

เอทานอลดีไฮเดรชันบนตัวเร่งปฏิกิริยา ZSM-5 ที่มีอัตราส่วนโดยโมลซิลิคอนต่ออะลูมิเนียมที่ต่างกัน
ซึ่งถูกปรับปรุงด้วยกรดฟอสฟอริกและแพลเลเดียม



บทคัดย่อและแฟ้มข้อมูลฉบับเต็มของวิทยานิพนธ์ตั้งแต่ปีการศึกษา 2554 ที่ให้บริการในคลังปัญญาจุฬาฯ (CUIR)
เป็นแฟ้มข้อมูลของนิสิตเจ้าของวิทยานิพนธ์ ที่ส่งผ่านทางบัณฑิตวิทยาลัย

The abstract and full text of theses from the academic year 2011 in Chulalongkorn University Intellectual Repository (CUIR)
are the thesis authors' files submitted through the University Graduate School.

วิทยานิพนธ์นี้เป็นส่วนหนึ่งของการศึกษาตามหลักสูตรปริญญาวิศวกรรมศาสตรมหาบัณฑิต

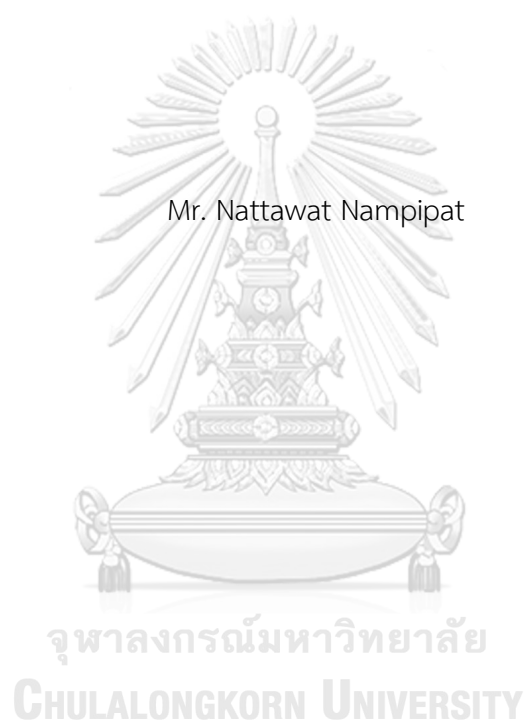
สาขาวิชาวิศวกรรมเคมี ภาควิชาวิศวกรรมเคมี

คณะวิศวกรรมศาสตร์ จุฬาลงกรณ์มหาวิทยาลัย

ปีการศึกษา 2560

ลิขสิทธิ์ของจุฬาลงกรณ์มหาวิทยาลัย

Dehydration of ethanol over ZSM-5
catalysts having different Si/Al molar ratios with H₃PO₄ and Pd modification



A Thesis Submitted in Partial Fulfillment of the Requirements
for the Degree of Master of Engineering Program in Chemical Engineering

Department of Chemical Engineering

Faculty of Engineering

Chulalongkorn University

Academic Year 2017

Copyright of Chulalongkorn University

Thesis Title	Dehydration of ethanol over ZSM-5 catalysts having different Si/Al molar ratios with H ₃ PO ₄ and Pd modification
By	Mr. Nattawat Nampipat
Field of Study	Chemical Engineering
Thesis Advisor	Professor Bunjerd Jongsomjit, Ph.D.

Accepted by the Faculty of Engineering, Chulalongkorn University in Partial Fulfillment of the Requirements for the Master's Degree

..... Dean of the Faculty of Engineering
(Associate Professor Supot Teachavorasinskun, Ph.D.)

THESIS COMMITTEE

..... Chairman
(Professor Muenduen Phisalaphong, Ph.D.)

..... Thesis Advisor
(Professor Bunjerd Jongsomjit, Ph.D.)

..... Examiner
(Chutimon Satirapipathkul, Ph.D.)

..... External Examiner
(Sasiradee Jantasee, Ph.D.)

มหาวิทยาลัย
CHULALONGKORN UNIVERSITY

ณัฐวัตร นำพิพัฒน์ : เอทานอลดีไฮเดรชันบนตัวเร่งปฏิกิริยา ZSM-5 ที่มีอัตราส่วนโดยโมลซิลิคอนต่ออะลูมิเนียมที่ต่างกันซึ่งถูกปรับปรุงด้วยกรดฟอสฟอริกและแพลเลเดียม (Dehydration of ethanol over ZSM-5 catalysts having different Si/Al molar ratios with H_3PO_4 and Pd modification) อ.ที่ปรึกษาวิทยานิพนธ์หลัก: ศ. ดร.บรรเจิด จงสมจิตร, หน้า.

Dehydration of ethanol was studied over ZSM-5, HZSM-5 and modified HZSM-5 catalysts under atmospheric pressure and temperature range of 200 °C to 400 °C. ZSM-5 catalysts were prepared by hydrothermal method using tetraphopylammonium bromide, sodium silicate solution and aluminium nitrate nonahydrate. The results showed that the various Si/Al molar ratios led to affect the amount of acidity on the surface of catalysts. The ZSM-5(20) catalyst exhibited the highest ethanol conversion at 400 °C about 70.3 % due to its high acid sites and large surface area. The commercial HZSM-5 catalysts, which had molar ratio similar to ZSM-5 Si/Al 20 catalysts, were modified with phosphoric acid and palladium metal by incipient wetness impregnation and co-impregnation methods. The results revealed that both modifications with phosphoric acid and palladium metal had effect on acidity and physical properties such as surface area of catalysts. These modifications resulted in increased weak acid and moderate to strong acid sites indicating that the total acidity increased. Both factors led to more ethylene formation at low temperature. In addition, Pd-HZSM-5 catalyst exhibited the highest activity among modified HZSM-5 catalysts. It had ethanol conversion about 22.3% at 200 °C. For Pd-P-HZSM-5 and Pd-P-HZSM-5 (Co-impregnation), they showed ethylene selectivity equal 12.6 % and 11.4 %, respectively at 200 °C. These results were due to modification with two metals resulting in more site that was suitable for occurring ethylene. Although the synthesized HZSM-5 catalyst, which was modified from ZSM-5 Si/Al20 by ion-exchange with ammonium nitrate, exhibited higher activity than commercial HZSM-5 catalyst and Pd-HZSM-5, it had higher coke formation due to this catalysts had higher acidity and surface area.

ภาควิชา วิศวกรรมเคมี

ลายมือชื่อนิสิต

สาขาวิชา วิศวกรรมเคมี

ลายมือชื่อ อ.ที่ปรึกษาหลัก

ปีการศึกษา 2560

5970165621 : MAJOR CHEMICAL ENGINEERING

KEYWORDS: ETHANOL DEHYDRATION / ZSM-5 / HZSM-5 / PHOSPHORUS / PALLADIUM

NATTAWAT NAMPIPAT: Dehydration of ethanol over ZSM-5 catalysts having different Si/Al molar ratios with H_3PO_4 and Pd modification. ADVISOR: PROF. BUNJERD JONGSOMJIT, Ph.D., pp.

ปฏิกิริยาเอทานอลดีไฮเดรชันบนตัวเร่งปฏิกิริยา ZSM-5, HZSM-5 และ HZSM-5 ที่ถูกพัฒนาภายใต้วัฏภาคแก๊สความดันบรรยากาศและอุณหภูมิช่วง 200 ถึง 400 องศาเซลเซียส โดยที่ตัวเร่งปฏิกิริยา ZSM-5 ถูกเตรียมด้วยวิธีไฮโดรเทอร์มัลซึ่งใช้สารผสมเตตระโพรพิลแอมโมเนียมโบรไมด์ สารละลายโซเดียมซิลิเกต และอะลูมิเนียมไตรเอทอโนนาไฮเดรท ผลการทดลองแสดงให้เห็นว่าสัดส่วนของซิลิคอนต่ออะลูมิเนียมโดยโมลนั้นนำไปสู่ผลกระทบต่อความเป็นกรดและปริมาณพื้นที่ผิวของตัวเร่งปฏิกิริยา โดยตัวเร่งปฏิกิริยา ZSM-5 ที่มีสัดส่วน 20 ให้ค่าการแปลงผันของเอทานอลสูงที่สุดเท่ากับ 70.3 เปอร์เซ็นต์ ที่อุณหภูมิ 400 องศาเซลเซียส เนื่องมาจากความเป็นกรดปริมาณมากและพื้นที่ผิวที่สูง ตัวเร่งปฏิกิริยา HZSM-5 เซิงพาณิชย์ที่มีสัดส่วนซิลิคอนต่ออะลูมิเนียมโดยโมลใกล้เคียง 20 ถูกปรับปรุงให้มิกับกรดฟอสฟอริกและโลหะแพลเลเดียมโดยใช้วิธีการเคลือบฝังและ การเคลือบฝังร่วม ซึ่งผลการทดลองถูกพบว่าการปรับปรุงตัวเร่งปฏิกิริยาด้วยกรดฟอสฟอริกและโลหะแพลเลเดียมส่งผลต่อความเป็นกรดและคุณสมบัติทางกายภาพเช่น พื้นที่ผิวของตัวเร่งปฏิกิริยา เป็นต้น การปรับปรุงนี้ทำให้ความแรงของกรดทั้ง กรดอ่อน และกรดปานกลางไปจนถึงกรดแก่ มีปริมาณที่เพิ่มมากขึ้นและทำให้ปริมาณความเป็นกรดโดยรวมมีค่าที่เพิ่มขึ้นอีกด้วย ทั้งสองปัจจัยนี้นำไปสู่การเกิดเอทิลีนที่อุณหภูมิต่ำ อีกทั้งการปรับปรุงเฉพาะโลหะแพลเลเดียมแสดงให้เห็นประสิทธิภาพสูงที่สุดท่ามกลางตัวเร่งปฏิกิริยา HZSM-5 ที่ถูกปรับปรุง ให้ร้อยละการแปลงผันของเอทานอลสูงถึง 22.3 เปอร์เซ็นต์ ที่อุณหภูมิ 200 องศาเซลเซียส สำหรับตัวเร่งปฏิกิริยาที่ถูกปรับปรุงด้วยกรดฟอสฟอริกและโลหะแพลเลเดียมแบบวิธีการเคลือบฝังและ การเคลือบฝังร่วมแสดงให้ค่าการเลือกเกิดของเอทิลีนที่อุณหภูมิต่ำ 200 องศาเซลเซียส เท่ากับ 12.6 และ 11.4 เปอร์เซ็นต์ ตามลำดับ เนื่องจากการปรับปรุงด้วยโลหะทั้ง 2 ชนิดนั้นส่งผลต่อจุดด่างไวที่เหมาะสมต่อการเกิดเอทิลีนมีปริมาณเพิ่มมากขึ้นถึงแม้ว่าตัวเร่งปฏิกิริยา HZSM-5 ที่ถูกสังเคราะห์จากการแลกเปลี่ยนไอออนกับแอมโมเนียมไนเตรท จะแสดงประสิทธิภาพที่เหนือกว่า HZSM-5 เซิงพาณิชย์ และ Pd-HZSM-5 แต่ก็เกิดโค้กในปริมาณที่มากกว่า เนื่องจากตัวมันมีปริมาณความเป็นกรดและพื้นที่ผิวสูงกว่า

Department: Chemical Engineering Student's Signature

Field of Study: Chemical Engineering Advisor's Signature

Academic Year: 2017

ACKNOWLEDGEMENTS

This research was successful by incorporation with several people. The author is really grateful my thesis advisor, Prof. Dr. Bunjerd jongsomjit for various suggestions, encouragement, research guideline, fault and guideline for improvement during research. The author cannot succeed in research without his advice. In addition, the author is also grateful

Prof. Dr. Muenduen Phisalaphong as the chairman, Dr. Chutimon Satirapipatkul and

Dr. Sasiradee Jantasee as a member of committee for their comments and suggestions.

Furthermore, the author would like to thank his parents for continuous encouragement during research and thank his senior in ethanol dehydration research and his friends who research at the same and different place for their suggestions and supports.

Finally, the author thanks the Grant for International Research Integration: Chula Research Scholar, Ratchadaphiseksomphot Endowment Fund and Department of Chemical engineering Chulalongkorn University for the financial support of this research.

CONTENTS

	Page
THAI ABSTRACT	iv
ENGLISH ABSTRACT	v
ACKNOWLEDGEMENTS	vi
CONTENTS	vii
FIGUER CONTENTS.....	xi
TABLE CONTENTS	xv
Chapter 1 Introduction.....	1
1.1 Introduction.....	1
1.2 Objective.....	2
1.3 Research Scope	2
1.4 Research methodology.....	4
Chapter 2 Background and literature review.....	7
2.1 Properties of ZSM-5.....	7
2.1.1 Synthesis of ZSM-5.....	8
2.1.2 Synthesis of HZSM-5.....	8
2.2 Properties of palladium.....	9
2.3 Properties of phosphorus.....	9
2.4 Ethanol dehydration reaction	10
2.5 Catalyst in ethanol dehydration reaction	14
2.5.1 Phosphoric acid catalyst.....	14
2.5.2 Oxide catalyst.....	14
2.5.3 Molecular sieve catalyst	14

	Page
2.5.4 Heteropolyacid catalyst.....	15
2.6 Literature review	15
Chapter 3 Experiment.....	19
3.1 Catalyst preparation	19
3.1.1 Synthesis of ZSM-5.....	19
3.1.2 Synthesis of phosphoric acid modified HZSM-5	20
3.1.3 Synthesis of noble metal modified HZSM-5 by incipient wetness impregnation	21
3.1.4 Synthesis of noble metal modified P-HZSM-5 by incipient wetness impregnation	22
3.1.5 Synthesis of noble metal and phosphoric acid modified HZSM-5 by incipient wetness co-impregnation.....	23
3.1.5 Synthesis of HZSM-5.....	24
3.2 Catalyst characterization	24
3.2.1 X-ray diffraction (XRD)	24
3.2.2 Atomic absorption spectroscopy (AAS).....	24
3.2.3 Ammonia temperature-programmed desorption (NH ₃ -TPD).....	25
3.2.4 Scanning electron microscope (SEM) and Energy dispersive X-ray spectroscopy (EDX).....	25
3.2.5 N ₂ physisorption (BET&BJH).....	25
3.2.6 X-ray fluorescence (XRF).....	25
3.2.7 Thermal gravimetric and differential analysis (TG/DTA).....	25
3.3 Catalytic Ethanol dehydration reaction	26
Chapter 4 Results and discussion.....	28

	Page
4.1 Characterization of synthesized ZSM-5.....	29
4.1.1 X-ray diffraction (XRD)	29
4.1.2 Scanning electron microscope (SEM) and energy dispersive X-ray spectroscopy (EDX).....	30
4.1.3 Atomic absorption spectroscopy (AAS).....	33
4.1.5 Ammonia temperature-programmed desorption (NH ₃ -TPD).....	34
4.1.4 N ₂ physisorption (BET&BJH).....	36
4.1.6 Ethanol dehydration reaction.....	38
4.2 Characterization of HZSM-5 and modified HZSM-5 with phosphoric acid and palladium	42
4.2.1 X-ray diffraction (XRD)	42
4.2.2 X-ray fluorescence (XRF).....	43
4.2.3 Scanning electron microscope (SEM) and Energy dispersive X-ray spectroscopy (EDX).....	44
4.2.4 N ₂ physisorption (BET&BJH).....	50
4.2.5 Ammonia temperature-programmed desorption (NH ₃ -TPD).....	54
4.2.6 Ethanol dehydration reaction.....	56
4.3 Characterization of synthesized HZSM-5 and commercial HZSM-5.....	63
4.3.1 X-ray diffraction (XRD)	63
4.3.2 X-ray fluorescence (XRF).....	64
4.3.2 Scanning electron microscope (SEM) and Energy dispersive X-ray spectroscopy (EDX).....	65
4.3.4 N ₂ physisorption (BET&BJH).....	71
4.3.5 Ammonia temperature-programmed desorption (NH ₃ -TPD).....	73

	Page
4.3.6 Thermal gravimetric and differential analysis (TG/DTA)	74
4.3.7 Ethanol dehydration reaction.....	76
Chapter 5 Conclusions and recommendations.....	81
5.1 Conclusion.....	81
5.2 Recommendations	83
REFERENCES	84
APPENDIX.....	88
Appendix A Calculation catalysts preparation.....	89
Appendix B Calculation catalysts preparation by incipient wetness impregnation.....	90
Appendix C Modification ZSM-5 catalyst by ion-exchange	94
Appendix D Calibration curve of Reactant and Product	95
Appendix E Calculation of acidity catalysts from NH ₃ -TPD.....	98
Appendix F Calculation of conversion , selectivity, yield rate of reaction and WHSV	99
Appendix G Catalytic activity, selectivity, yield and rate of reaction of product over all catalysts.....	100
VITA.....	105

FIGUER CONTENTS

Figure 1 Structure of pentasil unit, ZSM-5 and other zeolite. ¹⁷	7
Figure 2 Autoclave structure	8
Figure 3 Three routes of ethanol dehydration reaction.....	11
Figure 4 The mechanism of ethanol dehydration to ethylene	12
Figure 5 The mechanism of ethanol dehydration to diethyl ether (dissociative pathway).....	13
Figure 6 The mechanism of ethanol dehydration to diethyl ether (associative pathway).....	13
Figure 7 Schematics of the catalytic cycles.....	17
Figure 8 Diagram of ZSM-5 catalysts preparation by hydrothermal method.....	20
Figure 9 Diagram of P-HZSM-5 catalysts preparation by incipient wetness impregnation method.....	21
Figure 10 Diagram of Pd-HZSM-5 catalysts preparation by incipient wetness impregnation method.....	22
Figure 11 Diagram of Pd-P-HZSM-5 catalysts preparation by incipient wetness impregnation method.....	22
Figure 12 Diagram of Pd-HZSM-5 catalysts preparation by incipient wetness co-impregnation method.....	23
Figure 13 Schematic of the gas phase ethanol dehydration reaction	27
Figure 14 XRD patterns of ZSM-5 with different molar ratios of Si/Al	29
Figure 15 SEM image of synthesized ZSM-5 catalysts with molar ratio of Si/Al 20 (a), 40 (b) and 60 (c), respectively.	31
Figure 16 SEM-EDX mapping of synthesized ZSM-5 Si/Al 20	31

Figure 17 SEM-EDX mapping of synthesized ZSM-5 Si/Al 40.....	32
Figure 18 SEM-EDX mapping of synthesized ZSM-5 Si/Al 60.....	32
Figure 19 Isotherm graph of synthesized ZSM-5 catalysts; (a). ZSM-5 Si/Al at 20 (b). ZSM-5 Si/Al at 40 and (c). ZSM-5 Si/Al at 60	37
Figure 20 NH ₃ -TPD profiles of synthesized ZSM-5 with different molar ratios of Si/Al.....	35
Figure 21 Ethylene yield in ethanol dehydration over synthesized ZSM-5 catalysts with different silicon to aluminium molar ratio.	40
Figure 22 Diethyl ether yield in ethanol dehydration over synthesized ZSM-5 catalysts with different silicon to aluminium molar ratios.	41
Figure 23 XRD patterns of HZSM-5 and modified HZSM-5 catalysts.....	42
Figure 24 SEM image of HZSM-5 and modified HZSM-5 catalysts ; (a). HZSM-5, (b). P-HZSM-5, (c). Pd-HZSM-5, (d). Pd-P-HZSM-5 and (e). Pd-P-HZSM-5 Co- impregnation.....	45
Figure 25 SEM-EDX mapping of HZSM-5	46
Figure 26 SEM-EDX mapping of P-HZSM-5.....	46
Figure 27 SEM-EDX mapping of Pd-HZSM-5	47
Figure 28 SEM-EDX mapping of Pd-P-HZSM-5.....	47
Figure 29 SEM-EDX mapping of Pd-P-HZSM-5 (Co-impregnation)	48
Figure 30 Isotherm graph of HZSM-5 and modified HZSM-5 catalysts; (a). HZSM-5, (b). Pd-HZSM-5, (c). P-HZSM-5, (d). Pd-P-HZSM-5 and (e). Pd-P-HZSM-5 (Co- impregnation).....	52
Figure 31 Pore size distribution graph of HZSM-5 and modified HZSM-5 catalysts.....	53
Figure 32 NH ₃ -TPD profiles of HZSM-5 and modified HZSM-5 catalysts	54
Figure 33 Catalytic activity of HZSM-5 and modified HZSM-5 catalysts in ethanol dehydration reaction (line plot).....	56

Figure 34 Catalytic activity of HZSM-5 and modified HZSM-5 catalysts in ethanol dehydration reaction (bar chart).....	57
Figure 35 Ethylene yield of HZSM-5 and modified HZSM-5 catalysts in ethanol dehydration reaction (line plot).....	58
Figure 36 Ethylene yield of HZSM-5 and modified HZSM-5 catalysts in ethanol dehydration reaction (bar chart).....	59
Figure 37 Diethyl ether yield of HZSM-5 and modified HZSM-5 catalysts in ethanol dehydration reaction (line plot).....	60
Figure 38 Diethyl ether yield of HZSM-5 and modified HZSM-5 catalysts in ethanol dehydration reaction (bar chart).....	60
Figure 39 Acetaldehyde yield of HZSM-5 and modified HZSM-5 catalysts in ethanol dehydration reaction (line plot).....	61
Figure 40 Acetaldehyde yield of HZSM-5 and modified HZSM-5 catalysts in ethanol dehydration reaction (bar chart).....	62
Figure 41 XRD patterns of synthesized ZSM-5, HZSM-5 and commercial HZSM-5 catalysts.....	64
Figure 42 SEM image of commercial HZSM-5 (a) and synthesized HZSM-5.....	65
Figure 43 SEM-EDX mapping of Commercial HZSM-5 catalysts.....	66
Figure 44 SEM-EDX mapping of synthesized HZSM-5 catalysts.....	66
Figure 45 SEM image of fresh commercial HZSM-5 (a) and spent commercial HZSM-5 catalysts (b)......	68
Figure 46 SEM image of fresh synthesized HZSM-5 (a) and spent synthesized HZSM-5 catalysts (b)......	69
Figure 47 SEM-EDX of spent commercial HZSM-5 catalyst.....	69
Figure 48 SEM-EDX of spent synthesized HZSM-5 catalyst.....	70

Figure 49 Isotherm graph of commercial HZSM-5 and synthesized HZSM-5 catalysts	72
Figure 50 Pore size distribution of commercial HZSM-5 and synthesized HZSM-5 catalysts	72
Figure 51 NH ₃ -TPD profiles of commercial HZSM-5 and synthesized HZSM-5 catalysts	73
Figure 52 TG/DTA profile of commercial HZSM-5 catalyst	75
Figure 53 TG/DTA profile of synthesized HZSM-5 catalyst	75
Figure 54 Catalytic activity of commercial HZSM-5 and synthesized HZSM-5 catalysts in ethanol dehydration reaction.....	76
Figure 55 Ethylene yield of commercial HZSM-5 and synthesized HZSM-5 catalysts in ethanol dehydration reaction.....	77
Figure 56 Diethyl ether yield of commercial HZSM-5 and synthesized HZSM-5 catalysts in ethanol dehydration reaction.....	78
Figure 57 Acetaldehyde yield of commercial HZSM-5 and synthesized HZSM-5 catalysts in ethanol dehydration reaction.....	79

TABLE CONTENTS

Table 1 Palladium properties	9
Table 2 Phosphorus properties	10
Table 3 The chemical used in synthesis ZSM-5 catalyst	20
Table 4 The chemical used in synthesis P-HZSM-5 catalyst	21
Table 5 The chemical used in synthesis Pd-HZSM-5 catalyst	21
Table 6 The chemical used in synthesis HZSM-5 catalyst	24
Table 7 The chemical used in ethanol dehydration reaction	26
Table 8 The operating conditions in gas chromatograph	26
Table 9 Element distribution of synthesized ZSM-5 (weight percent)	33
Table 10 Element distribution of synthesized ZSM-5 (atomic percent)	33
Table 11 Element distribution of synthesized ZSM-5 from AAS	34
Table 12 Molar ratio of Si/Al between SEM-EDX and AAS techniques	34
Table 13 BET surface area, pore size and pore volume of synthesized ZSM-5 catalysts ..	36
Table 14 Total acidity from NH ₃ -TPD	36
Table 15 Conversion and product selectivity of synthesized ZSM-5 catalysts	39
Table 16 Element distribution from X-ray fluorescence (weight percent)	43
Table 17 Element distribution of HZSM-5 and modified HZSM-5 catalysts (weight percent)	49
Table 18 Element distribution of HZSM-5 and modified HZSM-5 catalysts (atomic percent)	49
Table 19 Amount of metal loading between SEM-EDX and XRF technique	50
Table 20 BET surface area, pore size and pore volume of HZSM-5 and modified HZSM-5 catalysts	50

Table 21 Total acidity of HZSM-5 and modified HZSM-5 catalysts from NH ₃ -TPD.....	55
Table 22 Element distribution of synthesized HZSM-5 and commercial HZSM-5 from X-ray fluorescence (weight percent).....	64
Table 23 Element distribution of commercial HZSM-5 and synthesized HZSM-5 catalysts (weight percent).....	67
Table 24 Element distribution of commercial HZSM-5 and synthesized HZSM-5 catalysts (atomic percent).....	67
Table 25 Molar ratio of Si/Al between SEM-EDX and XRF techniques.....	67
Table 26 Element distribution of commercial HZSM-5 and synthesized HZSM-5 catalysts (weight percent).....	70
Table 27 Element distribution of commercial HZSM-5 and synthesized HZSM-5 catalysts (atomic percent).....	70
Table 28 BET surface area, pore size and pore volume of commercial HZSM-5 and synthesized HZSM-5 catalysts.....	71
Table 29 Total acidity of commercial HZSM-5 and synthesized HZSM-5 catalysts from NH ₃ -TPD.	74
Table 30 Weight loss of commercial HZSM-5 and synthesized HZSM-5 catalysts from TG/DTA.....	76
Table 31 Ethanol conversion of all catalysts.....	80

CHAPTER 1

INTRODUCTION

1.1 Introduction

Nowadays, the Fossil fuels are used widely and emission greenhouse gas that damages the environment. Moreover, the damage from global warming is likely to increase each year. Causing in global temperature rising ¹. To limit the long term global temperature rise, renewable energy is a clean that can reduce greenhouse gas emissions and depletion of fossil fuel reserves. In addition, ethanol is one of renewable energies that can be easily produced from biomass materials such as cassava, sugarcane, corn, rice and others through fermentation process²⁻³. The dehydration of ethanol has long been of interest to produce ethylene and diethyl ether from non-petroleum feedstock. Generally, there are two competitive pathways during catalytic dehydration of ethanol. Ethanol can be dehydrated to produce ethylene at high temperature, while diethyl ether was formed at lower temperature. Ethylene is an essential chemical in the petrochemical and polymer industries ⁴, while diethyl ether has been also used as a solvent in the chemical, fragrance, and pharmaceutical industries and has a number of applications in fuel chemical industry. Diethyl ether has high octane and cetane number ⁵, thus, it is used as an ignition additive for gasoline and diesel engines. Although diethyl ether is used in many application areas, the dehydration of ethanol to diethyl ether has received less attention. It is well known that many solid acid catalysts such as zeolites, silica-alumina and alumina have been used for ethanol dehydration to produce diethyl ether ⁶. ZSM-5 is one type of zeolite catalysts that is widely used for catalytic dehydration of ethanol to diethyl ether because it has a good performance at lower reaction temperature and ethylene at higher reaction temperature with a higher product yield⁷. ZSM-5 zeolite can be easily synthesized via hydrothermal process. The molar ratio of silicon to aluminium of ZSM-5 can be controlled by changing the amount of sodium silicate solution⁸⁻⁹. HZSM-5 is a one form of ZSM-5 after ion-exchange with ammonium nitrate and use in ethanol dehydration more than ZSM-5 form due to high stability catalyst¹⁰.

In order to enhance activity in ethanol dehydration, some metals are modified in HZSM-5¹¹⁻¹². In addition, using phosphoric acid to modify in HZSM-5 form to PZSM-5 form can enhance selectivity of ethylene and stability¹³.

In present study, the effects of different molar ratios of Si/Al in ZSM-5 catalysts synthesized by hydrothermal process and effect of sequence in modification catalyst with phosphoric acid and noble metal (Pd) were investigated. The catalytic activity of ZSM-5 catalysts and modified HZSM-5 catalysts are studied in ethanol dehydration.

1.2 Objective

1. To investigate the effect of different molar ratios of silicon to aluminium in ZSM-5 catalysts synthesized by hydrothermal process in ethanol dehydration reaction.
2. To compare the effect of sequence in catalysts with phosphoric acid and noble metal (Pd) modification in ethanol dehydration reaction.
3. To compare catalytic activity between synthesized HZSM-5 and commercial HZSM-5 catalysts in ethanol dehydration reaction.

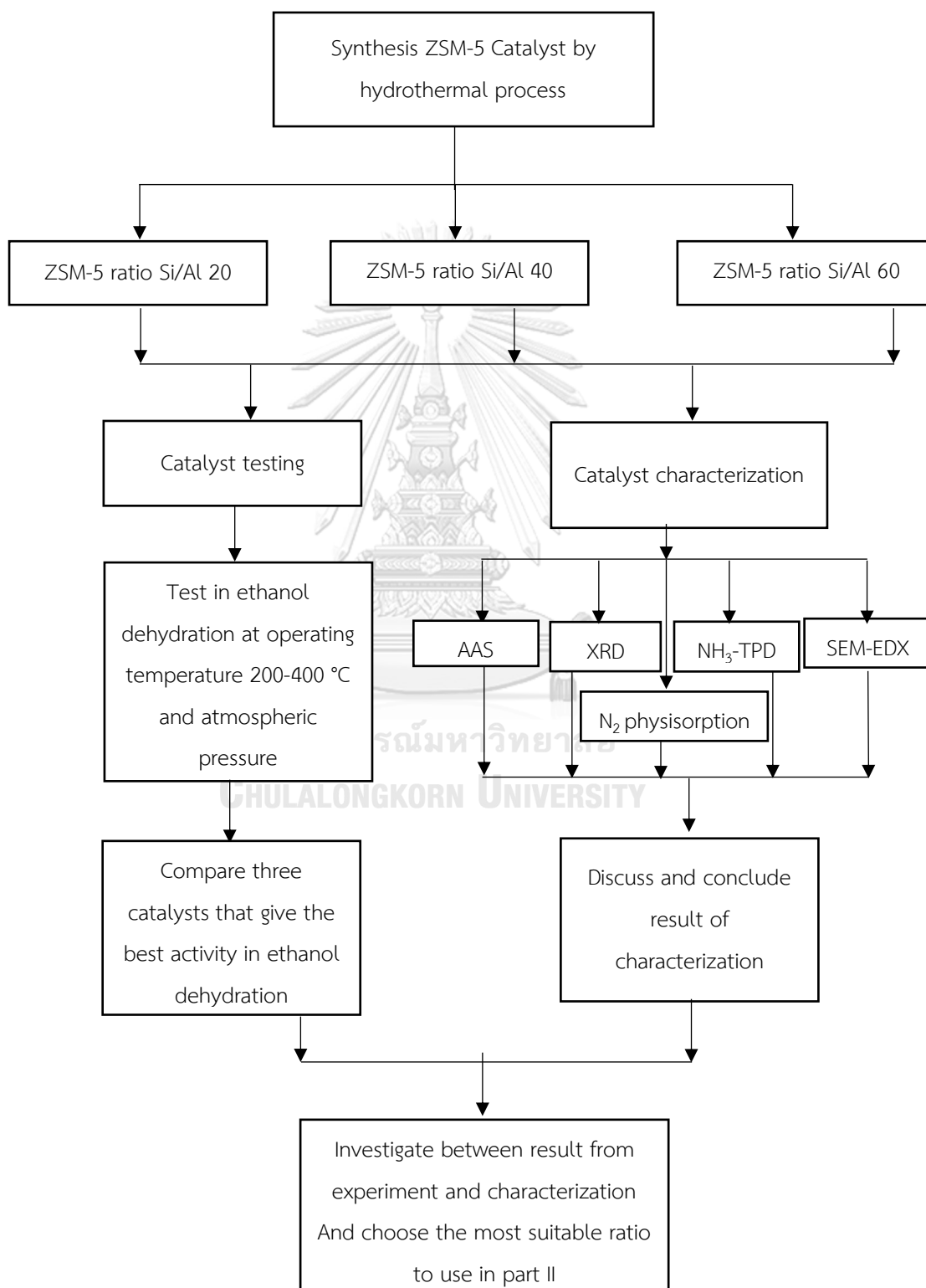
1.3 Research Scope

1. Three molar ratios of silicon to aluminium in ZSM-5 catalysts (20, 40 and 60) were prepared by hydrothermal process.
2. Characterization of synthesized catalysts with X-ray diffraction (XRD), Ammonia temperature programmed desorption (NH₃-TPD), Scanning electron microscope (SEM) and Energy dispersive X-ray spectroscopy (SEM-EDX) and N₂ physisorption (BET).
3. ZSM-5 molar ratio of silicon to aluminium 20, 40 and 60 were tested in ethanol dehydration at operation temperature 200 – 400 °C and atmospheric pressure.
4. Determining the most suitable ratio in ZSM-5, which gives the best activity in ethanol hydration.

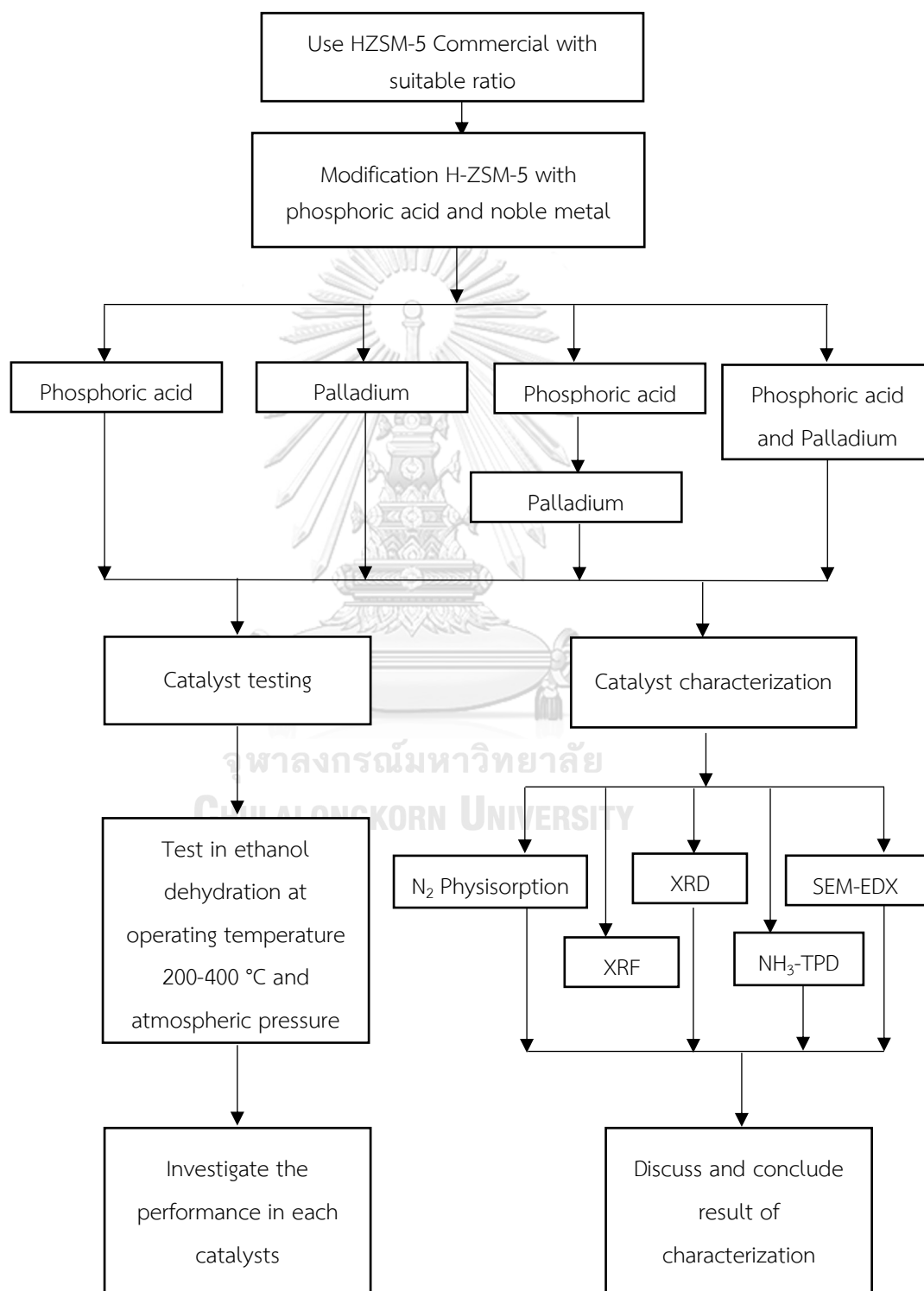
5. Modification Catalyst ,HZSM-5 commercial , with phosphoric acid and noble metal ,palladium, by varying the sequence of loading between acid and metal.
6. Reaction study of modified HZSM-5 in ethanol dehydration at operation temperature 200 – 400 °C and atmospheric pressure.
7. Comparing the performance of modified HZSM-5 with phosphoric acid and palladium that varied the sequence of loading, which gives the best activity in ethanol hydration.
8. Modification ZSM-5 catalyst by ion exchange method
9. Comparing the performance between synthesized HZSM-5 and commercial HZSM-5 catalysts
10. Characterization Synthesized catalyst with X-ray diffraction (XRD), Ammonia temperature programmed desorption (NH₃-TPD), Scanning electron microscope (SEM) and Energy dispersive X-ray spectroscopy (SEM-EDX) N₂ physisorption (BET), X-ray fluorescence (XRF) , Thermal gravimetric and differential analysis (TG/DTA) and Atomic absorption spectroscopy (AAS).

1.4 Research methodology

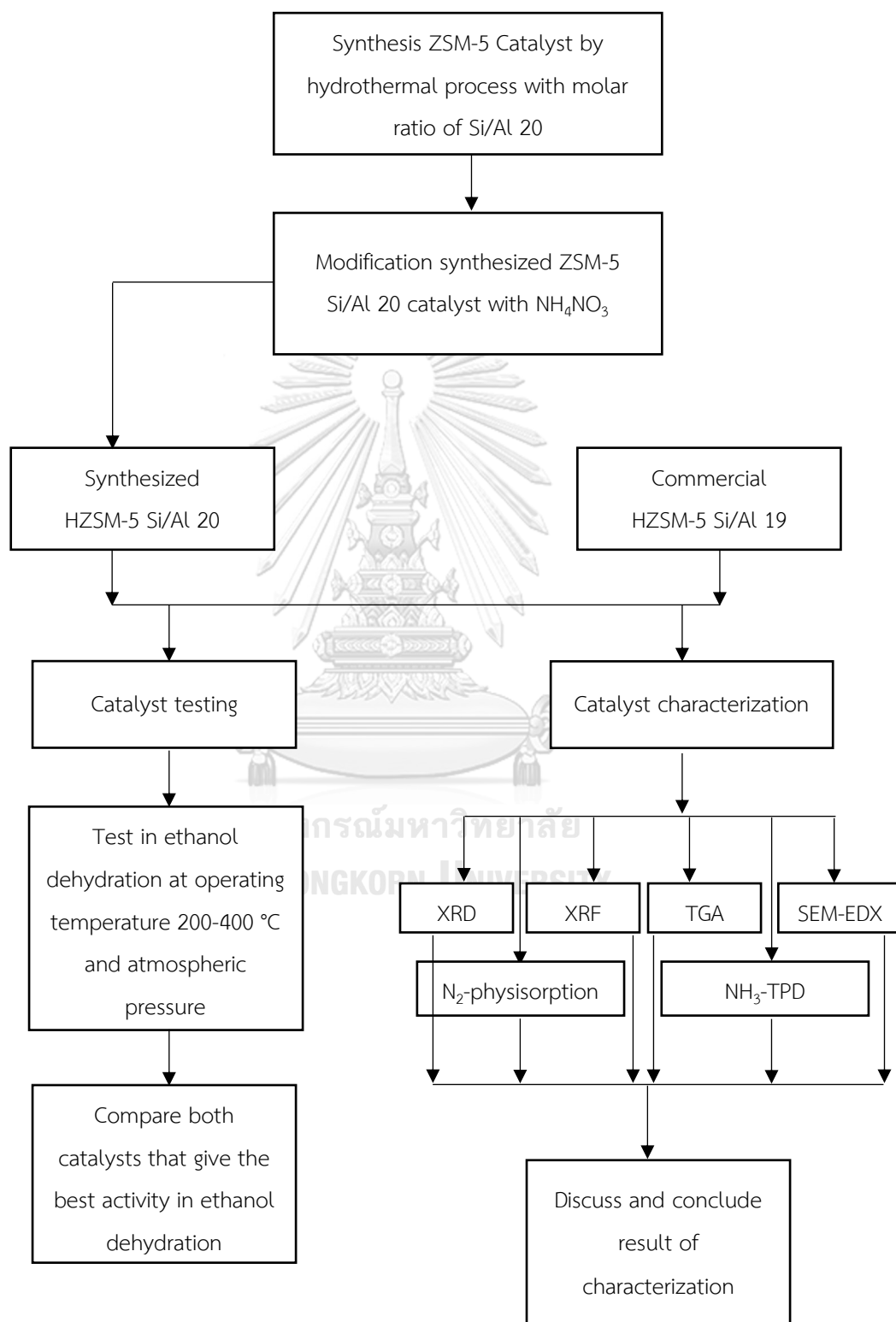
Part I: Investigation of the most suitable molar ratio of silicon to aluminium in ZSM-5 catalyst in ethanol dehydration reaction.



Part II: Investigation on the effect of metal Pd and P, and effect of sequence in modification of catalyst with phosphoric acid and noble metal (Pd) in ethanol dehydration reaction.



Part III: Comparison catalytic activity between synthesized HZSM-5 and commercial HZSM-5 catalysts in ethanol dehydration reaction.



CHAPTER 2

BACKGROUND AND LITERATURE REVIEW

2.1 Properties of ZSM-5

ZSM-5 catalysts were used as heterogeneous catalysts in widely industries such as oil refinery and petro chemical industry due to high physical and chemical properties including unique structure, shape selectivity, thermal stability, and acidity.¹⁴ Actually, ZSM-5 was a microspores catalyst (<2 nm.) but in recent year, It success to synthesis mesopores catalysts (<50 nm.)¹⁵⁻¹⁶. ZSM-5 or Pentasil zeolite has channel with three dimensional channels defined by 10-membered rings liked pentasil unit. Physical and chemical properties such as morphology, acidity, crystal size and ratio of silicon to aluminium were depend on chemical composition in precursor, source of silicon and aluminium, the alkalinity, seeds presence, the molar ratio of OH/SiO₂ and system dynamics⁹. The structure of ZSM-5 and pentasil unit are representing in Figure 2.1

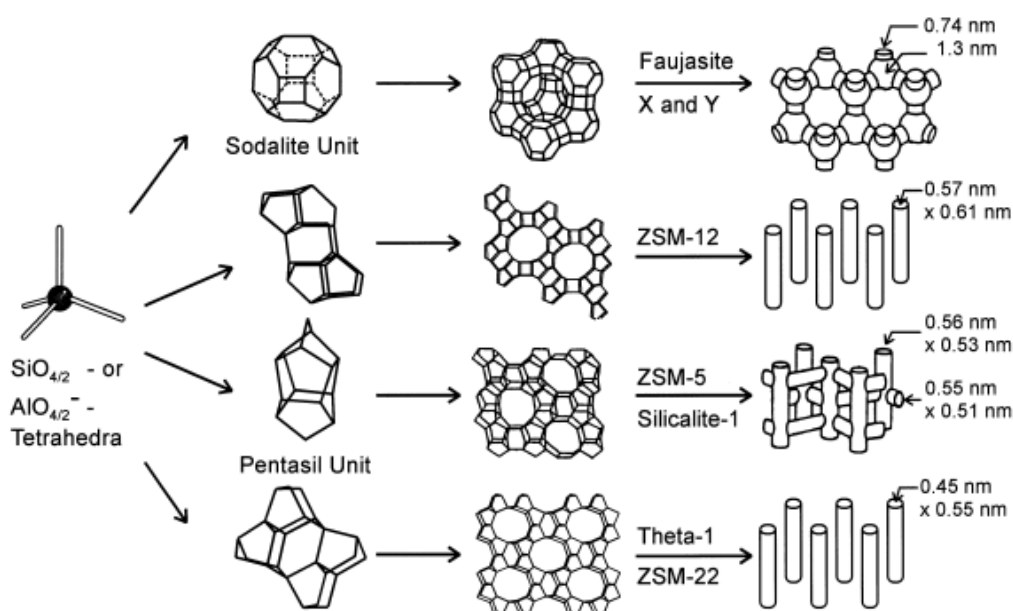


Figure 1 Structure of pentasil unit, ZSM-5 and other zeolite.¹⁷

2.1.1 Synthesis of ZSM-5

In synthesis ZSM-5 catalyst, the most common technic for preparing zeolite was hydrothermal process by using stainless steel reactor (autoclave). Hydrothermal method was used water as a solvent for maintained pressure at high temperature. Many organic materials were used as template example, tetrapropylammonium hydroxide (TPAOH), tetraethylorthosilicate (TEOS)¹⁸ and tetrapropylammonia bromide (TPABr). Moreover, the solid waste from Mae-Moh coal-fired power generation could use as silicon and aluminium source instead of synthesized chemical⁸. Furthermore, from Kumar et al.¹⁴ investigation. Effect of time and mode stirring in synthesis method influenced to properties of ZSM-5 catalyst. The structure of autoclave shows in Figure 2.2

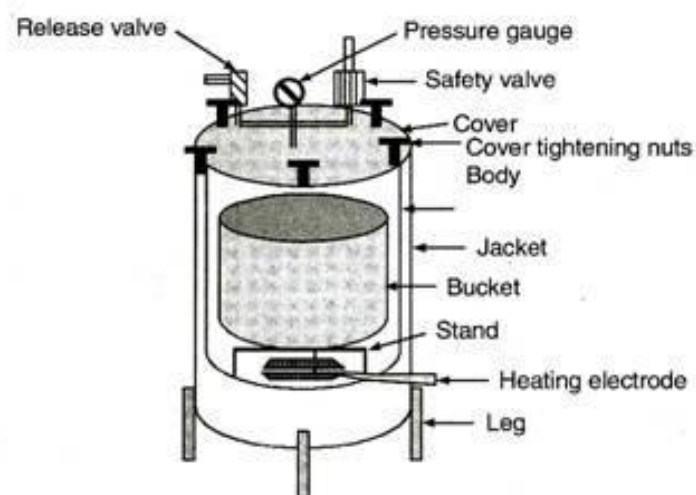


Figure 2 Autoclave structure

2.1.2 Synthesis of HZSM-5

Synthesized ZSM-5 is a Sodium form (NaZSM-5) due to Sodium silicate solution as a precursor. In synthesis of HZSM-5, it uses ion-exchange technic with 1 M ammonium hydroxide solution (NH_4OH) or ammonium nitrate (NH_4NO_3). The cation of ZSM-5 is exchanged by H^+ ion and turn ZSM-5 into HZSM-5 catalysts¹⁹⁻²⁰.

2.2 Properties of palladium

Palladium or Pd is a chemical element with an atomic number 46. It is discovered in the 1803 by William Hyde Wollaston. The Physical properties of Palladium is reported in Table 1

Platinum group metals (PGMs) are consist of Palladium platinum, rhodium, ruthenium, iridium, and osmium. Although these substances have similar chemical properties but Palladium has the lowest melting point and lowest density. More than half of the supply of palladium and platinum group metal are used in catalytic converters that convert up to 90% of the harmful gases in the exhaust car such as hydrocarbons, carbon monoxide and nitrogen dioxide into less toxic (nitrogen, carbon dioxide and water vapor). Furthermore, Palladium is also used in electronics, dentistry, hydrogenation, chemical applications, groundwater treatment and palladium jewelry. In recent year, Palladium was used as promoter to promote activity in reaction

Table 1 Palladium properties

Properties	Specification
Group, Period, Block	10 , 5 , d
Atomic number, mass	46, 106.42 g/mol
Appearance	Silvery white
Phase	Solid
Density near r.t.	12.023 g/cm ³
Melting point	1,828.05 K
Boiling point	3,236 K

2.3 Properties of phosphorus

Phosphorus or P is a chemical element with an atomic number 15. Phosphorus was first made by Hennig Brandt at Hamburg in 1669 when he evaporated urine and heated the residue until it was red hot, whereupon phosphorus vapor distilled which he collected by condensing it in water. The Physical properties of Phosphorus is reported in Table 2 Phosphorus is a variety of forms, but there are only two main

forms, white phosphorus and red phosphorus, to be used. Because it is highly reactive, Phosphorus never appears as a free element. Moreover, Phosphorus is used as a promoter to increase stability of HZSM-5 in selective conversion ethanol to propylene²¹. In this research, Phosphoric is a precursor of phosphorus that used to modify HZSM-5 catalyst for enhancing activity of catalyst.

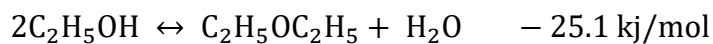
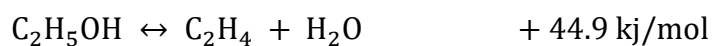
Table 2 Phosphorus properties

Properties	Specification
Group, Period, Block	15 , 3 , p
Atomic number, mass	15, 30.974 g/mol
Appearance	Colorless, waxy white, yellow, scarlet, red, violet, black
Phase	Solid
Density near r.t.	white: 1.823 g/cm ³ red: \approx 2.2–2.34 g/cm ³ violet: 2.36 g/cm ³ black: 2.69 g/cm ³
Melting point	317.25 K
Boiling point	553.15 K

2.4 Ethanol dehydration reaction

Actually, Ethanol is a renewable energy that produced from biomass such as corn, cassava, rice and sugarcane. Because ethanol emit less greenhouse gases and high octane number, it is used as additive in gasoline. Moreover, ethanol is used as a raw material to produce a variety of products including ethylene, diethyl ether, acetaldehyde and etc.

Ethanol dehydration reaction has two competitive pathways: a unimolecular pathway to form ethylene and water and a bimolecular pathway to form diethyl ether (DEE) and water. Ethylene can occur at high temperature due to endothermic reaction as the first reaction, while diethyl ether is produced at low temperature (exothermic reaction) as the second reaction.



The mechanism research of ethanol dehydration reaction considers in generation of ethylene and diethyl ether that can be concluded in 3 routes. As report in Figure 2.3 These are parallel reaction, a series of reactions and a parallel series reaction ²².

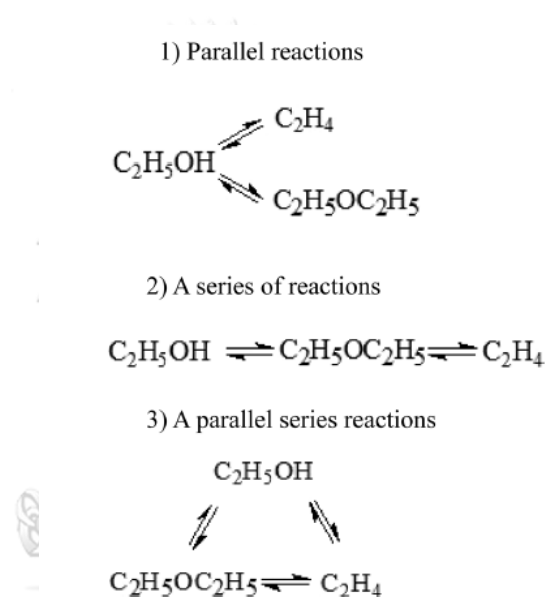
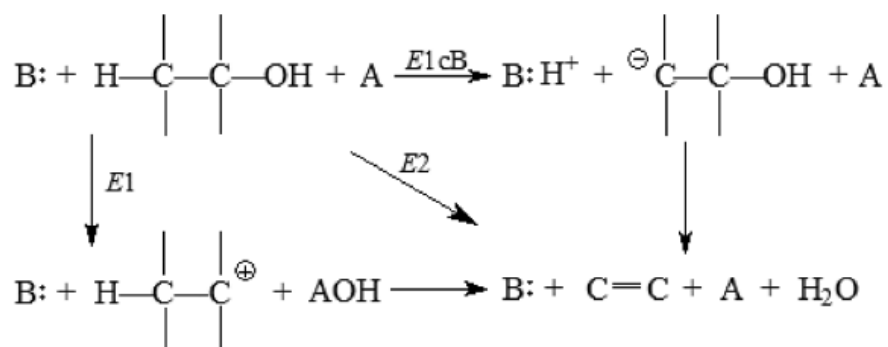


Figure 3 Three routes of ethanol dehydration reaction



: electrons pair \oplus positive charge \ominus negative charge

Figure 4 The mechanism of ethanol dehydration to ethylene

The mechanism of ethanol dehydration to ethylene is represented in Figure 2.4, It has three reaction mechanisms of ethanol catalytic dehydration to ethylene under different reaction conditions (E1, E2 and E1cb) While A and B are the acidic and basic centers of the catalyst, respectively. Three reaction (E1, E2 and E1cb) are competitive reaction and elimination reaction. In E1 reaction, one molecule of ethanol dissociate OH^- and generate carbonation intermediate. Ethylene is formed when intermediate loses β -hydrogen. The E2 reaction elimination reaction and it is finished in one step only. The E1cb reaction is a single molecule conjugate base elimination reaction. β -hydrogen of the reactant is captured with the nucleophilic center to generate carbanion (conjugate base), and then the hydroxyl of the conjugate base leaves to generate olefin and water²².

The mechanism of ethanol dehydration to diethyl ether is divided into two pathways, namely dissociative path way and associative pathway. In dissociative pathway is shown in Figure 2.5, the reaction starts like E1 elimination reaction in mechanism of ethanol dehydration to ethylene but carbonation captures one molecule of ethanol and leaves H^+ ion. H^+ ion capture with OH^- group and generates water. In Figure 2.6 shows the associative pathway of mechanism of ethanol dehydration to diethyl ether. The mechanism starts with one proton attack ethanol to form electrophilic then, it captures with another ethanol to form intermediate. Diethyl ether is formed when the intermediate removes water and base group. Both of intermediate in dissociative pathway and associative pathway can break bond at high

temperature and form ethylene after generate carbocation, following E1 reaction in mechanism of ethanol to ethylene ²².

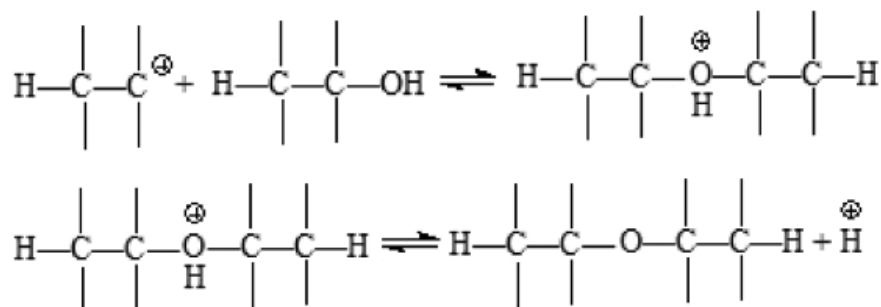


Figure 5 The mechanism of ethanol dehydration to diethyl ether (dissociative pathway)

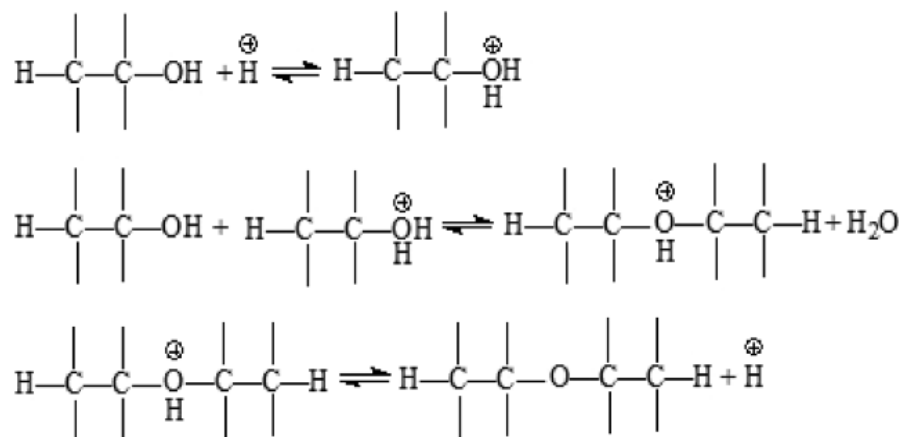


Figure 6 The mechanism of ethanol dehydration to diethyl ether (associative pathway)

2.5 Catalyst in ethanol dehydration reaction

In ethanol dehydration reaction, it has widely catalysts are used such as clay, activated alumina, silicon oxide, magnesium oxide, zirconium oxide, phosphate, calcium phosphate, zinc aluminates, heteropoly salt, and molecular sieve, etc., that can be classified into 4 categories such as phosphoric acid, oxides, molecular sieves, and heteropolyacid catalyst ²².

2.5.1 Phosphoric acid catalyst

In manufacturing ethylene, phosphoric acid catalyst is the first catalysts which used in ethylene industries. It was developed by the British Imperial Chemical (ICI) by loading phosphate on clay or coke in the 1930s ²³. In 1981, Donald et al. ²⁴ study about effect of reaction condition and catalyst regeneration on ethanol dehydration with phosphoric acid. Although the performance of phosphoric acid catalyst gives high purity of ethylene as product, but it uses long time to regeneration and easies deactivation by coke. Since the 1950s, this catalyst have been used.

2.5.2 Oxide catalyst

The representative of oxide catalyst is alumina. It is used in dehydration of alcohol, isomerization, alkylation and cracking reaction ²⁵. In the 1950s, Alumina and clay were used as catalyst in ethanol dehydration to produce ethylene. The performance of alumina and clay are compared in deactivation and purity of ethylene. The deactivation in alumina catalysts is less than clay, but the purity of ethylene is less than clay too ²⁶. It can be concluded that alumina catalyst has good stability.

2.5.3 Molecular sieve catalyst

The properties of molecular sieve catalyst are high surface area, acid-base properties and unique pore structure w. In the 1980s, molecular sieve catalyst such as ZSM-5 and Si-Al phosphate (SAPO) were used in ethanol dehydration to ethylene. In

addition, these catalysts have higher activity than alumina at lower temperature. Because these catalysts highly active, it can be deactivated easily

2.5.4 Heteropolyacid catalyst

Heteropolyacid catalyst includes oxygen atom bridging multiacid that formed by central atom and lig-atom. It can use as acid or oxidation-reduction catalyst²⁷. The advantage of heteropolyacid catalyst in ethanol dehydration is using low temperature to generate ethylene but decreasing in ethanol conversion rate.

2.6 Literature review

In the part literature review, it has many of catalysts which used in ethanol dehydration. From the previous section, the catalysts in ethanol dehydration are separated into 4 groups and all four groups have different advantages and disadvantages. While this reaction is intensively studied, the catalysts in the four groups are developed together.

In 2005, Machado N. et al.²⁸ studied iron modification on ZSM-5 zeolite catalyst to the catalytic activity of ethanol to hydrocarbon such as ethylene, ethane, propylene, propane, C₄, C₅ and heavy hydrocarbon by varying technic of iron loading on ZSM-5 catalysts example impregnation and ion-exchange. The best result was obtained from the iron ion-exchange sample at low iron content.

In 2005, Zaki T.²⁹ investigated catalytic dehydration of ethanol over transition metal oxide catalysts such as Fe₂O₃, Mn₂O₃, Al₂O₃, SiO₂ and mixed transition metal oxide at operating temperature 200 °C - 500 °C. The result shown the catalyst that had high surface acidity gave high activity and the activity increased while temperature increased.

In 2007, Varisli D. et al.³⁰ studied ethanol dehydration to ethylene and diethyl ether over heteropolyacid (HPA) catalysts, namely tungstophosphoricacid (TPA), silicotungsticacid (STA) and molybdophosphoricacid (MPA) at operating temperature 140°C - 250 °C. Diethyl ether was main product at temperature 180 °C. STA was the best HPA catalysts followed by TPA and MPA in ethanol dehydration. The presence of water vapor results in reducing activity.

In 2008, Zhang D. et al.³¹ reported effect of phosphorus modified on HZSM-5 in ethanol dehydration reaction. Addition of phosphorus decreased strong acid site and the weak acid site presented instead. Moreover, it was found amount of phosphorus involved selectivity of ethylene and hydrocarbon. As phosphorus more than loading 3.4 wt %, only ethylene presented as product at high temperature

In 2010, Ramesh K. et al.¹³ studied about effect of phosphorus modified on HZSM-5 in selective ethanol dehydration. It was found phosphorus enhanced the stability of HZSM-5 which easily deactivate to stable more than 200 h. From result of NH₃-TPD, the strong acid site was decreased clearly when phosphorus was added. The P-modified ZSM-5 catalyst was highly active in ethanol dehydration to ethylene. It made ethylene selectivity more than 98 % at lower temperature 623 K.

In 2010, Zhan N. et al.³² investigated addition of lanthanum and phosphorus on HZSM-5 catalysts at low temperature (200 °C – 300 °C) in ethanol dehydration . Effect of phosphorus was anti-coke and effect of lanthanum with phosphorus slightly enhanced activity in ethanol hydration at low temperature.

In 2015, Phung T.K. et al.¹¹ studied the conversion of ethanol to hydrocarbon over P, Fe and Ni modified HZSM-5. Phosphorus affected to reduce formation of coke and increase selectivity of ethylene. The role of iron was decreased acidity of catalyst. Nickel modified HZSM-5 enhanced selectivity of C₄ and aromatic due to decreasing of Brønsted acid site.

In 2015, Phung T.K. et al.³³ investigated the catalytic of ethanol to diethyl ether over acid catalysts such as alumina, zeolite types MFI, FER and USY, silica-alumina and calcined hydrotalcite. It was found 4 reaction, namely diethyl ether cracking, diethyl ether hydrolysis dehydration of ethanol to ethylene and diethyl ether occurred at temperature range 453 K– 573 K. Zeolite was active more than alumina and silica-alumina. At high temperature, ethylene was produced by ethanol dehydration (one step) and ethanol to diethyl ether as intermediate followed by diethyl ether cracking to ethylene (two step). The generating of ethylene and diethyl was found these products involved ethoxy group.

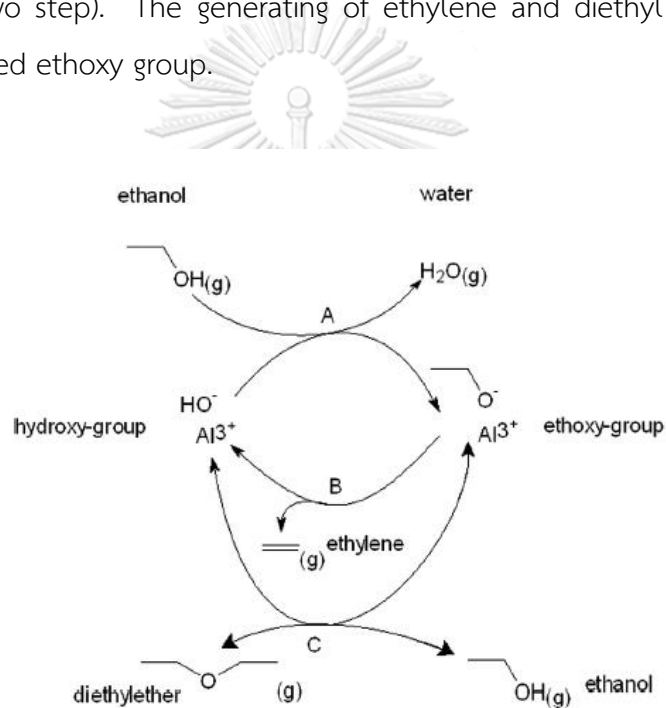


Figure 7 Schematics of the catalytic cycles.

In 2015, Bagal L.K.³⁴ investigated effect of noble metal such as palladium (Pd) and cerium (Ce) on the enhancement of ethanol vapor response modified SnO_2 thick films. Even small loading of Pd could reduce operating temperature with rapid response time, better selectivity and at lower concentration of target gas. The result was summarized that the dissociative adsorption of O_2 on Pd particles with following spill-over onto the Ce-doped SnO_2 surface becomes an important step in the process of detection of ethanol on the surface of Pd loaded Ce-doped SnO_2 .

In 2016, Chen B. et al.³⁵ reported effect of iron modified HZSM-5 with ratio of Si/Al 25 to 300 by ion-exchange in ethanol dehydration to ethylene and effect of adjusting liquid hourly space velocity. The results showed Fe-ZSM-5 that had ratio Si/Al equal 25 gave the best catalytic performance at 260 °C and 0.81 h⁻¹ LHSV. More than 97 % yield of ethylene was obtained at these condition. Increasing LHSV influenced to decreasing of conversion and selectivity of ethylene. While selectivity of diethyl ether increased due to the contact time was shortened

In 2017,⁵ studied the catalytic of ethanol dehydration to diethyl ether over noble metal, namely ruthenium (Ru) and platinum (Pt) modified H-beta zeolite catalyst at operating temperature 200 °C – 250 °C. Both of Ru and Pt enhanced yield of diethyl ether because increasing of ethanol conversion at low temperature without changing of diethyl ether selectivity. The Ru-HBZ gave the highest diethyl ether yield about 47 % at temperature 250 °C.

In 2018, de Oliveira T.K.R. et al.³⁶ experimented about turning ethanol to diethyl ether over copper (Cu) and iron (Fe) modified ZSM-5 at low temperature. Effect of Fe did not effect on acidity of ZSM-5 but decreased in crystalizes of ZSM-5. The presence of Cu changed strong acid site to weak and moderate acid site. Ethanol dehydration to diethyl ether favored low temperature and weak to medium acid site of catalysts.

From all of literature review, these have many of catalysts which used in ethanol dehydration are interesting. Each promoter has different function to enhance system. For phosphorus, It is found to be very useful for ethanol dehydration but it is a small amount of research that indicates that phosphorus is used with the noble metal as catalyst or promoter. Therefore, Investigation about effect of phosphorus with palladium in ethanol dehydration is interesting.

CHAPTER 3

EXPERIMENT

This chapter explains detail in experiment that consist of synthesis ZSM-5 catalyst by hydrothermal process, modification catalyst with acid and noble metal , procedure in testing ethanol dehydration reaction and catalyst characterization example X-ray diffraction (XRD), Ammonia temperature programmed desorption (NH₃-TPD), Scanning electron microscope (SEM) and Energy dispersive X-ray spectroscopy (EDX) N₂ physisorption (BET), X-ray fluorescence (XRF) and X-ray photoelectron spectroscopy (XPS).

3.1 Catalyst preparation

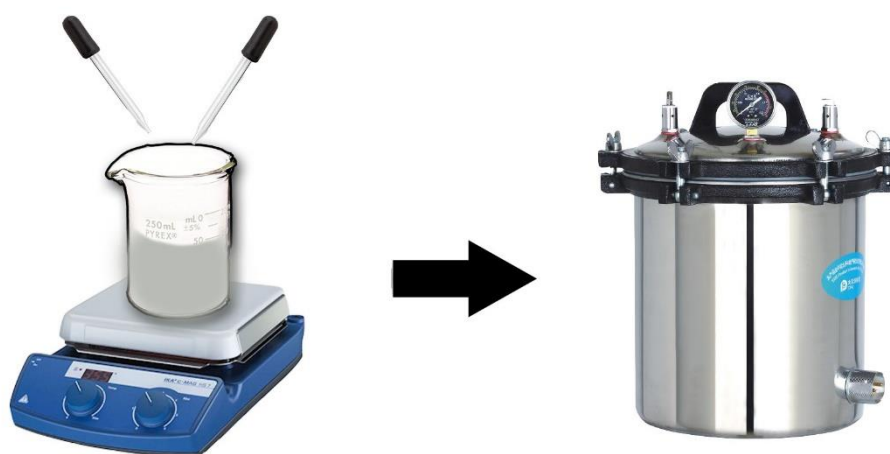
3.1.1 Synthesis of ZSM-5

ZSM-5 catalyst was synthesized by hydrothermal using Tetrapropylammonium bromide, sodium silicate, aluminium nitrate nonahydrate and hydrochloric acid as reported in Table 3. The molar ratio of silicon to aluminum is depend on amount of sodium silicate solution which added in mixture solution.

First, Tetrapropylammonium bromide was dissolved in de-ionized water and mixed with sodium silicate and aluminium nitrate that was dissolved in de-ionized water. 1 M HCl was added to the mixture solution for adjusting the final pH = 10.5. The mixture solution of aluminium, silicon and tetrapropylammonium bromide was stirred until it was a homogenous solution on the hot plate stirrer. The homogenous solution was brought into stainless-steel autoclave for synthesis at 210 °C for 24 h. After synthesis completed, the solution was centrifuged at 2000 rpm with de-ionized water for 20 minutes at 5 cycles in order to adjust pH to 7. Then, the precipitate was dried at 110 °C overnight in oven. Finally, the dried solid catalysts were calcined in air at 550 °C for 4.5 h.

Table 3 The chemical used in synthesis ZSM-5 catalyst

Chemical	Formula	Supplier
98% Tetrapropylammonium bromide	$C_{16}H_{36}BrN$	Aldrich
Sodium silicate solution	$Na_{2x}SiO_{2+x}$	Merck
Aluminium nitrate nonahydrate	$Al(NO_3)_3 \cdot 9H_2O$	Aldrich
37% hydrochloric acid	HCl	Qręc

**Figure 8** Diagram of ZSM-5 catalysts preparation by hydrothermal method.

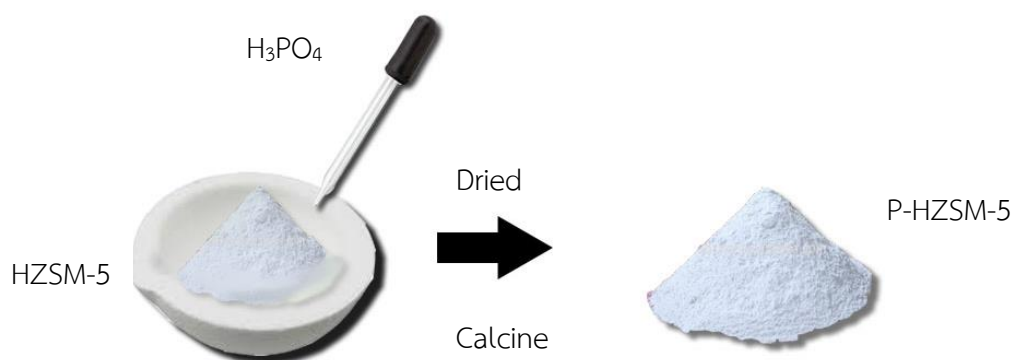
CHULALONGKORN UNIVERSITY

3.1.2 Synthesis of phosphoric acid modified HZSM-5

The 5 wt% P-HZSM-5 catalysts were prepared by incipient wetness impregnation technique. Phosphoric acid (H_3PO_4) as reported in Table 4 was used as precursor and dissolved with distilled water. The amount of desired solution was same the total pore volume of HZSM-5 catalyst. After impregnation, the catalyst was placed at room temperature for 2 hours to ensure a thorough distribution. Next, drying at 110 °C for one day with air and subsequent calcination at 550 °C for 4.5 h.

Table 4 The chemical used in synthesis P-HZSM-5 catalyst

Chemical	Formula	Supplier
85% Phosphoric acid	H_3PO_4	Merck

**Figure 9** Diagram of P-HZSM-5 catalysts preparation by incipient wetness impregnation method.

3.1.3 Synthesis of noble metal modified HZSM-5 by incipient wetness impregnation

The Pd-HZSM-5 catalysts were prepared by incipient wetness impregnation technique. 10 % Tetraamminepalladium(II)nitrate in water as reported in Table 5 was used as precursor and dissolved with distil water. The amount of desired solution was same the total pore volume of HZSM-5 catalyst. After impregnation, the catalyst was placed at room temperature for 2 hours to ensure a thorough distribution. Next, drying at 110 °C for one day with air and subsequent calcination at 550 °C for 4.5 h.

Table 5 The chemical used in synthesis Pd-HZSM-5catalyst

Chemical	Formula	Supplier
10% Tetraamminepalladium(II)nitrate	$Pd(NO_3)_2 \cdot 4(NH_3)$	Aldrich

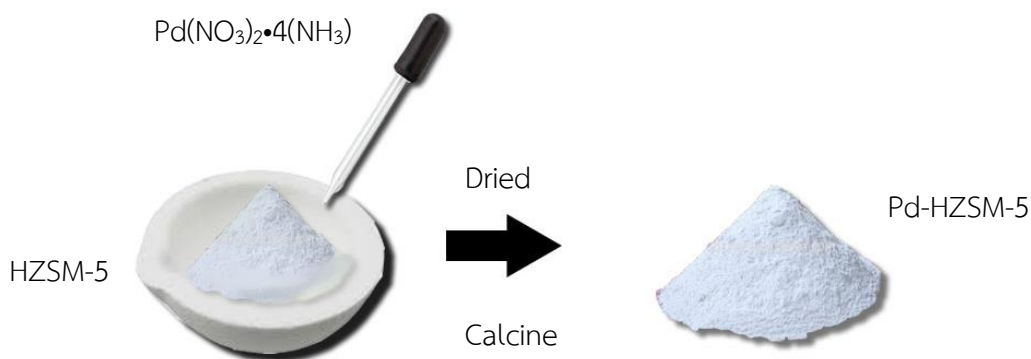


Figure 10 Diagram of Pd-HZSM-5 catalysts preparation by incipient wetness impregnation method.

3.1.4 Synthesis of noble metal modified P-HZSM-5 by incipient wetness impregnation

Pd metal from 10% Tetraamminepalladium(II)nitrate was loaded into P-HZSM-5 catalyst by incipient wetness impregnation technique. A noble metal precursor was dissolved with distill water and added into P-HZSM-5 catalyst. The amount of desired solution was same the total pore volume of HZSM-5 catalyst. After impregnation, the catalyst was placed at room temperature for 2 hours to ensure a thorough distribution. Next, drying at 110 °C for one day with air and subsequent calcination at 550 °C for 4.5 h.

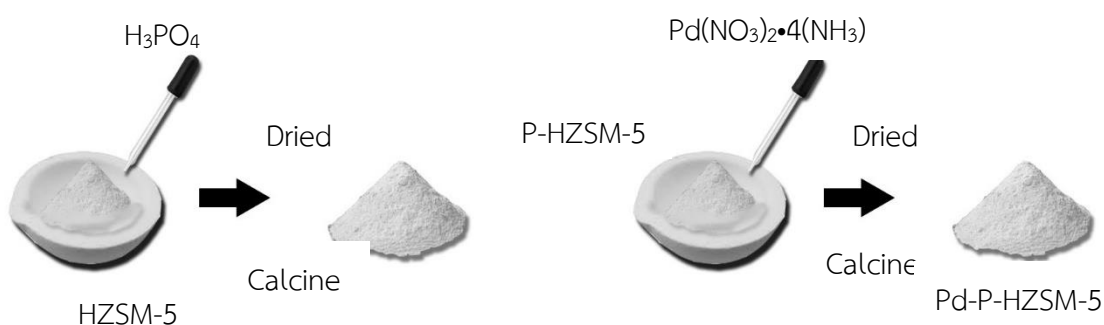


Figure 11 Diagram of Pd-P-HZSM-5 catalysts preparation by incipient wetness impregnation method.

3.1.5 Synthesis of noble metal and phosphoric acid modified HZSM-5 by incipient wetness co-impregnation

The Pd-P-HZSM-5 catalysts were prepared by incipient wetness co-impregnation technique. Distil water was added in (Precursor of Pd) that mixed with phosphorus acid until volume of mixture solution was equal total pore volume of HZSM-5. After impregnation, the catalyst was placed at room temperature for 2 hours to ensure a thorough distribution. Next, drying at 110 °C for one day with air and subsequent calcination at 550 °C for 4.5 h.

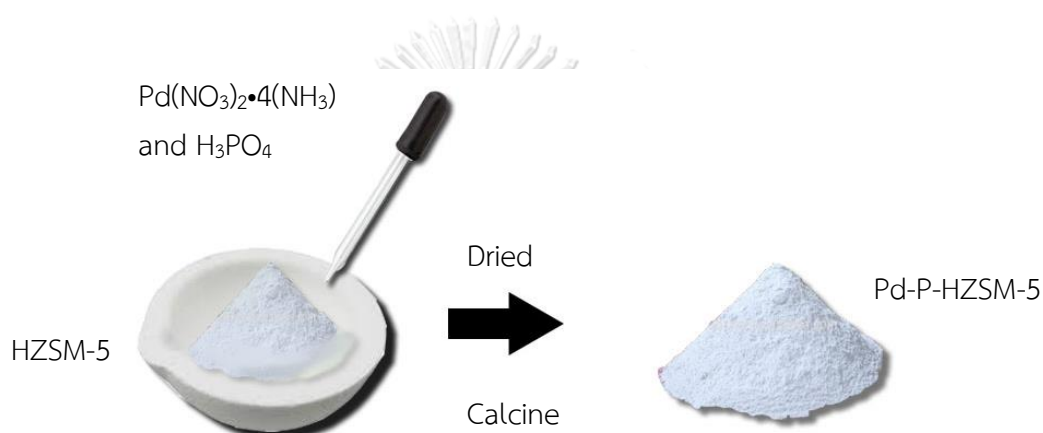


Figure 12 Diagram of Pd-HZSM-5 catalysts preparation by incipient wetness co-impregnation method.

3.1.5 Synthesis of HZSM-5

ZSM-5 catalyst was modified by ion exchange method using ammonium nitrate (NH_4NO_3) as reported in Table 6. The sodium form (Na^+) of ZSM-5 was exchange with NH_4^+ of ammonium nitrate solution and generated new form into HZSM-5 catalyst¹⁹⁻²⁰.

First, ZSM-5 catalyst from synthesis by hydrothermal method was dissolved in 1 M of ammonium nitrate solution. Then, the mixture solution was stirred on the hot plate stirrer at room temperature for 2 hours after that the mixture solution was filtered by vacuum pump. These methods were repeated more than 3 rounds. After repetition completed, the precipitate was dried at 110 °C overnight in oven. Finally, the dried solid catalysts were calcined in air at 550 °C for 4.5 h.

Table 6 The chemical used in synthesis HZSM-5 catalyst

Chemical	Formula	Supplier
Ammonium nitrate	NH_4NO_3	Ajax Finechem

3.2 Catalyst characterization

3.2.1 X-ray diffraction (XRD)

Synthesized ZSM-5 in part I and modified H-ZSM-5 in part II were characterized by SIEMENS D-5000 X-ray diffractometer with $\text{Cu K}\alpha$ ($\lambda = 1.54439 \text{ \AA}$) for analyzing bulk crystalline phase and crystalline size. The patterns of synthesized ZSM-5 and Modified H-ZSM-5 were recorded over the 2θ between 5° and 60° and between 5° and 80° respectively.

3.2.2 Atomic absorption spectroscopy (AAS)

Silicon and aluminium in ZSM-5 catalysts were detected Atomic absorption spectroscopy (AAS) instrument for analyzing amount of element distribution in catalysts

3.2.3 Ammonia temperature-programmed desorption (NH₃-TPD)

Acidity of synthesized ZSM-5 and Modified H-ZSM-5 were measured by using Micromeritics chemisorp 2750 pulse chemisorption system. In the measurement, 0.1 g of catalysts were packed in a U-tube glass with 0.03 g of quartz wool and pretreated at 500 °C under helium flow for 1 h. Then, the catalysts were saturated with 15% of NH₃/He and the physisorbed ammonia was desorbed under helium gas flow after saturation. The catalyst was heated from 40 °C to 800 °C at heating rate of 10 °C /min to desorb the chemisorbed NH₃.

3.2.4 Scanning electron microscope (SEM) and Energy dispersive X-ray spectroscopy (EDX)

Morphologies of catalysts were investigated by using a JEOL JSM-5800LV model Scanning electron microscope and elemental distribution of catalysts were examined by using Link Isis series 300 program energy dispersive X-ray spectroscopy.

3.2.5 N₂ physisorption (BET&BJH)

Surface area, pore volume, pore diameter, isotherm graph and pore size distribution of catalysts were detected by adsorptiometer (Micromeritics ASAP 2010) and using BET&BJH method to analyzing

3.2.6 X-ray fluorescence (XRF)

XRF is a technique that used to determine the elemental composition of materials. XRF analyzers determine the sample by measuring the fluorescent X-ray emitted from a sample when it is excited by a primary X-ray source. This release of energy is then registered by the detector in then XRF instrument, which in turn categorizes the energies by element. The amounts of metal in each catalyst were measured by using Panaanalytical MINIPAL 4 instrument.

3.2.7 Thermal gravimetric and differential analysis (TG/DTA)

Commercial HZSM-5 and synthesized HZSM-5 catalysts were characterized by thermal gravimetric and differential analysis using TA instruments SDTQ 600 analyzer at temperature range 30 °C – 600 °C for detected weight loss and amount of coke.

3.3 Catalytic Ethanol dehydration reaction

The catalytic dehydration of ethanol was carried out in a fixed-bed continuous flow microreactor made from a borosilicate glass with an inside diameter of 0.7 cm and length of 33 cm. The chemicals used in Ethanol dehydration reaction are reported in Table 7. The catalyst (0.05 g) was packed with quartz wool into the middle of microreactor. The impurity was eliminated from surface of catalyst prior to reaction by pretreating with nitrogen with 60 ml/min at 200 °C for 1 h. Then, ethanol was vaporized and fed with controlled by a single syringe pump at total flow rate of 1.45 ml/h (WHSV = 22.9 h⁻¹). Finally, all products were collected and analyzed at operation temperatures 200 °C, 250 °C, 300 °C, 350 °C and 400 °C by a GC-FID equipped with a DB-5 capillary column, which had operating condition as reported in Table 8

Table 7 The chemical used in ethanol dehydration reaction

Chemical	Formula	Supplier
99 wt % Ethanol	C ₂ H ₅ OH	Merch
UHP Nitrogen gas 99.99 %	N ₂	Linde

Table 8 The operating conditions in gas chromatograph

Gas Chromatograph	Shimadzu GC 14-A
Detector	FID
Capillary column	DB-5
Carrier gas	Nitrogen gas Hydrogen gas
Column temperature	Initial 40 °C Final 40 °C
Injector temperature	150 °C
Detector temperature	150 °C
Time analysis	6 min.

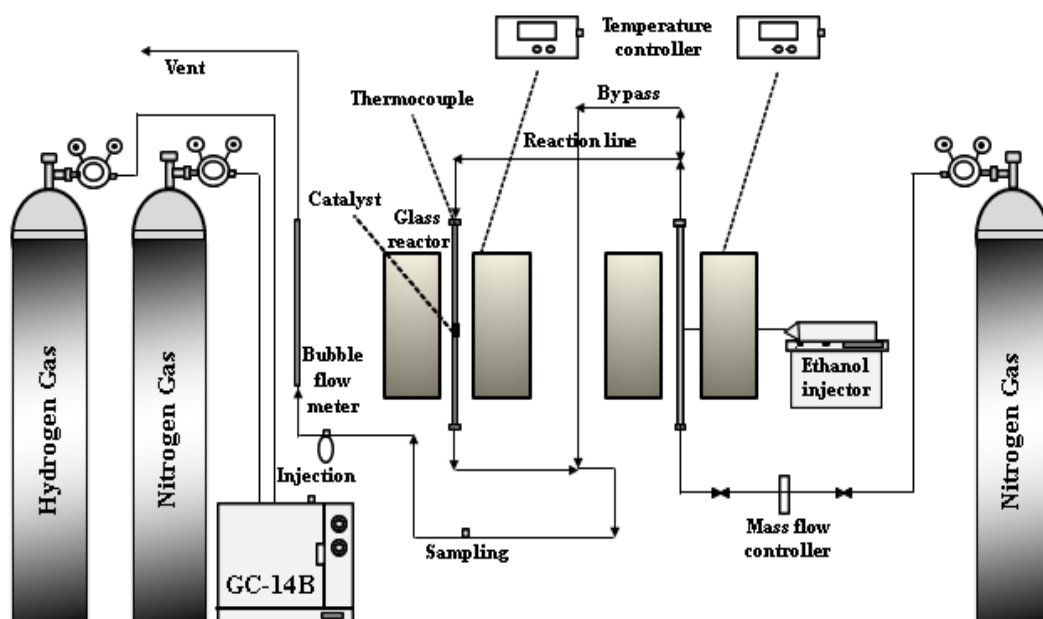


Figure 13 Schematic of the gas phase ethanol dehydration reaction

CHAPTER 4

RESULTS AND DISCUSSION

Chapter 4 discusses about catalytic activity and characterization of synthesized ZSM-5 catalysts, modified HZSM-5 catalysts with acid and noble metal and synthesized HZSM-5 catalyst in ethanol dehydration. The results and discussion are divided into three parts. For the first part ZSM-5, which was synthesized from hydrothermal process with different silicon to aluminium molar ratios (20, 40 and 60) were characterized with XRD, SEM-EDX, N₂ physisorption and NH₃-TPD techniques. The second part is investigation effect of modification catalyst with noble metal (palladium) and acid (Phosphoric acid). HZSM-5 catalyst from commercial that had ratio similar to the synthesized ZSM-5 catalyst which gave the best catalytic activity in the first part was modified by the incipient wetness impregnation method with palladium of loading 0.5 wt% and phosphoric acid with loading of 5 wt% and was analyzed with XRD, XRF, SEM-EDX, N₂-physisorption and NH₃-TPD techniques. Finally, the last part is comparing catalytic activity of ZSM-5 catalysts in the first part, which was modified by ion-exchange method to HZSM-5 catalyst and commercial HZSM-5 catalysts. Both catalysts were characterized by XRD, XRF, SEM-EDX, N₂-physisorption, NH₃-TPD and TG/DTA techniques. The catalytic activity of three parts were tested in fixed-bed tubular reactor which has nitrogen gas as carrier gas and vapor of ethanol pass through. After reaction complete, the product gas was analyzed with GC type FID.

Part 1: Investigation of the most suitable molar ratio of silicon to aluminium in ZSM-5 catalyst in ethanol dehydration reaction.

4.1 Characterization of synthesized ZSM-5

ZSM-5 catalysts are synthesized via hydrothermal process in stainless steel at 210 °C for 24 hr. and calcined at 550 °C. The physical properties of catalysts are investigated by X-ray diffraction (XRD), scanning electron microscope (SEM) and energy dispersive X-ray spectroscopy (EDX), N₂ physisorption (BET&BJH) and ammonia temperature-programmed desorption (NH₃-TPD)

4.1.1 X-ray diffraction (XRD)

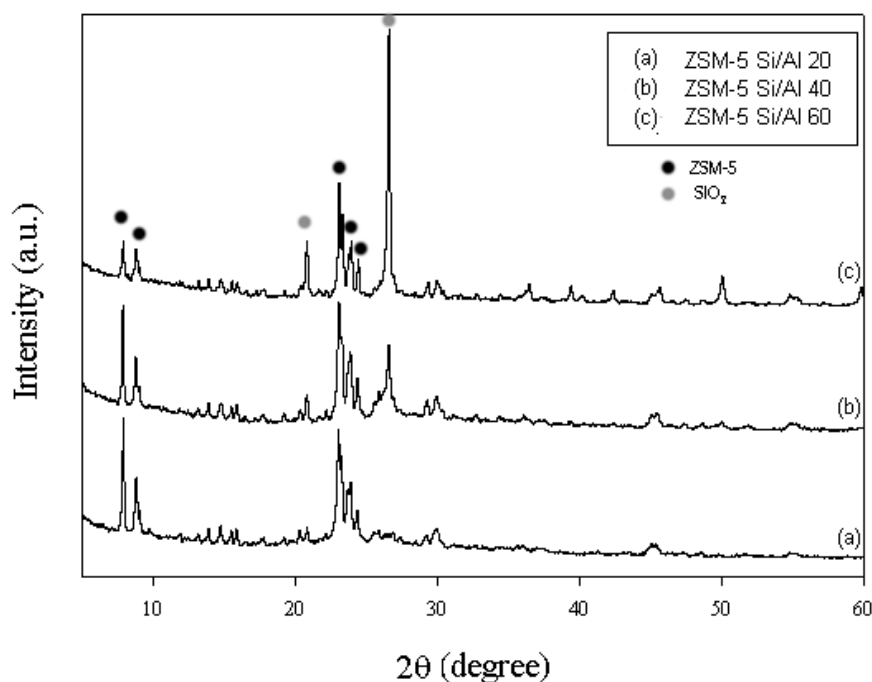


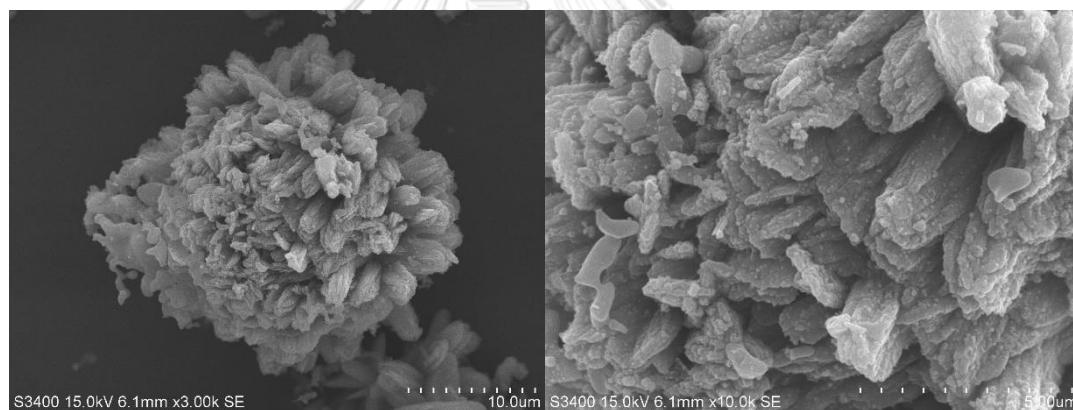
Figure 14 XRD patterns of ZSM-5 with different molar ratios of Si/Al

The XRD patterns of synthesized ZSM-5 catalysts with different molar ratios of Si/Al at 20,40 and 60 are reported in Figure 14 .The measurement was carried out at diffraction angle 5° to 60°. It can be observed that all catalysts exhibited the characteristic sharp peaks of ZSM-5 presenting at $2\theta = 7.8^\circ, 8.7^\circ, 22.94^\circ, 23.6^\circ$ and

24.26°³⁷ and the other peaks that presented ($2\theta = 21^\circ$ and 27°) are characteristic peaks of SiO_2 ³⁸. Therefore, the intensity of the characteristic peaks at $2\theta = 21^\circ$ and 27° are high as the proportion increased of silicon to aluminium due to the excessive amount of silicon precursors that can be confirmed the intensity of the characteristic peaks at $2\theta = 7.8^\circ$ and 8.7° decreased, too.

4.1.2 Scanning electron microscope (SEM) and energy dispersive X-ray spectroscopy (EDX)

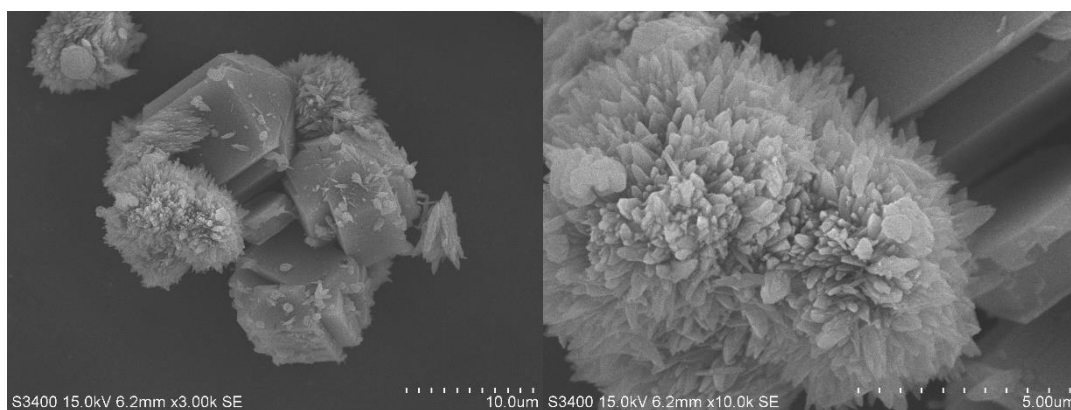
Analysing of morphology and element distribution of synthesized ZSM-5 catalysts are investigated by scanning electron microscope (SEM) and energy dispersive X-ray spectroscopy (EDX), respectively. The morphology of synthesized ZSM-5 catalysts with different silicon to aluminium molar ratios are shown in Figure 15. Effect of Si/Al



(a).



(b).



(c).

Figure 15 SEM image of synthesized ZSM-5 catalysts with molar ratio of Si/Al 20 (a), 40 (b) and 60 (c), respectively.

molar ratio could be observed from SEM image of the synthesized ZSM-5 catalyst. The molar ratio of Si/Al at 20 had worm-like or flake-like morphology. On the other hand, the cubic crystals morphology will appear when increased molar ratio to 40 and 60 by increased amount of silicon source. The size of cubic crystals increases when the ratio of Si/Al increased over 40⁸.

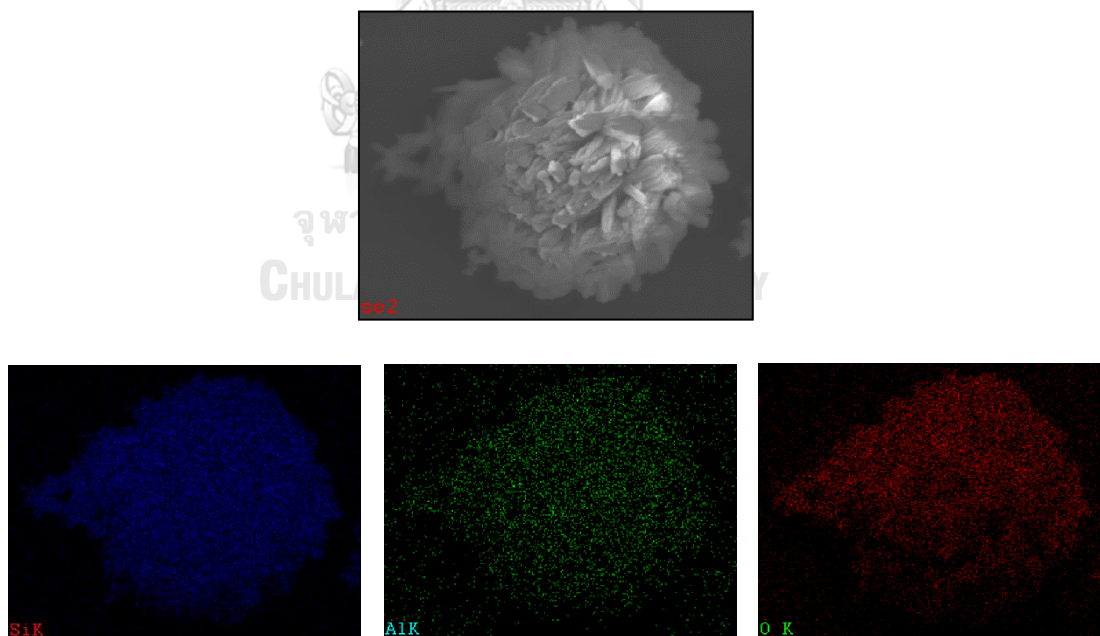


Figure 16 SEM-EDX mapping of synthesized ZSM-5 Si/Al 20

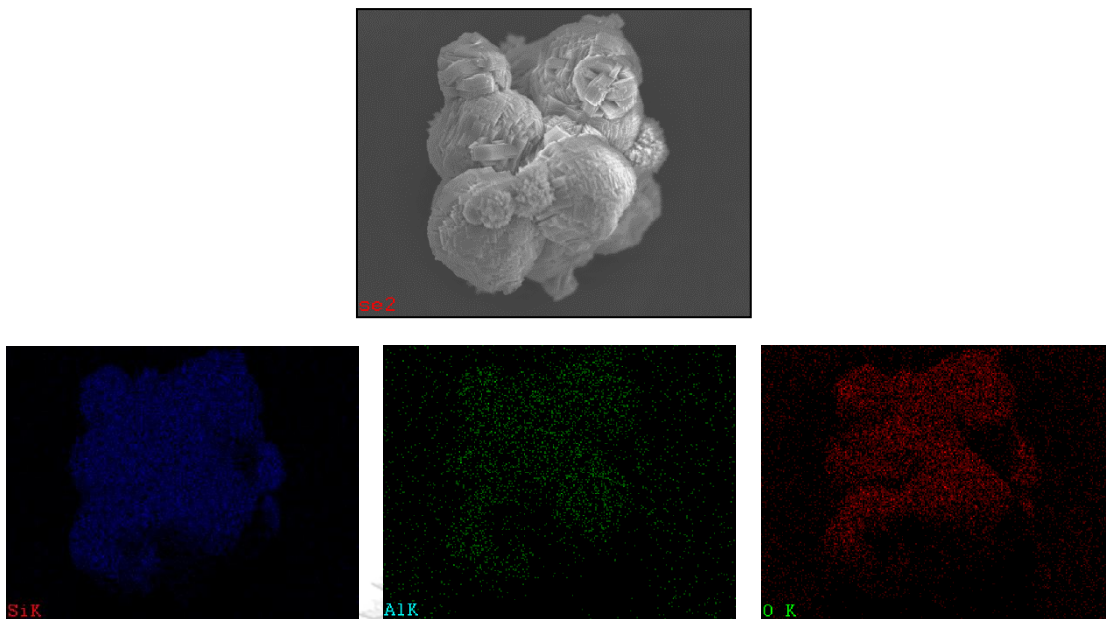


Figure 17 SEM-EDX mapping of synthesized ZSM-5 Si/Al 40

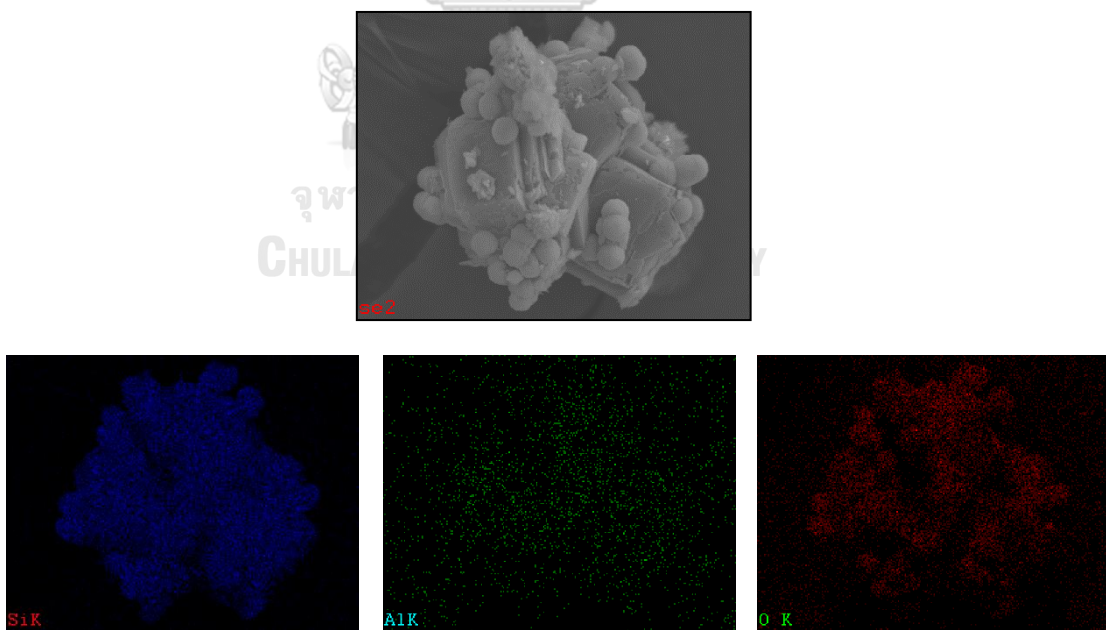


Figure 18 SEM-EDX mapping of synthesized ZSM-5 Si/Al 60

The SEM-EDX mappings in Figures 16 to 18 are shown element distribution of metal silicon, aluminium and oxygen (Si, Al and O) on all three molar ratios of synthesized ZSM-5 catalysts. It can be concluded that all metals (Si, Al and O) have well dispersion on surface catalysts. The amounts of elements distribution are shown in Tables 9 and 10 in weight percent and atomic percent, respectively. The proportion of silicon to aluminium in weight percent and atomic percent increased when the ratio of silicon to aluminium increased.

Table 9 Element distribution of synthesized ZSM-5 (weight percent)

Catalysts	Element distribution (wt%)			Si/Al (wt%/wt%)
	Si	Al	O	
ZSM-5 Si/Al 20	50.82	3.28	45.89	15.49
ZSM-5 Si/Al 40	51.28	1.8	46.92	28.49
ZSM-5 Si/Al 60	54.77	1.24	43.99	44.17

Table 10 Element distribution of synthesized ZSM-5 (atomic percent)

Catalysts	Element distribution (at%)			Si/Al (at%/at%)
	Si	Al	O	
ZSM-5 Si/Al 20	37.70	2.54	59.76	14.84
ZSM-5 Si/Al 40	37.84	1.38	60.78	27.42
ZSM-5 Si/Al 60	41.09	0.97	57.94	42.36

4.1.3 Atomic absorption spectroscopy (AAS)

Amount of silicon and aluminum in ZSM-5 catalysts with different molar ratio of silicon to aluminium were dissolved in solution and analyzed amount of element by desorption spectrum of individual substance in bulk catalysts after absorption with light source. The amount of Si and Al of ZSM-5 catalysts with different ratio are shown in Table 11

Table 11 Element distribution of synthesized ZSM-5 from AAS

Catalysts	Element		Element		Si/Al (wt%/wt%)
	distribution (at%)		distribution (wt%)		
	Si	Al	Si	Al	
ZSM-5 Si/Al 20	37.2	2.3	50.3	3.0	16.77
ZSM-5 Si/Al 40	38.8	1.3	52.2	1.7	30.71
ZSM-5 Si/Al 60	39.3	0.9	52.9	1.2	44.08

Table 12 Molar ratio of Si/Al between SEM-EDX and AAS techniques

Catalysts	SEM-EDX	AAS
	(Surface catalyst)	(Bulk catalyst)
	Si/Al (mol/mol)	Si/Al (mol/mol)
ZSM-5 Si/Al 20	14.94	16.17
ZSM-5 Si/Al 40	27.47	29.61
ZSM-5 Si/Al 60	42.59	42.51

Table 12 shows actual molar ratio of Si/Al from SEM-EDX and AAS techniques. Although the molar ratio from SEM-EDX was investigated on surface catalyst but these results were similar to molar ratio of Si/Al, which was investigated in bulk catalyst. This is due to the particle size of catalysts were small about (10-20 μm) and SEM-EDX techniques could detect depth up to 5 micrometer from surface of catalyst.

4.1.5 Ammonia temperature-programmed desorption (NH_3 -TPD)

Ammonia gas is adsorbed on surface catalysts, would desorb via physisorption (carrier gas), chemisorption (bond breaking during temperature ramping). The ammonia was detected by detector and plotted in TCD signal (a.u.) versus temperature or time.

The acidities of ZSM-5 catalysts with different Si/Al molar ratios are determined by NH_3 -TPD as shown in Figure 20. The typical acid site distributions of these graphs are weak acid site (below 250 $^\circ\text{C}$), medium acid site (250 $^\circ\text{C}$ – 400 $^\circ\text{C}$) and strong acid site (above 400 $^\circ\text{C}$) from NH_3 -TPD in all of ZSM-5 ratios. Moreover, the intensity of TCD

signal decreases when the ratio of ZSM-5 increases. It can be said that the acidity decreases as the ratio of silica to aluminum increases due to the amount of sodium silicate solution with high pH was added to adjust ratio of silicon to aluminium and makes total acidity drops. Amount of total acidity is shown in Table 14. This table shows that the total acid sites of ZSM-5 decreases with increasing Si/Al molar ratio.

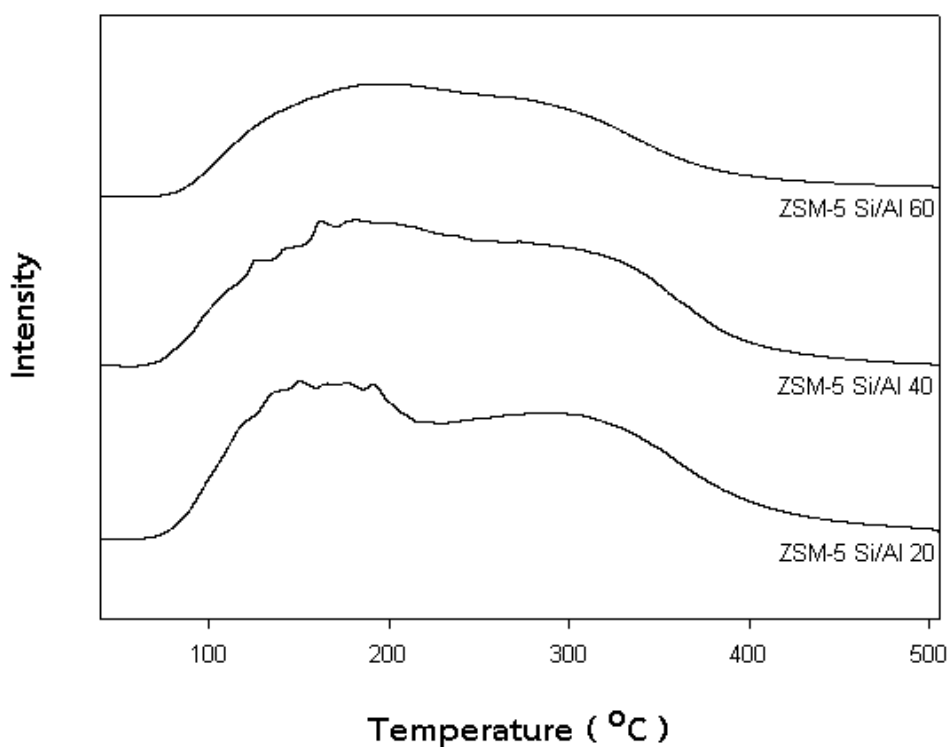


Figure 19 NH₃-TPD profiles of synthesized ZSM-5 with different molar ratios of Si/Al

Table 13 Total acidity from NH₃-TPD.

Catalyst	NH ₃ desorption (μmol NH ₃ /g _{cat})		Total acidity (μmol NH ₃ /g _{cat})
	Weak	Medium to strong	
ZSM-5 Si/Al 20	500	956	1456
ZSM-5 Si/Al 40	493	717	1210
ZSM-5 Si/Al 60	240	695	935

4.1.4 N₂ physisorption (BET&BJH)

Surface area, pore size, pore volume, and isotherm graph of synthesized ZSM-5 catalysts were investigated by N₂ physisorption technique. The results from N₂ physisorption are reported in Table 13. The BET surface area and total pore volume of all catalysts decreased with increasing Si/Al ratio. The pore size can indicate that all catalysts are in mesoporous range. In addition, Isotherm graph from adsorption-desorption of nitrogen gas of all synthesized ZSM-5 catalysts are displayed in Figure 19 that show similar type of isotherm (isotherm type 4) and appear hysteresis loop in all catalysts. The hysteresis loop is an obvious evidence that the three catalysts were mesoporous structure. Moreover, increasing molar ratio of silicon to aluminium can increase amount of nitrogen adsorption capacity that mean synthesized ZSM-5 with Si/Al 60 had highest pore volume.

Table 14 BET surface area, pore size and pore volume of synthesized ZSM-5 catalysts

Catalysts	Surface area ^a	Pore volume ^b	Pore size ^c
	(m ² /g)	(cm ³ /g)	(Å)
ZSM-5 Si/Al 20	207	0.0146	26.6
ZSM-5 Si/Al 40	172	0.0255	69.4
ZSM-5 Si/Al 60	177	0.0305	36.2

^a Determined from BET method

^{b,c} Determined from BJH desorption method

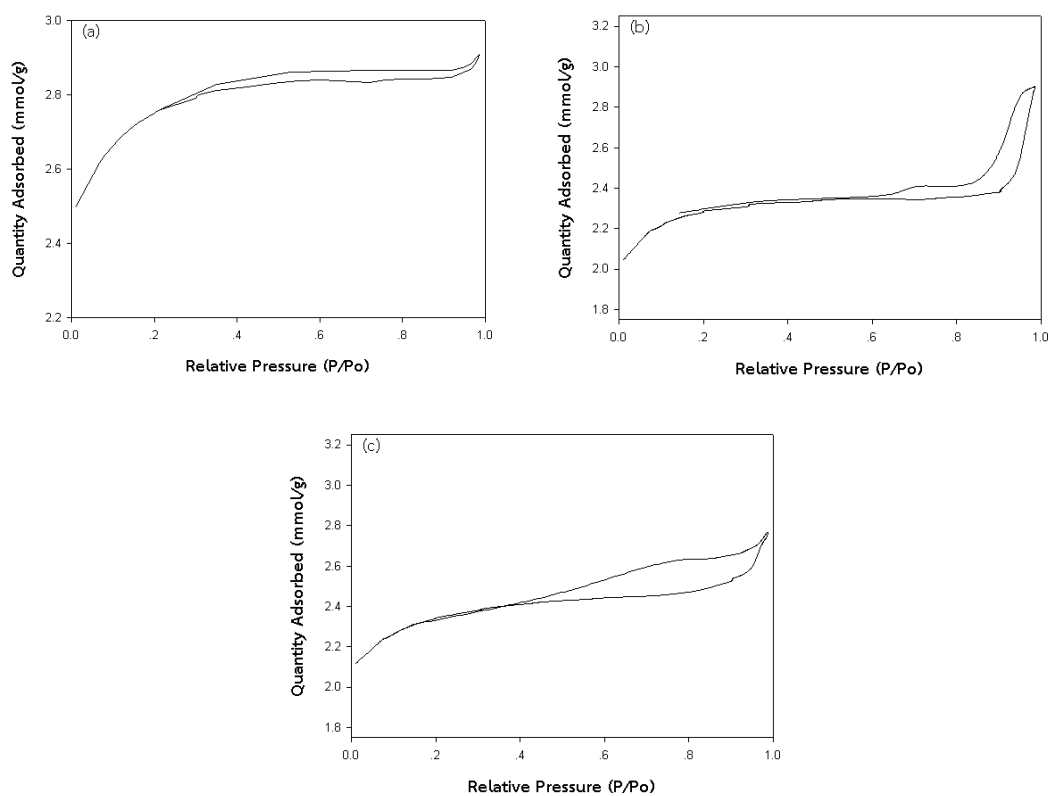


Figure 20 Isotherm graph of synthesized ZSM-5 catalysts; (a). ZSM-5 Si/Al at 20
(b). ZSM-5 Si/Al at 40 and (c). ZSM-5 Si/Al at 60

4.1.6 Ethanol dehydration reaction

The catalytic ethanol dehydration to diethyl ether, acetaldehyde and ethylene over ZSM-5 catalysts having different Si/Al molar ratios was tested in fixed-bed continuous flow microreactor at temperature of 200 °C to 400 °C and atmospheric pressure. The conversion and selectivity of ZSM-5 zeolite catalysts are reported in Table 15. It shows that the ethanol conversion increases with increased reaction temperature for all catalysts. The ZSM-5 Si/Al 20 catalyst exhibited the highest activity. It can be observed that at 400 °C the conversions 70.3, 38.2, and 3.5% are obtained for catalysts having the Si/Al molar ratios of 20, 40 and 60, respectively.

The selectivity to ethylene decreases with increasing Si/Al ratio. This is attributed to the decrease in the acidity and surface area. For diethyl ether selectivity, it was found that the selectivity of diethyl ether is high at low temperatures and decreased when temperature is increased because of the ethanol dehydration to diethyl ether favours exothermic reaction and undergoes diethyl ether cracking reaction and diethyl ether hydrolysis that turned into ethylene and ethanol at high temperature³³. This results in the observation of high ethylene selectivity at high temperature and has ethanol dehydrogenation as side reaction that changed ethanol to acetaldehyde when temperature is increased more than 200 °C.

Table 15 Conversion and product selectivity of synthesized ZSM-5 catalysts

Catalysts	Temperature (°C)	Ethanol	Product selectivity (%)		
		Converaion (%)	Ethylene	Diethyl ether	Acetaldehyde
ZSM-5 Si/Al 20	200	7.1	0.0	100.0	0.0
	250	12.8	4.9	94.4	0.8
	300	16.4	32.4	66.5	1.1
	350	43.1	80.0	18.4	1.6
	400	70.3	95.6	2.5	2.0
ZSM-5 Si/Al 40	200	2.8	0.0	100.0	0
	250	9.4	3.1	85.7	11.2
	300	12.0	11.0	84.5	4.5
	350	20.5	43.3	51.5	5.2
	400	38.2	83.6	12.7	3.8
ZSM-5 Si/Al 60	200	0.0	0.0	0.0	0.0
	250	0.0	0.0	0.0	0.0
	300	1.2	0.0	0.0	100.0
	350	2.1	4.2	0.6	95.3
	400	3.5	10.3	3.7	86.0

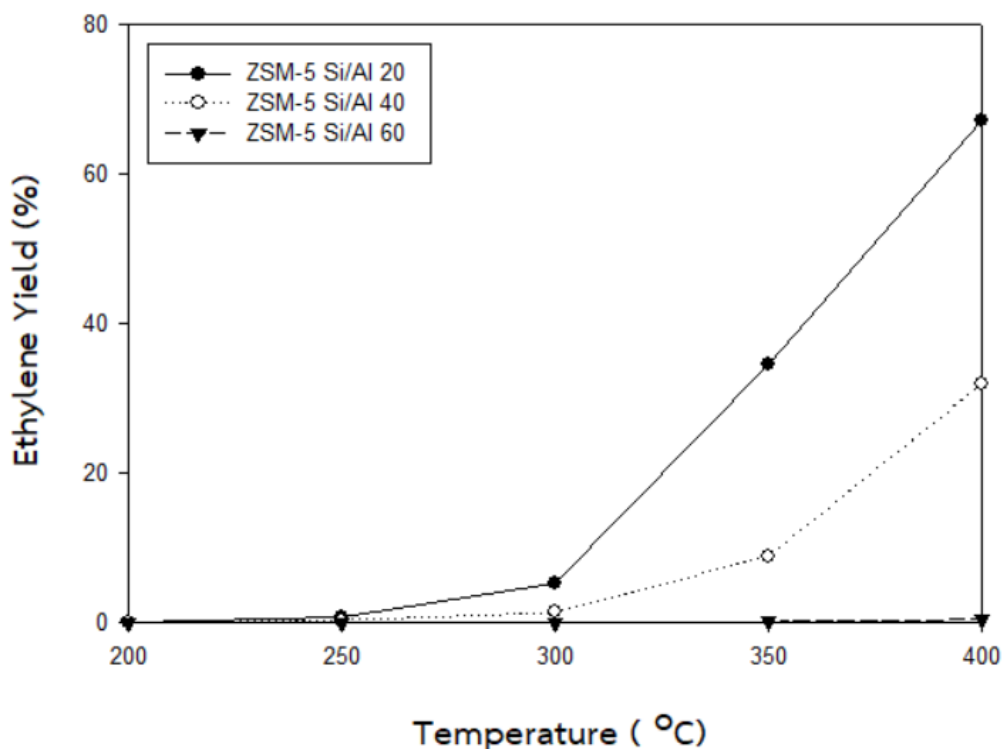


Figure 21 Ethylene yield in ethanol dehydration over synthesized ZSM-5 catalysts with different silicon to aluminium molar ratio.

Figure 21 shows the ethylene yield of synthesized ZSM-5 catalysts at temperature range of 200 °C – 400 °C. Yield of ethylene increased when temperature was increased due to ethylene favored endothermic reaction and diethyl ether cracking that changed diethyl ether as other product to ethylene at high temperature. Moreover, diethyl ether hydrolysis occurred and made the selectivity of diethyl ether drops. Therefore, both of ethylene selectivity and yield were increasing. At temperature of 400 °C was the highest ethylene yield and it increases if the temperature is higher. On the other hand, the diethyl ether yield that displays in Figure 22 has opposite trend when compared with ethylene yield. Synthesized ZSM-5 Si/Al 60 catalyst showed the lowest diethyl ether yield because ethanol dehydration reaction occurred only slightly. In case of ZSM-5 Si/Al 20 catalyst, it had optimum diethyl ether yield at temperature 250 °C about 12.1%, which is greater than optimum point in case of ZSM-5 Si/Al 40 catalyst (10.5% diethyl ether yield and 350 °C)

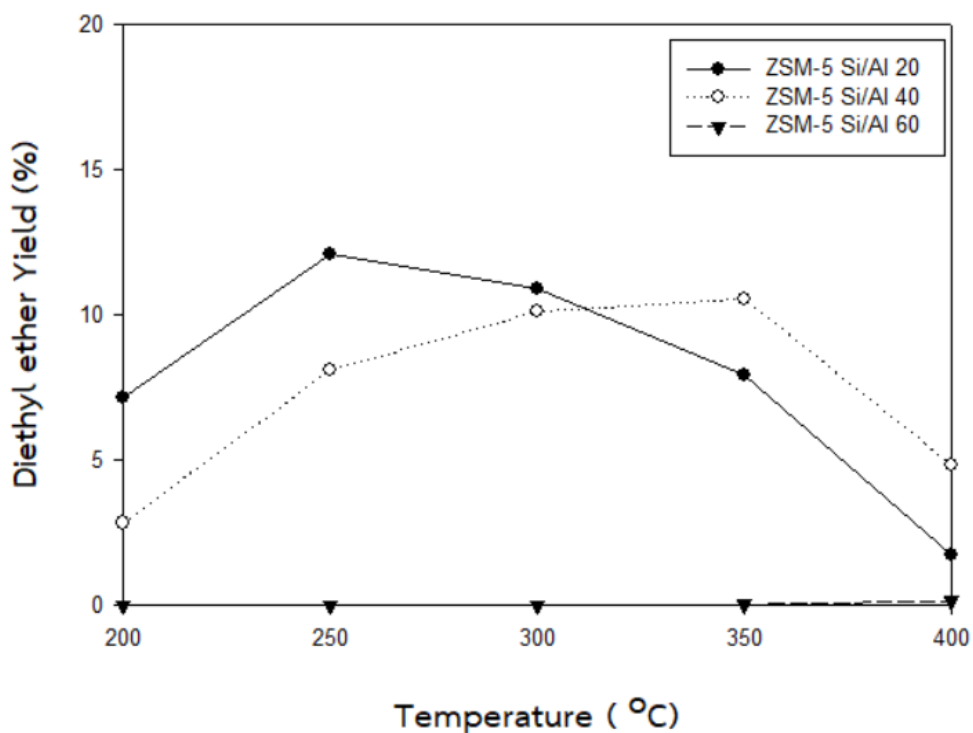


Figure 22 Diethyl ether yield in ethanol dehydration over synthesized ZSM-5 catalysts with different silicon to aluminium molar ratios.

From all results, it can be concluded that the ratio of Si/Al in ZSM-5 catalyst essentially affects the catalytic ethanol dehydration to diethyl ether and ethylene due to surface area, acidity and appearing of SiO_2 peak in XRD pattern. These factors were the important keys to obtain the highest activity in ethanol dehydration.

Part 2: Investigation on the effect of Pd and P, and effect of sequence in modification of catalyst with phosphoric acid and noble metal (Pd) on ethanol dehydration reaction.

4.2 Characterization of HZSM-5 and modified HZSM-5 with phosphoric acid and palladium

From part 4.1, ZSM-5 catalysts with Si/Al 20 catalyst gave the highest catalytic activity in ethanol dehydration reaction (70.3 % of ethanol conversion). Thus, HZSM-5 catalysts from commercial that had Si/Al ratio similar to ZSM-5 Si/Al 20 catalyst are tested and modified with phosphoric acid and palladium. These catalysts are characterized by various techniques in part 4.2. The properties of catalysts are investigated by X-ray diffraction (XRD), X-ray fluorescence (XRF), scanning electron microscope (SEM) and energy dispersive X-ray spectroscopy (EDX), N₂ physisorption (BET&BJH) and ammonia temperature-programmed desorption (NH₃-TPD)

4.2.1 X-ray diffraction (XRD)

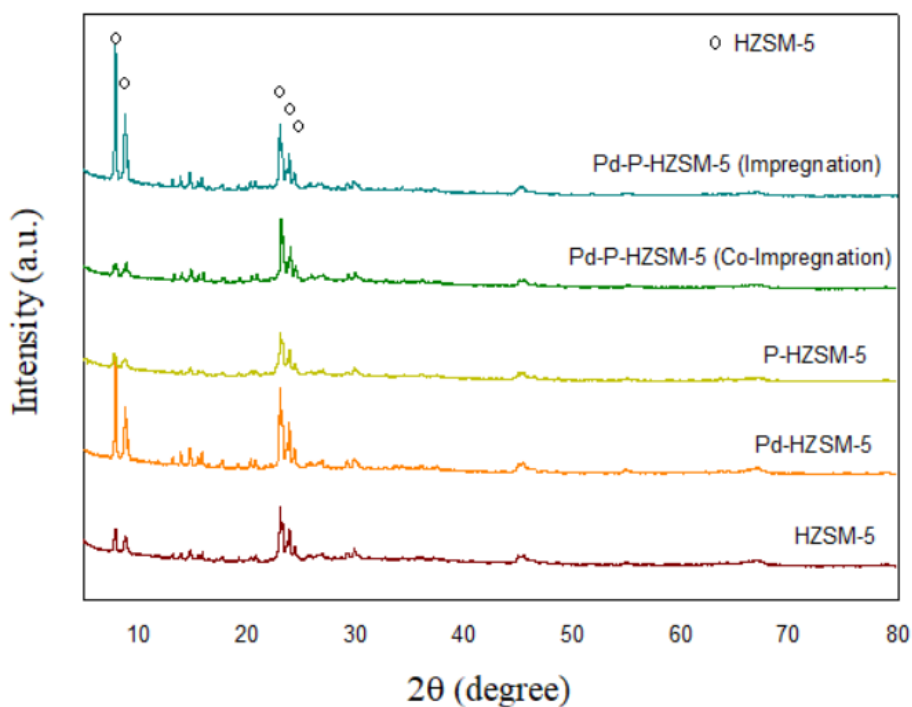


Figure 23 XRD patterns of HZSM-5 and modified HZSM-5 catalysts

The XRD patterns of HZSM-5 catalyst and modified HZSM-5 catalysts with phosphoric acid and Pd at diffraction angle (2θ) 5° from 80° are illustrated in Figure 23. The XRD patterns of HZSM-5 and modified HZSM-5 catalysts had sharp peak at $2\theta = 7.8^\circ, 8.7^\circ, 22.94^\circ, 23.6^\circ$ and 24.26° ³⁷, which is similar with those of synthesized ZSM-5 catalysts in part 4.1. Furthermore, adding phosphoric acid by incipient wetness impregnation technique made the intensity of XRD peak for HZSM-5 catalysts peak became weaker due to slight dealumination of tetrahedral framework aluminum (TFAL) in HZSM-5 catalysts^{13, 19, 21, 31}. However, improvement of HZSM-5 catalysts with palladium enhanced the intensity of HZSM-5 catalysts when compared with HZSM-5 catalysts. This is a result of improvement with palladium that can affect the crystallize structure of HZSM-5 catalysts. Although modification of phosphoric acid and palladium had effect on MFI structure of HZSM-5 catalysts, it did not have appearance of XRD pattern of phosphoric acid and palladium. Therefore, adding of phosphoric acid and palladium by incipient wetness impregnation technique had no effect on basic phase structure of catalysts³².

4.2.2 X-ray fluorescence (XRF)

Table 16 Element distribution from X-ray fluorescence (weight percent)

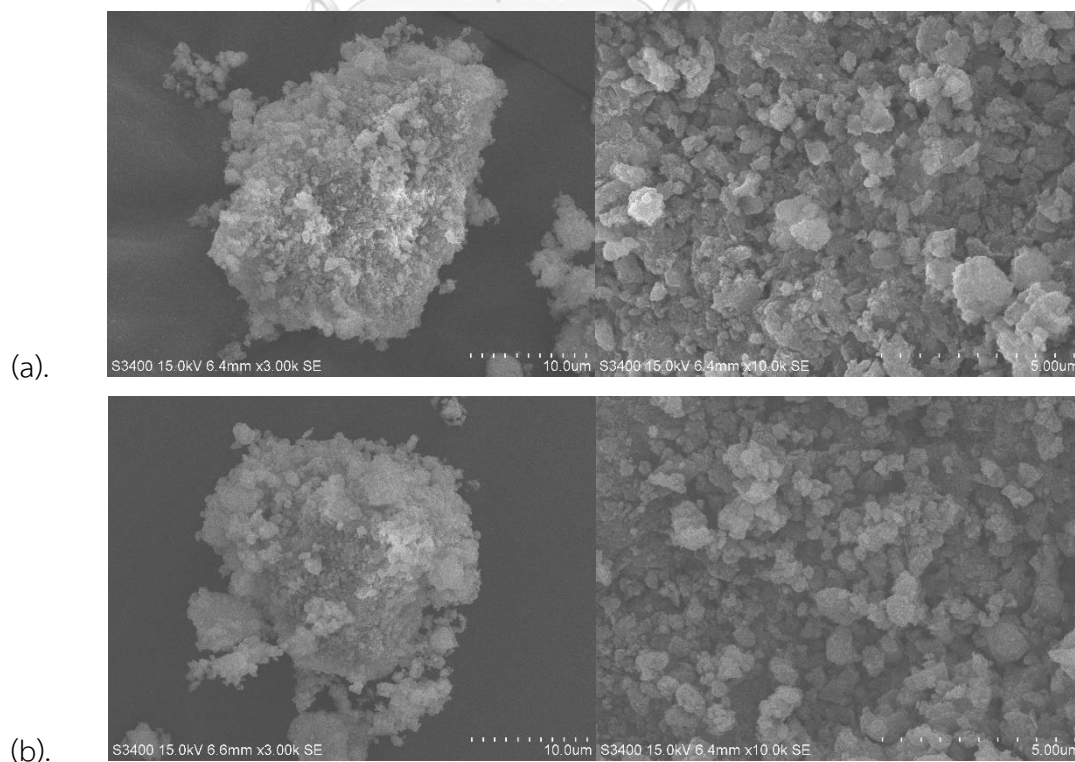
Catalysts	Element distribution (wt%)				Si/Al (mol/mol)	Metal/HZSM-5 ($\times 100$ %)
	Si	Al	Pd	P		
HZSM-5	64.21	35.30	-	-	1.75	-
P-HZSM-5	59.34	31.00	-	9.25	1.85	10.24
Pd-HZSM-5	62.87	34.63	2.14	-	1.75	2.20
Pd-P-HZSM-5	57.78	30.64	1.90	9.26	1.82	12.62
Pd-P-HZSM-5 (Co-impregnation)	57.27	30.58	1.77	9.97	1.81	11.36

The element distribution of each catalysts was investigated by X-ray fluorescence (XRF) and reported in Table 16. The actual loading of phosphorus and palladium metals that were loaded on surface of HZSM-5 catalysts was more than 5 wt% of phosphorus and 0.5 wt% of palladium respectively. Considering molar ratio

of Si/Al for each catalysts, HZSM-5 and Pd-HZSM-5 had same Si/Al or it can be said the adding of palladium had no effect on HZSM-5 structure, but molar ratio of Si/Al of other catalysts increased after modification with phosphoric acid. From result of X-ray diffraction, N_2 physisorption and X-ray fluorescence, it can be confirmed that modification with phosphoric acid had effect on HZSM-5 structure, especially structure that structure involved aluminium (dealumination of tetrahedral framework aluminum (TFAL))³¹.

4.2.3 Scanning electron microscope (SEM) and Energy dispersive X-ray spectroscopy (EDX)

Figure 24 displays the morphology of HZSM-5 and modified HZSM-5 catalysts investigated by scanning electron microscope (SEM). The morphologies of all catalysts have irregular shape and similar size. This can be concluded that improvement of HZSM-5 with phosphoric and palladium by incipient wetness impregnation technique may had little or no effect on morphology.



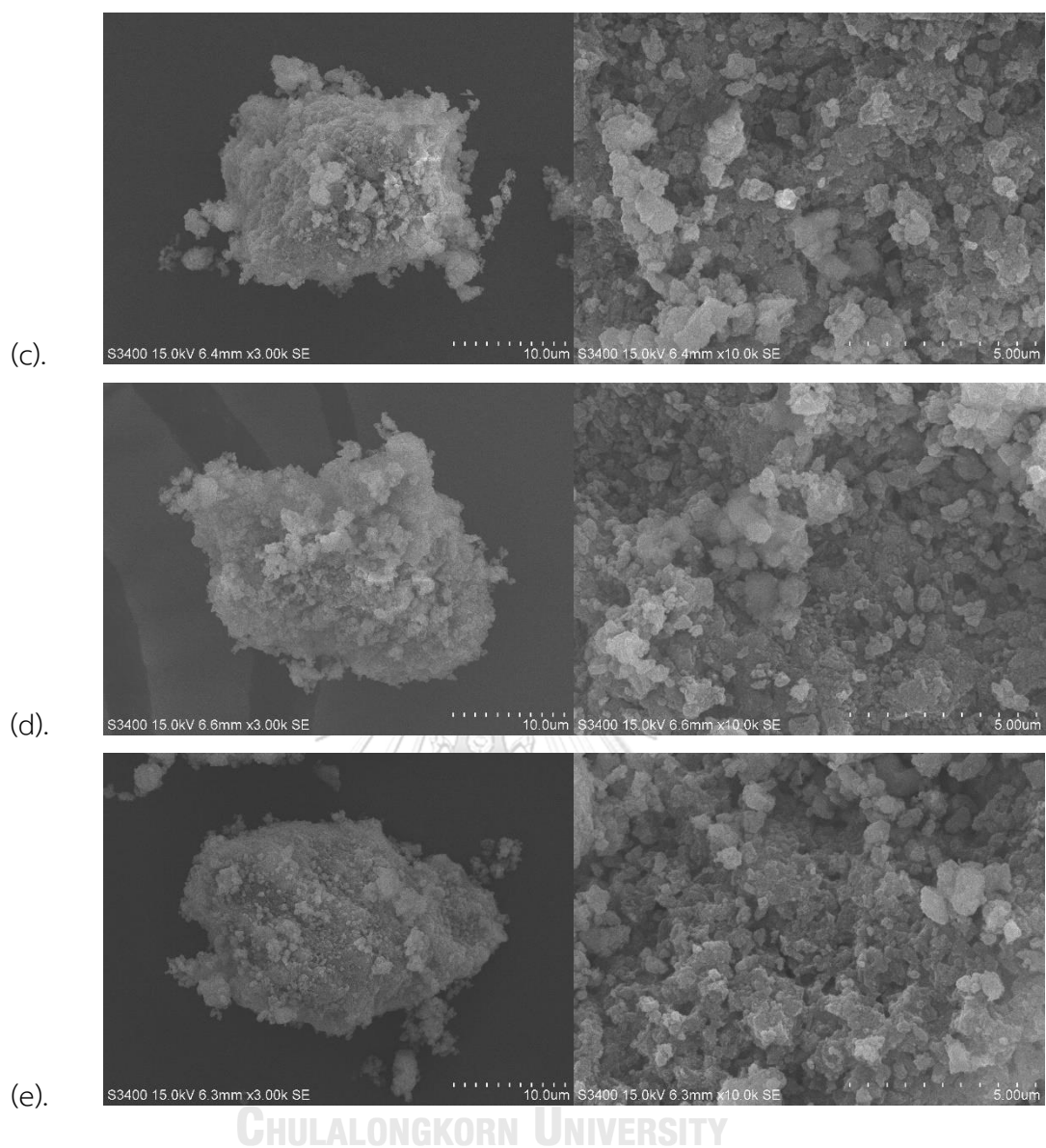


Figure 24 SEM image of HZSM-5 and modified HZSM-5 catalysts ; (a). HZSM-5, (b). P-HZSM-5, (c). Pd-HZSM-5, (d). Pd-P-HZSM-5 and (e). Pd-P-HZSM-5 Co-impregnation

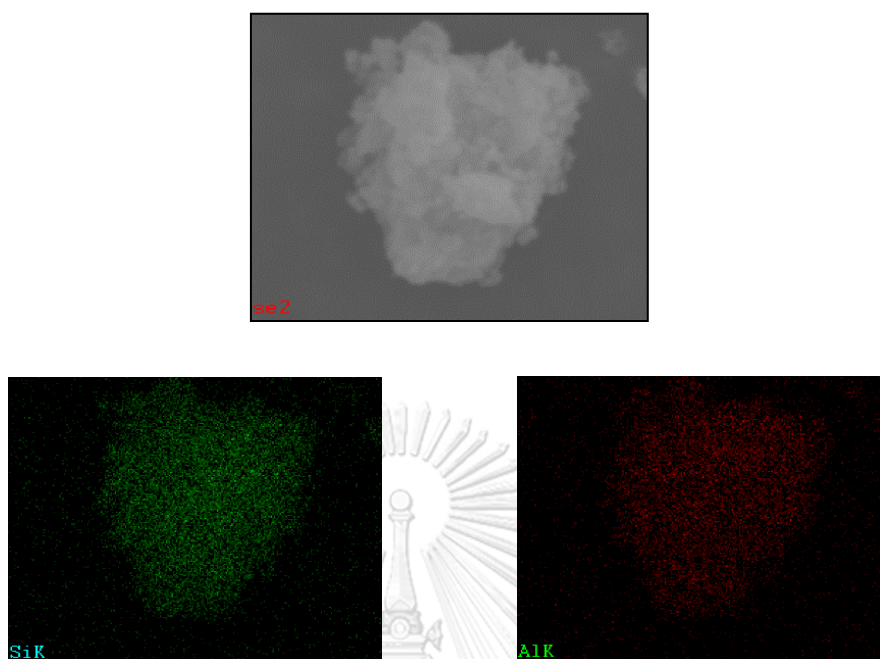


Figure 25 SEM-EDX mapping of HZSM-5

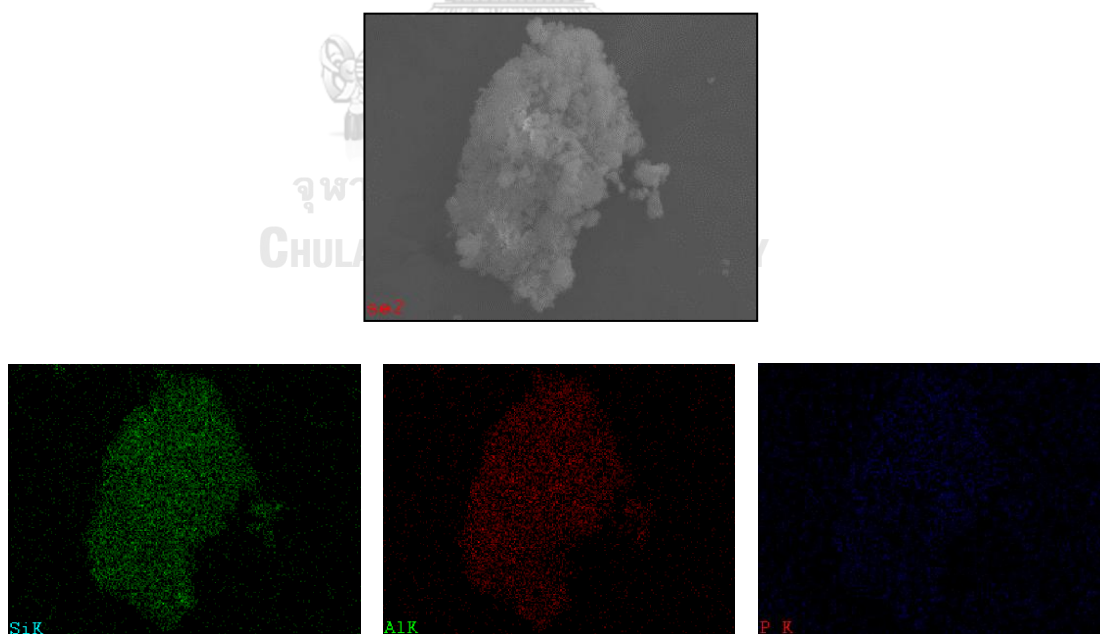


Figure 26 SEM-EDX mapping of P-HZSM-5

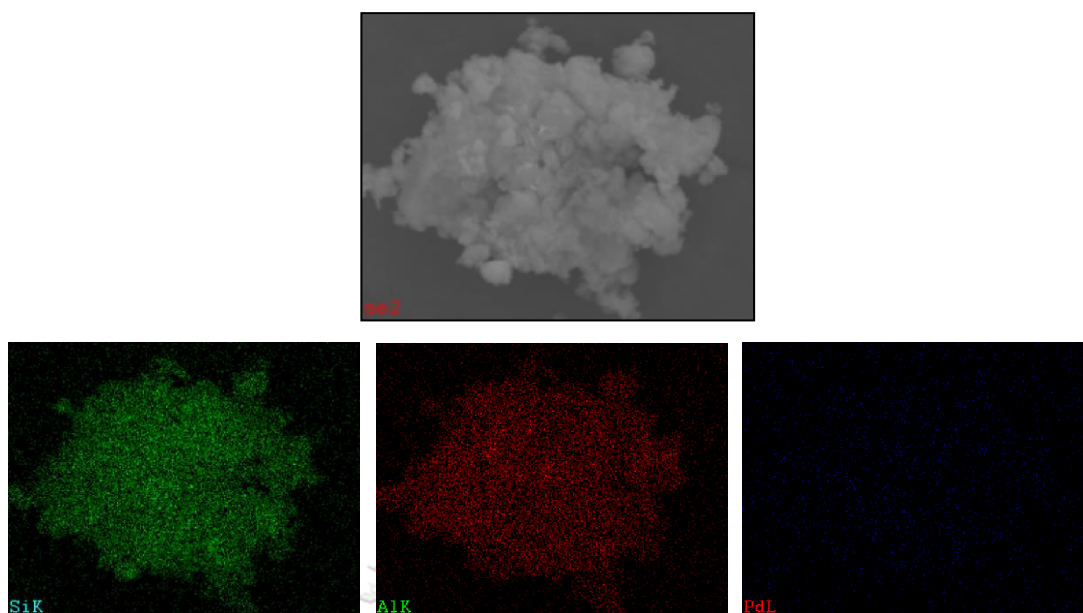


Figure 27 SEM-EDX mapping of Pd-HZSM-5

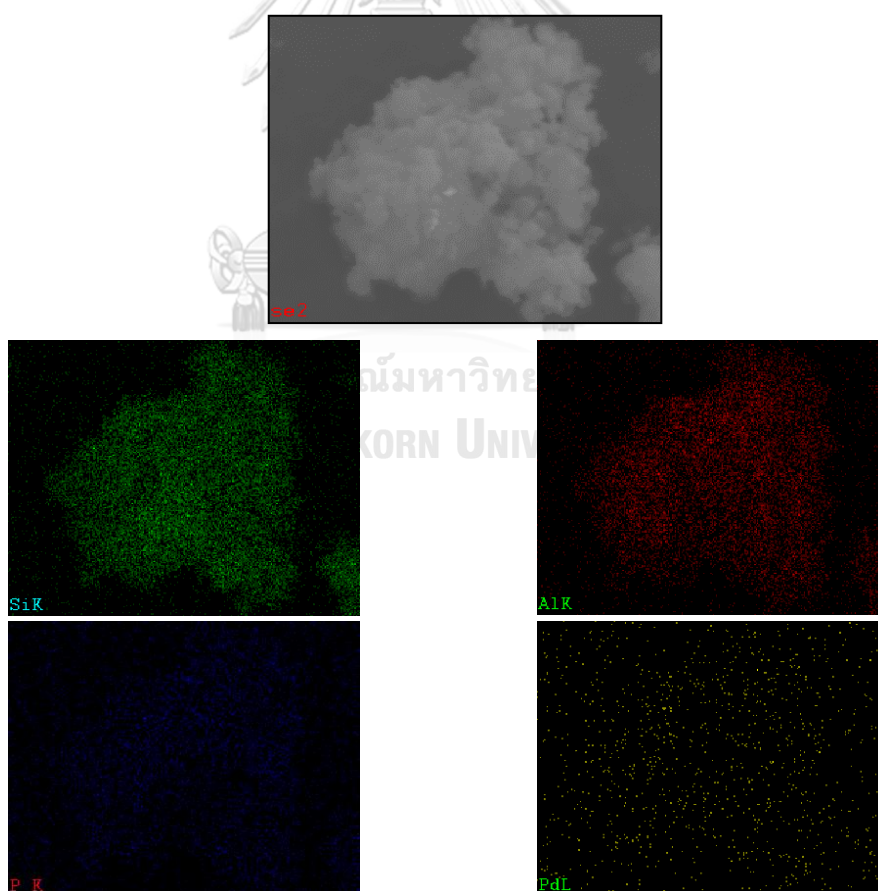


Figure 28 SEM-EDX mapping of Pd-P-HZSM-5

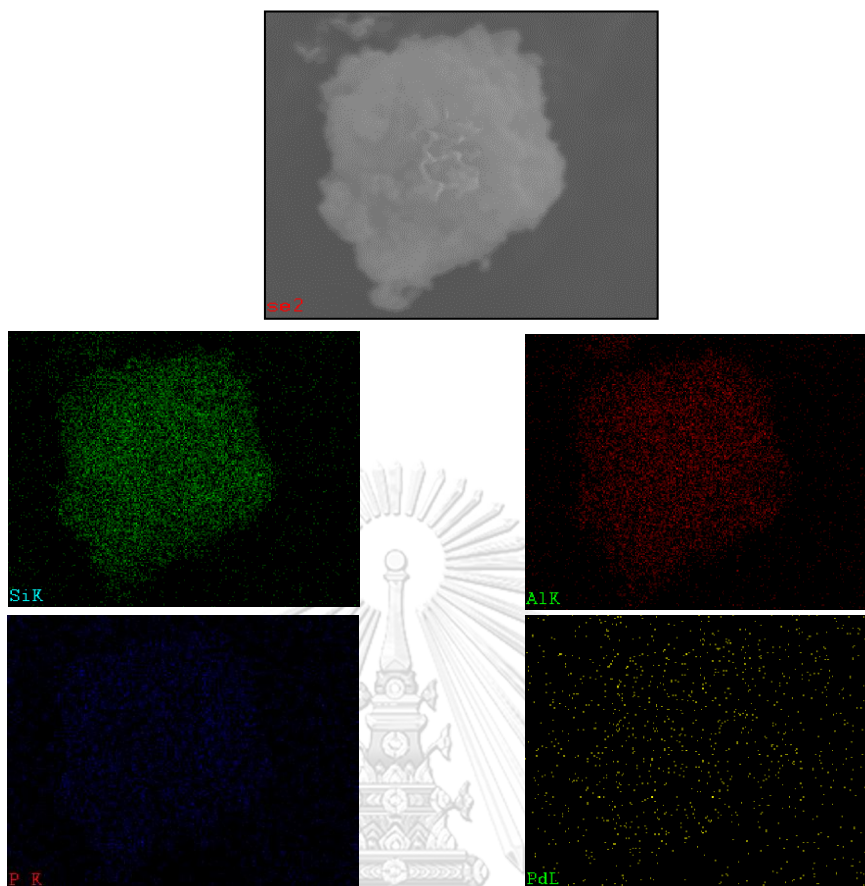


Figure 29 SEM-EDX mapping of Pd-P-HZSM-5 (Co-impregnation)

Figures 25 to 29 display element distribution of silicon (green) , aluminium (red) , phosphorus (blue) and palladium (yellow) over HZSM-5, P-HZSM-5, Pd-HZSM-5, Pd-P-HZSM-5 and Pd-P-HZSM-5 (Co-impregnation) respectively. From SEM-EDX image, it can be summarized that all of metals (Si, Al, P and Pd) have well dispersion on surface of catalysts. The amount of element distribution over catalysts is reported in Tables 17 and 18 in weight percent and atomic percent respectively. The amount of element distribution on each surface catalysts in both of weight and atomic percent was greater than amount of actual loading, especially amount of phosphorus element. This is caused by coating with platinum metal for having conductivity and platinum metal had peak overlap with phosphorus peak.

Table 17 Element distribution of HZSM-5 and modified HZSM-5 catalysts (weight percent)

Catalysts	Element distribution wt%			
	Si	Al	P	Pd
HZSM-5	64.01	35.99	-	-
P-HZSM-5	47.75	23.97	28.28	-
Pd-HZSM-5	31.82	65.65	-	2.53
Pd-P-HZSM-5	49.42	22.21	24.57	3.8
Pd-P-HZSM-5 (Co-impregnation)	46.02	23.67	27.38	2.93

Table 18 Element distribution of HZSM-5 and modified HZSM-5 catalysts (atomic percent)

Catalysts	Element distribution at%			
	Si	Al	P	Pd
HZSM-5	63.09	36.91	-	-
P-HZSM-5	48.55	25.37	26.08	-
Pd-HZSM-5	33.31	66.02	-	0.67
Pd-P-HZSM-5	51.58	24.13	23.05	1.05
Pd-P-HZSM-5 (Co-impregnation)	47.81	25.60	25.79	0.80

Analyzing between results from SEM-EDX in Table 17 and results from XRF in Table 18, amount of phosphorus and palladium in weight percent were more than results from XRF because SEM-EDX is a technique that investigates only surface of catalysts. In contrast, XRF analyzes element distribution in bulk of catalysts. The amount of metal loading (P and Pd) between SEM-EDX and XRF techniques are reported in Table 19.

Table 19 Amount of metal loading between SEM-EDX and XRF technique

Catalysts	Amount of metal loading on surface catalysts (wt%) investigated by SEM-EDX		Amount of metal loading in bulk catalysts (wt%) investigated by XRF	
	P	Pd	P	Pd
	HZSM-5	-	-	-
P-HZSM-5	28.28	-	9.25	-
Pd-HZSM-5	-	2.53	-	2.14
Pd-P-HZSM-5	24.57	3.8	9.26	1.90
Pd-P-HZSM-5 (Co-impregnation)	27.38	2.93	9.97	1.77

4.2.4 N₂ physisorption (BET&BJH)

Table 20 shows surface area, pore size and pore volume of HZSM-5 and modified catalysts. Adsorption – desorption Isotherm graph of HZSM-5 and modified HZSM-5 catalysts are illustrated as type IV in Figure 30. Pore size distribution graph of HZSM-5 and modified HZSM-5 catalysts are displayed in Figure 31. All information were investigated by N₂ physisorption technique.

Table 20 BET surface area, pore size and pore volume of HZSM-5 and modified HZSM-5 catalysts

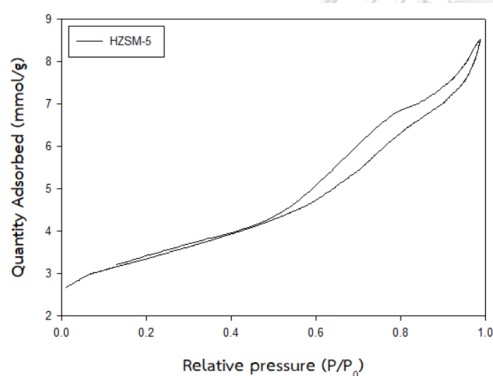
Sample	Surface area (m ² /g)	Pore size (nm)	Pore volume (cm ³ /g)
HZSM-5	257.972	5.3	0.268361
Pd-HZSM-5	301.982	5.3	0.273870
P-HZSM-5	212.620	5.6	0.161153
Pd-P-HZSM-5	227.380	5.9	0.161431
Pd-P-HZSM-5 (Co-impregnation)	233.062	5.5	0.163954

^a Determined from BET method

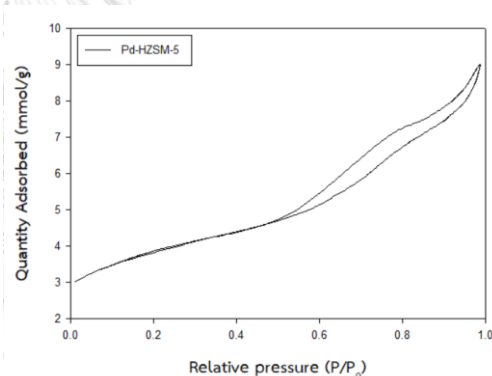
^{b,c} Determined from BJH desorption method

After improving HZSM-5 catalysts with palladium metal, the surface area and pore volume increased. It is caused of palladium is embedded within the porous and porous mouth and without effect on pore structure. That can verify by N_2 adsorption and desorption isotherm graph between HZSM-5 and Pd-HZSM-5 as shown in Figure 30 (a,b).

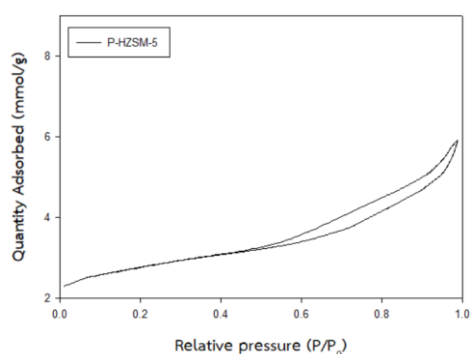
Effect of phosphoric acid is found to decrease of surface area ($258 \text{ m}^2/\text{g}$ to $213 \text{ m}^2/\text{g}$) and pore volume ($0.27 \text{ cm}^3/\text{g}$ to $0.16 \text{ cm}^3/\text{g}$) due to pore blockage by phosphorus species, whereas pore size slightly increases after impregnation^{4, 32}. The isotherm graph in Figure 30 (a,c) can be confirmed that the pore structure was changed. The sequence for impregnation of phosphoric acid and palladium between impregnation two times (phosphoric was first) and co-impregnation have only little effect on surface area, pore size and pore volume. Pd-P-HZSM-5 (Co-impregnation) avoided



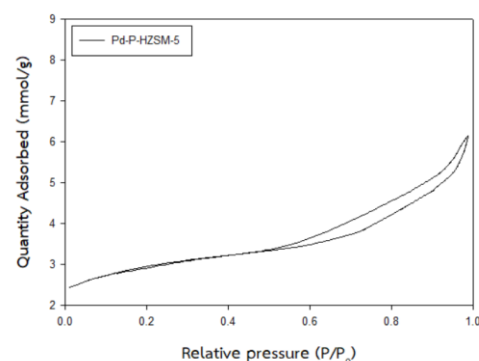
(a). HZSM-5



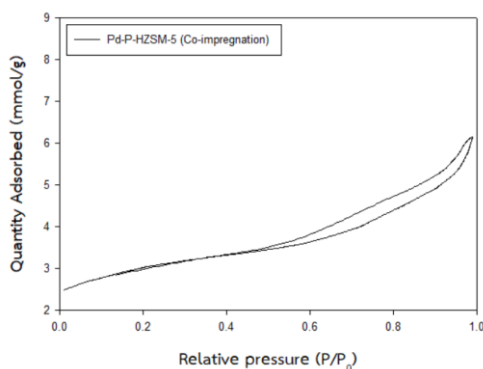
(b). Pd-HZSM-5



(c). P-HZSM-5



(d). Pd-P-HZSM-5



(e). Pd-P-HZSM-5 (Co-impregnation)

Figure 30 Isotherm graph of HZSM-5 and modified HZSM-5 catalysts; (a). HZSM-5, (b). Pd-HZSM-5, (c). P-HZSM-5, (d). Pd-P-HZSM-5 and (e). Pd-P-HZSM-5 (Co-impregnation)

The effect of sintering from second calcination at high temperature. It is caused Pd-P-HZSM-5 (Co-impregnation) to exhibit higher surface area of surface area than Pd-P-HZSM-5 that impregnation and calcination two times. Considering Isotherm graph between Pd-P-HZSM-5 and Pd-P-HZSM-5 (Co-impregnation), they also have similar have adsorption and desorption of N_2 . It can be confirmed that the structure of catalysts were not change after second impregnation.

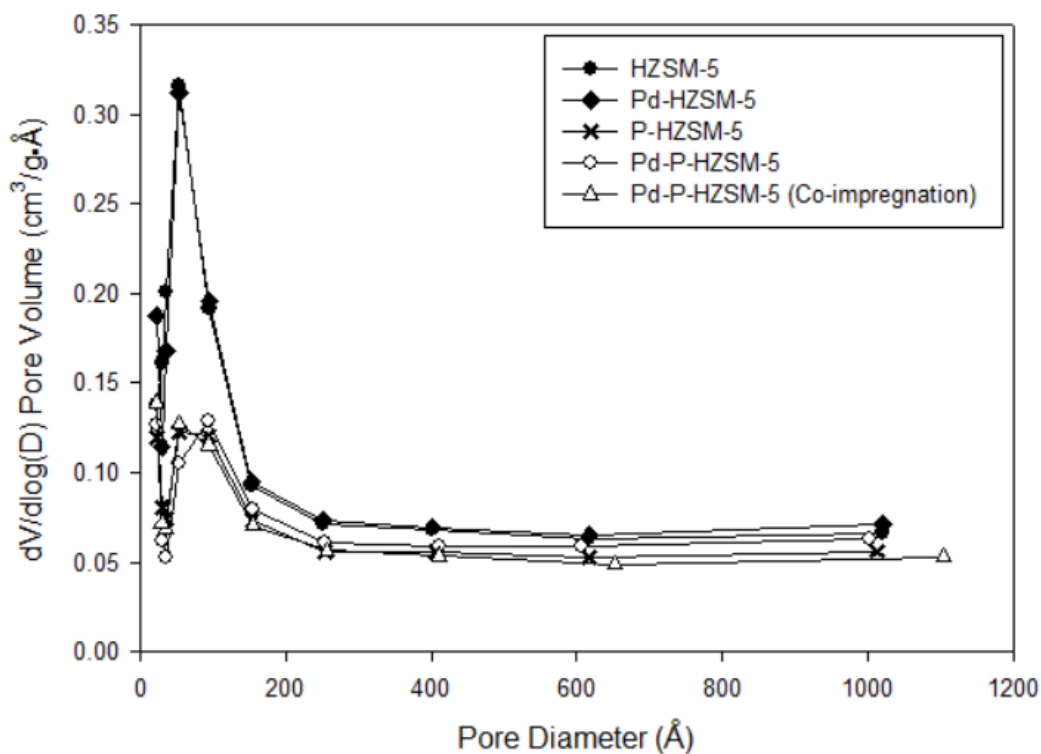


Figure 31 Pore size distribution graph of HZSM-5 and modified HZSM-5 catalysts

Pore size distribution of each catalysts is displayed as similar trend in Figure 31. In case of HZSM-5 and Pd-HZSM-5, these have high peak in pore diameter range 0 – 200 \AA because both of these catalysts have same average pore volume. After impregnation of phosphoric acid, P-HZSM-5 Pd-P-HZSM-5 and Pd-P-HZSM-5 (Co-impregnation) catalysts had lower peak in pore diameter range 0 – 200 \AA . Moreover, the effect of sequence for impregnation of phosphoric acid and palladium had no effect on pore size distribution

4.2.5 Ammonia temperature-programmed desorption (NH₃-TPD)

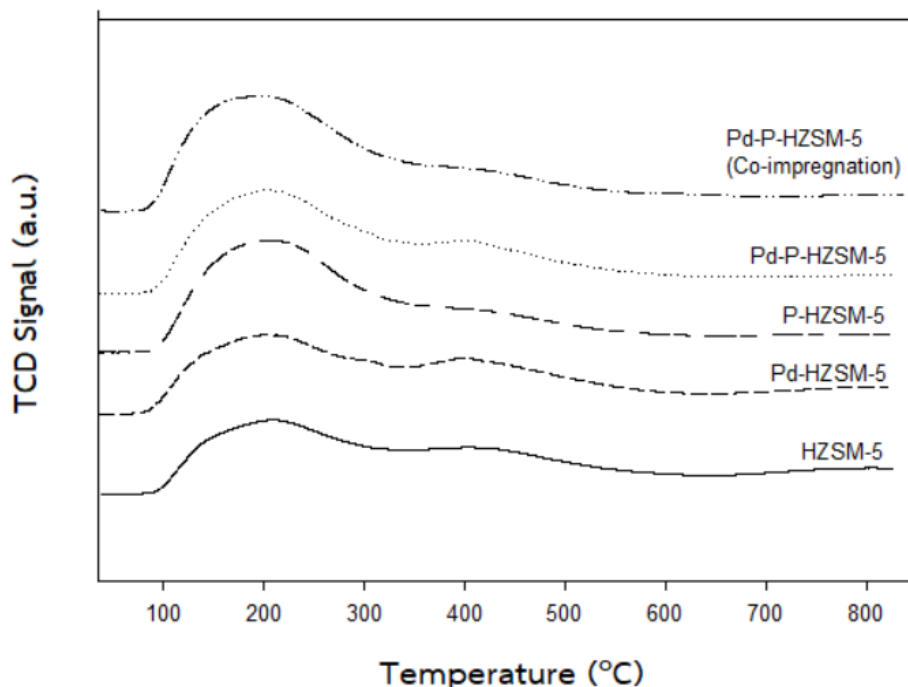


Figure 32 NH₃-TPD profiles of HZSM-5 and modified HZSM-5 catalysts

Acidity of HZSM-5 and modified HZSM-5 catalysts are measured by ammonia temperature-programmed desorption technique and plotted in Figure 32. The acidity of all catalysts was divided clearly into two desorption peaks; weak acid site and moderate to strong acid sites. From Figure 32, it can be concluded that the temperature in range moderate to strong of HZSM-5 catalyst is greater than other catalysts because improving HZSM-5 catalysts with phosphoric acid can shift high temperature desorption peak (acid in range moderate to strong acid site) to lower temperature^{19, 39}.

The data in Table 21 reveals that after Impregnation with phosphoric acid or palladium, the amount of total acidity increased when compared with unmodified HZSM-5 catalysts. It can be summarized that both of phosphoric acid and palladium improve in both of weak acid site and moderate to strong acid sites

Table 21 Total acidity of HZSM-5 and modified HZSM-5 catalysts from NH₃-TPD.

Catalyst	Temperature (°C)		NH ₃ desorption ($\mu\text{mol NH}_3/\text{g}_{\text{cat}}$)		Total acidity ($\mu\text{mol NH}_3/\text{g}_{\text{cat}}$)
	1 st peak	2 nd peak	Weak	Medium to strong	
HZSM-5	200	410	439.39	517.65	957.04
P-HZSM-5	196	354	649.78	565.30	1215.08
Pd-HZSM-5	200	400	600.00	604.29	1204.29
Pd-P-HZSM-5	194	388	625.74	595.67	1221.39
Pd-P-HZSM-5 (Co-impregnation)	190	355	667.91	588.85	1256.76

The effect between impregnation for rounds and co-impregnation on surface acidity was obviously in temperature at maximum TCD signal of second peak (moderate to strong acid site). In case of Pd-P-HZSM-5, it shifts into lower temperature when compared with Pd-P-HZSM-5 (Co-impregnation) (388 °C to 355 °C). Although step by step impregnation and co-impregnation had effect on temperature at maximum TCD signal of second peak, it only had slight effect on the total acidity.

4.2.6 Ethanol dehydration reaction

From part 4.1, It reveals that the ZSM-5 catalyst with the lowest molar ratio of silicon to aluminium gave the highest activity in ethanol dehydration in all of temperature range (200 °C – 400 °C). In part 4.2, the work was conducted based on using the commercial HZSM-5 with Si/Al = 19 and modified HZSM-5 by incipient wetness impregnation and co-impregnation with phosphoric acid and palladium in ethanol dehydration using same condition with part 4.1 (temperature programmed 200 °C - 400 °C, atmospheric pressure and WHSV 22.9 h⁻¹).

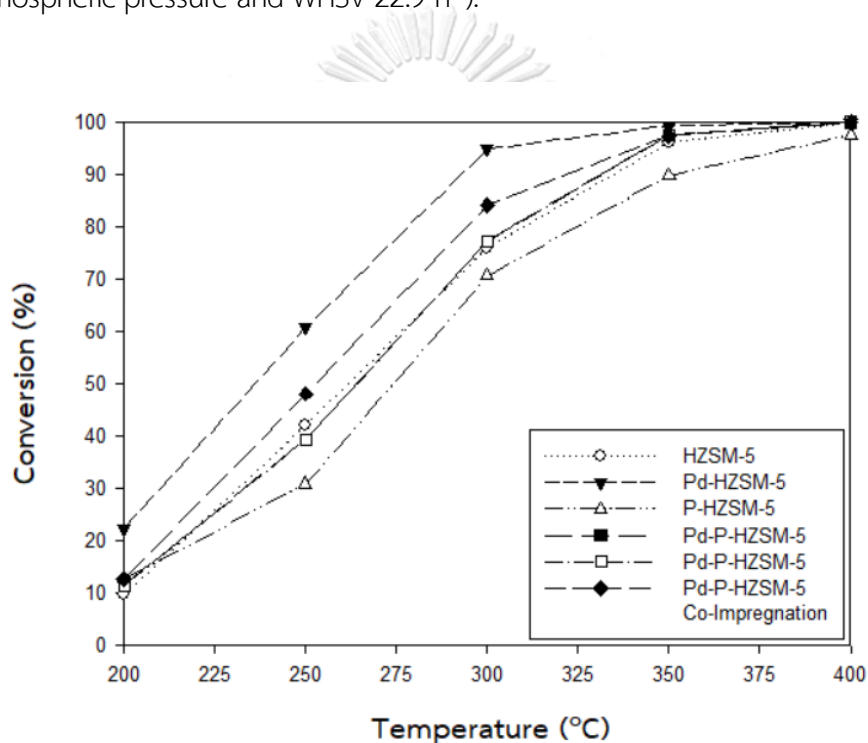


Figure 33 Catalytic activity of HZSM-5 and modified HZSM-5 catalysts in ethanol dehydration reaction (line plot)

The catalytic activity in ethanol dehydration reaction over HZSM-5 and modified HZSM-5 catalysts is shown in Figure 33 and Figure 34. It is found that ethanol conversion of each catalyst increased with increasing temperature. Modification of HZSM-5 catalysts with palladium can enhance catalytic activity in ethanol dehydration reaction (more than 90 % at temperature 300 °C), while modification with phosphoric acid slightly degraded ethanol conversion when temperature programmed was more

than 250 °C. Ethanol conversion of Pd-P-HZSM-5 (Co-impregnation) was greater than Pd-P-HZSM-5 (impregnation phosphoric first) due to surface area and total acidity of Pd-P-HZSM-5 (Co-impregnation), which was slightly higher than Pd-P-HZSM-5.

Most catalysts had ethanol conversion more than 90 % at temperature 350 °C and reached 100 percent at temperature 400 °C, excepting for the modified HZSM-5 with phosphoric acid. From the results above, it can be concluded that the addition of phosphoric acid can inhibit the ethanol dehydration reaction.

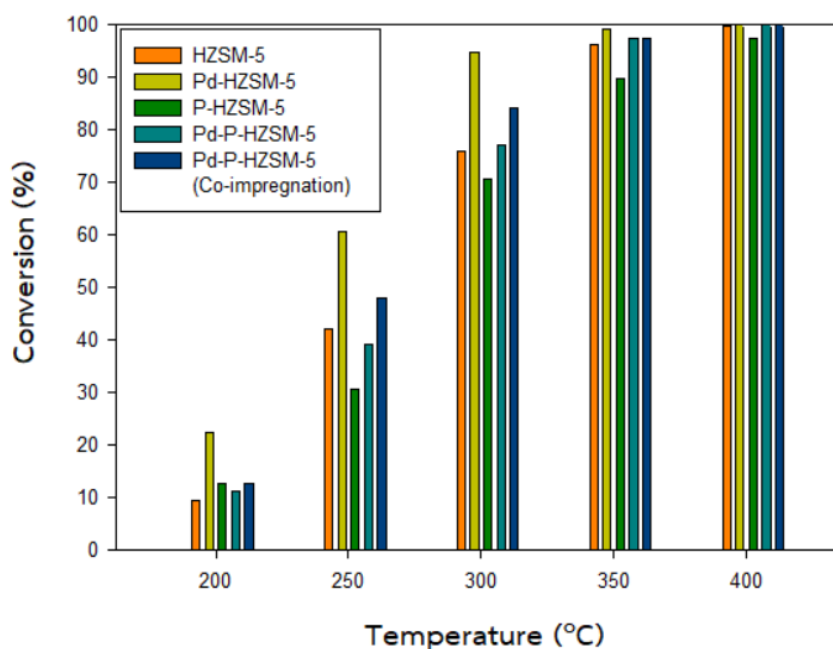


Figure 34 Catalytic activity of HZSM-5 and modified HZSM-5 catalysts in ethanol dehydration reaction (bar chart)

Ethylene is one product from ethanol dehydration reaction. It is an endothermic reaction. Therefore, ethylene prefers high temperature. From Figures 35 and 36, It can be observed that at low temperature had a little ethylene yield. This is due to ethanol conversion at low temperature had about 10 %. On the other hand, the main product of ethanol dehydration reaction was ethylene, so the ethylene yield had almost 100 % at high temperature (400 °C).

Effect of modification with palladium in ethylene yield was found to decrease activation energy in turning ethanol to ethylene. It made ethylene produced more at low temperature (200 °C – 250 °C). As observed from Figures 35 and 36, HZSM-5 catalysts can not produce ethylene at temperature 200 °C but Pd-HZSM-5, Pd-P-HZSM-5 and Pd-HZSM-5 (Co-impregnation) can product ethylene at 200 °C. When temperature increased to 250 °C, modified HZSM-5 catalysts preferred to produce higher ethylene than unmodified HZSM-5 and modified HZSM-5 with phosphoric acid.

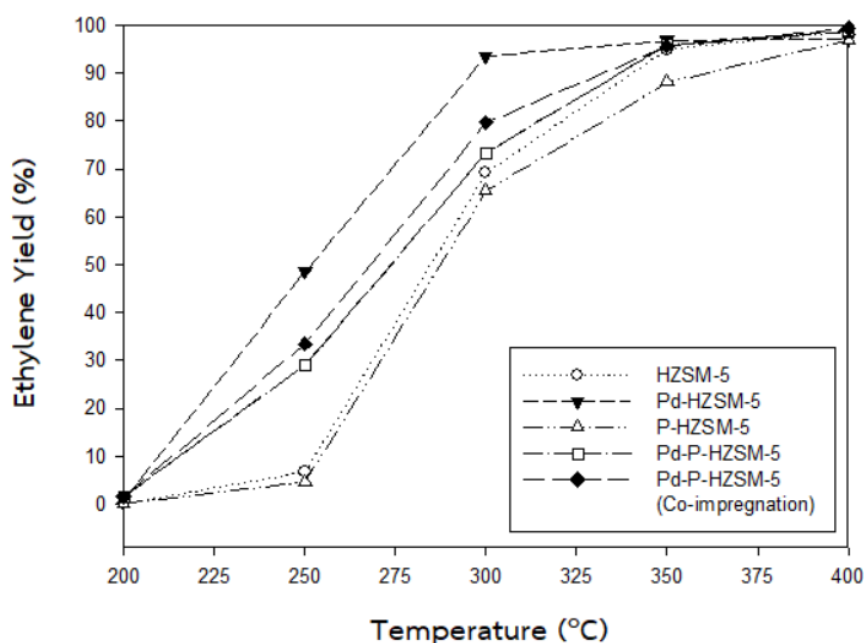


Figure 35 Ethylene yield of HZSM-5 and modified HZSM-5 catalysts in ethanol dehydration reaction (line plot)

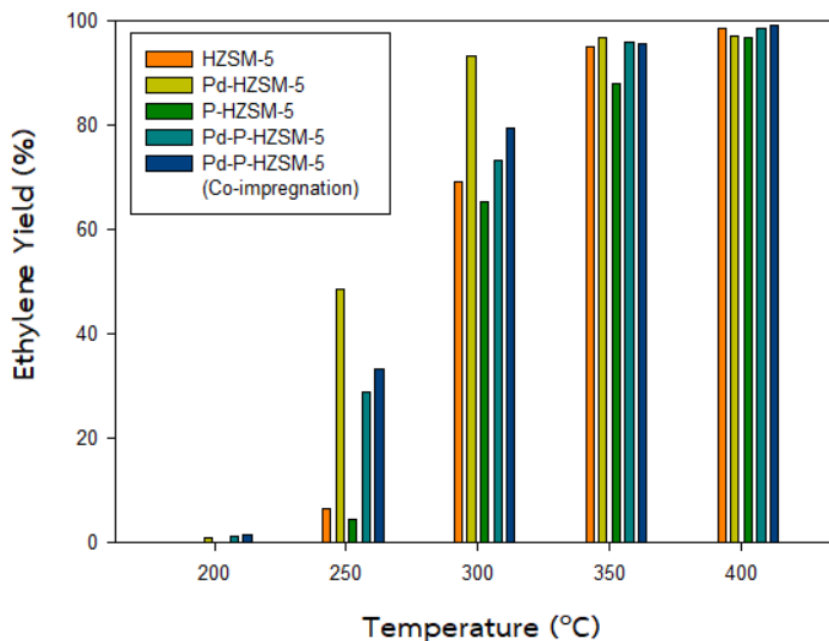


Figure 36 Ethylene yield of HZSM-5 and modified HZSM-5 catalysts in ethanol dehydration reaction (bar chart)

The product distribution of ethanol dehydration over modified HZSM-5 with phosphoric acid (P-HZSM-5) was similar to those of HZSM-5. It prefers to produce diethyl ether at low temperature (200 °C - 250 °C), but a little amount of ethylene can occur at 200 °C

Impregnation of phosphoric acid and palladium (Pd-P-HZSM-5) and co-impregnation of phosphoric acid and palladium (Pd-P-HZSM-5 (Co-impregnation)) had no effect on ethylene yield when compared together. Ethylene yield of Pd-P-HZSM-5 (Co-impregnation) was more than Pd-P-HZSM-5 due to physical and chemical properties (surface area, acidity, etc.). At temperature of 200 °C , although Pd-HZSM-5 gave higher ethylene yield than Pd-P-HZSM-5 (Co-impregnation) and Pd-P-HZSM-5 at high temperature, both of Pd-P-HZSM-5 (Co-impregnation) and Pd-P-HZSM-5 catalysts produced ethylene more than using one metal in impregnation due to effect of bimetallic.

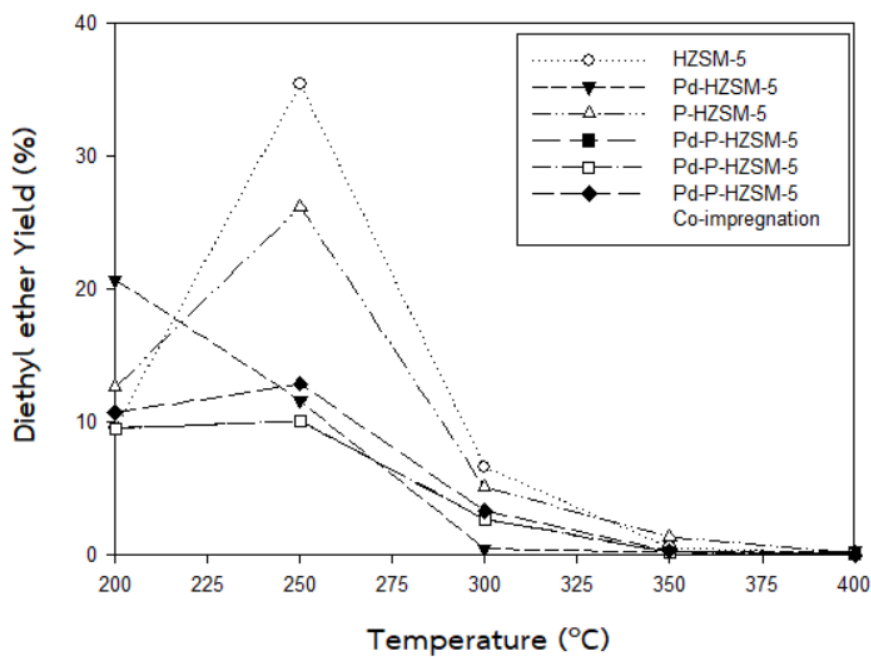


Figure 37 Diethyl ether yield of HZSM-5 and modified HZSM-5 catalysts in ethanol dehydration reaction (line plot)

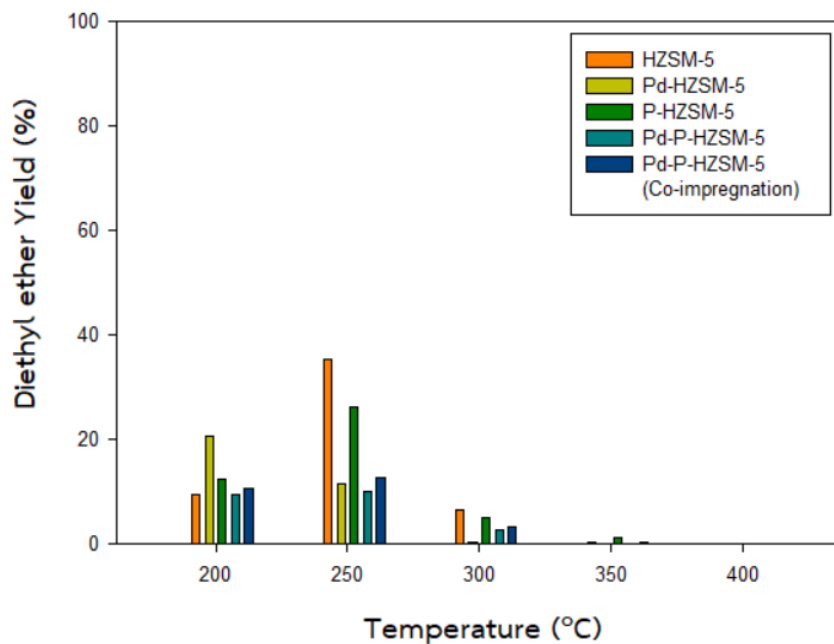


Figure 38 Diethyl ether yield of HZSM-5 and modified HZSM-5 catalysts in ethanol dehydration reaction (bar chart)

Besides ethylene product, diethyl ether is also product from ethanol dehydration reaction that prefers to occur at low temperature (200 °C – 250 °C) because it is an exothermic reaction. As observed from Figures 37 and 38, which were reported the diethyl ether yield, it was found that ethylene yield had the opposite trend with diethyl ether yield or it can be conclude diethyl ether yield decreases when temperature was higher than 250 °C. modified HZSM-5 catalysts with palladium had the highest diethyl ether yield at 200 °C (21% of diethyl ether yield) and HZSM-5 catalysts gave the highest diethyl ether yield in all temperature range (35% diethyl ether yield at 250 °C).

Effect of modification with palladium was found to decrease diethyl ether yield at high temperature. It made diethyl ether turned into ethylene (diethyl ether cracking reaction) and ethanol (diethyl ether hydrolysis reaction). For bimetallic , Pd-P-HZSM-5 (Co-impregnation), it had similar trend of diethyl ether to Pd-P-HZSM-5 or it can be said that the effect of loading sequece with phosphoric acid and palladium had no effect on each temperature.

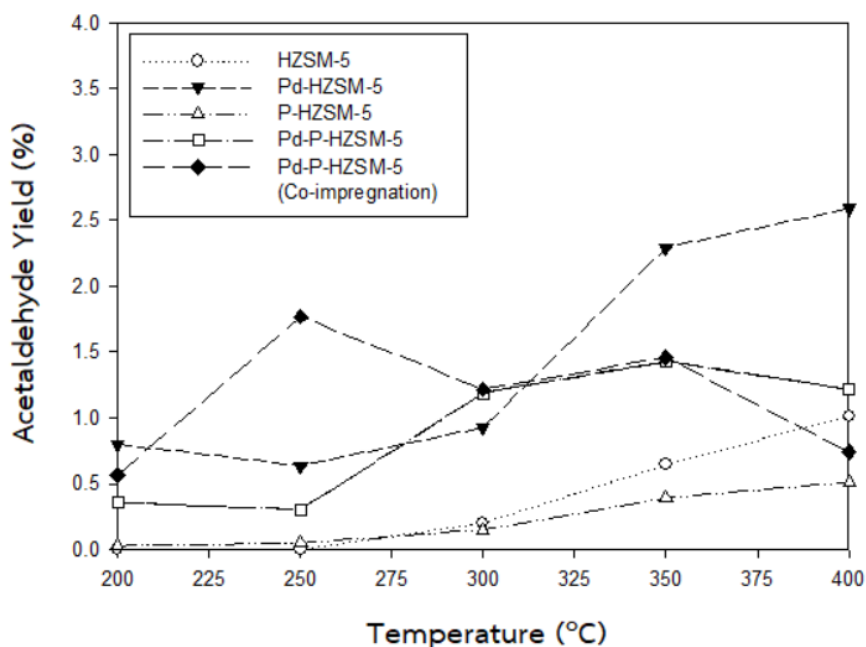


Figure 39 Acetaldehyde yield of HZSM-5 and modified HZSM-5 catalysts in ethanol dehydration reaction (line plot)

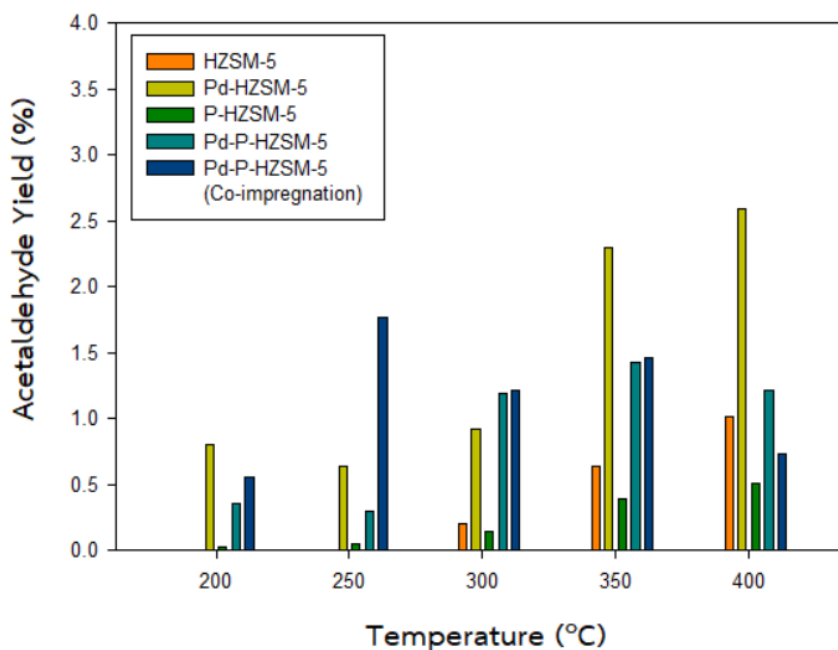


Figure 40 Acetaldehyde yield of HZSM-5 and modified HZSM-5 catalysts in ethanol dehydration reaction (bar chart)

Acetaldehyde is a byproduct from ethanol dehydrogenation, which is a side reaction of ethanol dehydration reaction, over HZSM-5 and modified HZSM-5 catalysts. From Figures 39 and 40, acetaldehyde yield for most catalysts tended to increase with increasing temperature. Moreover, Pd-HZSM-5 catalysts gave the highest acetaldehyde yield.

Part 3: Comparison catalytic activity between synthesized HZSM-5 and commercial HZSM-5 catalysts in ethanol dehydration reaction.

4.3 Characterization of synthesized HZSM-5 and commercial HZSM-5

From part 4.1, ZSM-5 catalysts with Si/Al of 20 gives the highest catalytic activity in ethanol dehydration reaction (70.3 % ethanol conversion). Therefore, ZSM-5 catalysts with molar ratio of Si/Al of 20 was improved into HZSM-5 with molar ratio of Si/Al = 20 by ion-exchange with ammonium nitrate (NH_4NO_3) and calcine at 550°C . Next, comparing catalytic activity with HZSM-5 from commercial that have similar Si/Al ratio of ZSM-5 Si/Al = 20. These catalysts are characterized by various techniques in part 4.3. The properties of catalysts are investigated by X-ray diffraction (XRD), X-ray fluorescence (XRF), scanning electron microscope (SEM) and energy dispersive X-ray spectroscopy (EDX), N_2 physisorption (BET&BJH), ammonia temperature-programmed desorption (NH_3 -TPD) and thermal gravimetric and differential thermal analysis (TG/DTA)

4.3.1 X-ray diffraction (XRD)

The XRD patterns in Figure 41 shows The XRD patterns of synthesized ZSM-5, HZSM-5 and commercial HZSM-5 catalysts, which were measured at diffraction angle (2θ) 5° from 80° . Three catalysts had sharp peak at same position or it can be said that these catalysts have composition of ZSM-5 structure. The XRD patterns of synthesized ZSM-5, HZSM-5 and commercial HZSM-5 catalysts appeared at $2\theta = 7.8^\circ, 8.7^\circ, 22.94^\circ, 23.6^\circ$ and 24.26° ³⁷. Furthermore, ion-exchange with ammonium nitrate (NH_4NO_3) made the intensity of ZSM-5 XRD peak became stronger due to improving of tetrahedral framework aluminum (TFAL) in HZSM-5 catalysts, whereas the commercial HZSM-5 catalysts exhibited the lowest intensity of ZSM-5 XRD peak when compared to both synthesized ZSM-5 and commercial HZSM-5 catalysts.

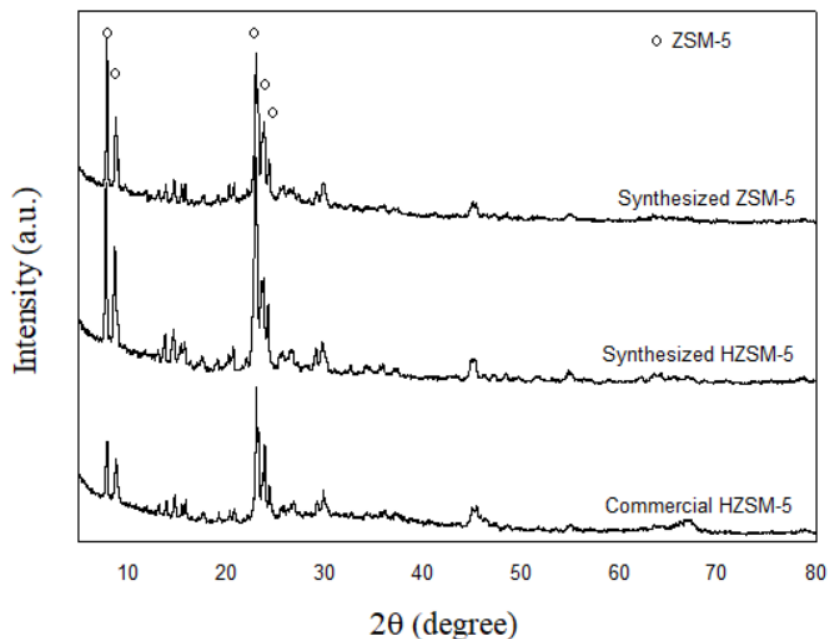


Figure 41 XRD patterns of synthesized ZSM-5, HZSM-5 and commercial HZSM-5 catalysts

4.3.2 X-ray fluorescence (XRF)

Table 22 Element distribution of synthesized HZSM-5 and commercial HZSM-5 from X-ray fluorescence (weight percent)

Catalysts	Element distribution (wt%)		Si/Al (mol/mol)
	Si	Al	
Commercial HZSM-5	64.21	35.30	1.75
Synthesized HZSM-5	93.68	6.01	15.03

Table 22 shows element distribution of silicon and aluminium in bulk catalyst. HZSM-5 catalysts with silicon to aluminium molar ratio of 19 from commercial was analyzed by XRF and the detected amount of aluminium metal was about 6 times greater than the amount of aluminium metal from the synthesized HZSM-5 catalysts. Moreover, molar ratio of Si/Al of commercial HZSM-5 catalyst was 1.75. It was 10 times

less than molar ratio of Si/Al, which was defined on label of commercial product. In case of synthesized HZSM-5 catalyst that was calculated molar ratio of Si/Al equal 20, the actual molar ratio of Si/Al was 15.03 that had value less than expected proportion.

4.3.2 Scanning electron microscope (SEM) and Energy dispersive X-ray spectroscopy (EDX)

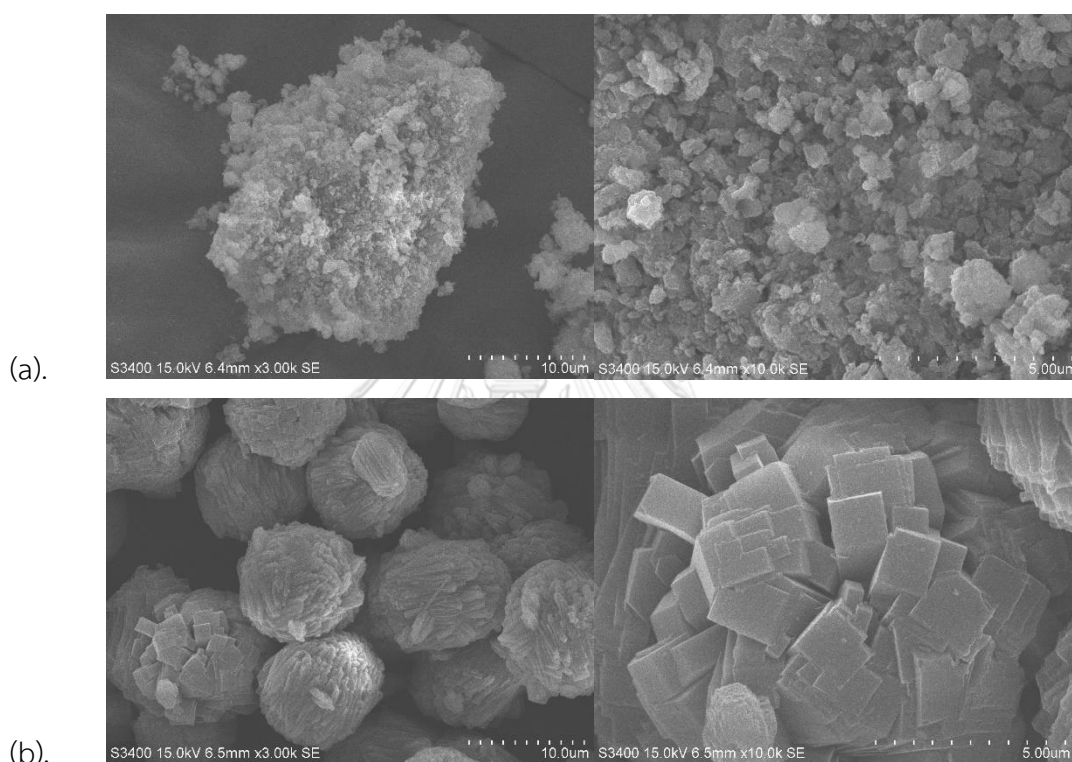


Figure 42 SEM image of commercial HZSM-5 (a) and synthesized HZSM-5 catalysts (b).

The morphology of synthesized HZSM-5 and commercial HZSM-5 catalysts was determined by SEM and displayed in Figure 42. The shape of commercial HZSM-5 catalyst was irregular shape having an average diameter 20 μm while the synthesized HZSM-5 catalyst had morphology of the cubic crystal or prismatic⁴⁰ with aggregation into spherical shape particles. Each spherical particle of synthesized HZSM-5 catalyst had average diameter of 10 μm.

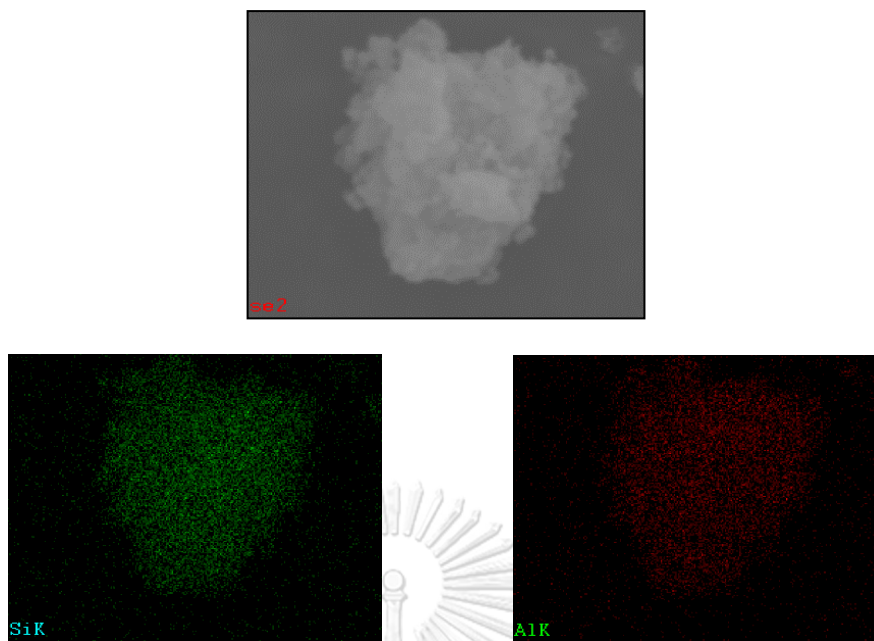


Figure 43 SEM-EDX mapping of Commercial HZSM-5 catalysts

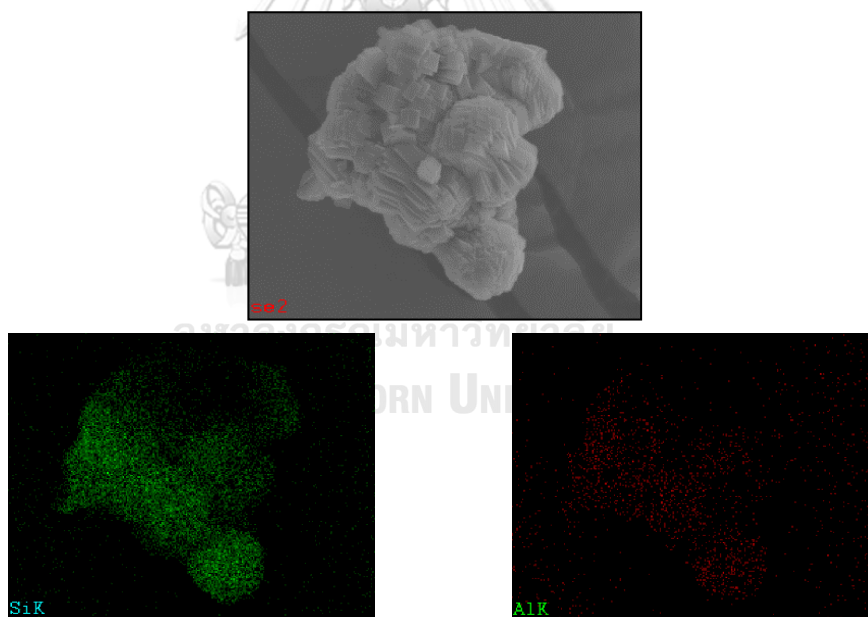


Figure 44 SEM-EDX mapping of synthesized HZSM-5 catalysts

From Figures 43 and 44, silicon and aluminium distributions of each catalysts are displayed. Each element is represented by a different color such as green represents silicon metal and red represents aluminium metal. From element distribution in these figure, it can be said that commercial HZSM-5 catalyst had more aluminium distribution than synthesized HZSM-5 catalyst. Amount of silicon and aluminium distribution was reported in Tables 23 and 24 in weight and atomic percent. The data in these tables can be confirmed that the aluminium distribution in commercial HZSM-5 catalyst was higher than synthesized HZSM-5 catalyst.

Table 23 Element distribution of commercial HZSM-5 and synthesized HZSM-5 catalysts (weight percent)

Catalysts	Element distribution (wt%)		Si/Al (wt%/wt%)
	Si	Al	
Commercial HZSM-5	64.01	35.99	1.78
Synthesized HZSM-5	92.95	7.05	13.18

Table 24 Element distribution of commercial HZSM-5 and synthesized HZSM-5 catalysts (atomic percent)

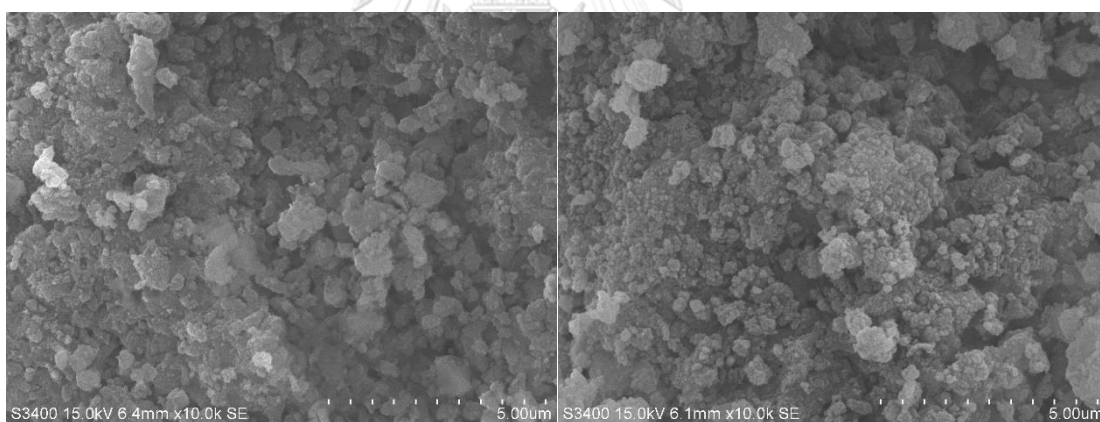
Catalysts	Element distribution (at%)		Si/Al (at%/at%)
	Si	Al	
Commercial HZSM-5	63.09	36.91	1.71
Synthesized HZSM-5	92.68	7.32	12.66

Table 25 Molar ratio of Si/Al between SEM-EDX and XRF techniques

Catalysts	SEM-EDX	XRF
	(Surface catalyst)	(Bulk catalyst)
	Si/Al (mol/mol)	Si/Al (mol/mol)
Commercial HZSM-5	1.67	1.75
Synthesized HZSM-5	12.71	15.03

The actual molar ratios of Si/Al in each catalyst are calculated and reported in Table 25. Both of SEM-EDX and XRF reported in the similar trend of results. Synthesized HZSM-5 catalyst had molar ratio of Si/Al, which was higher than commercial HZSM-5 catalyst due to amount of aluminium composition in commercial HZSM-5 catalyst is more than synthesized HZSM-5 catalyst.

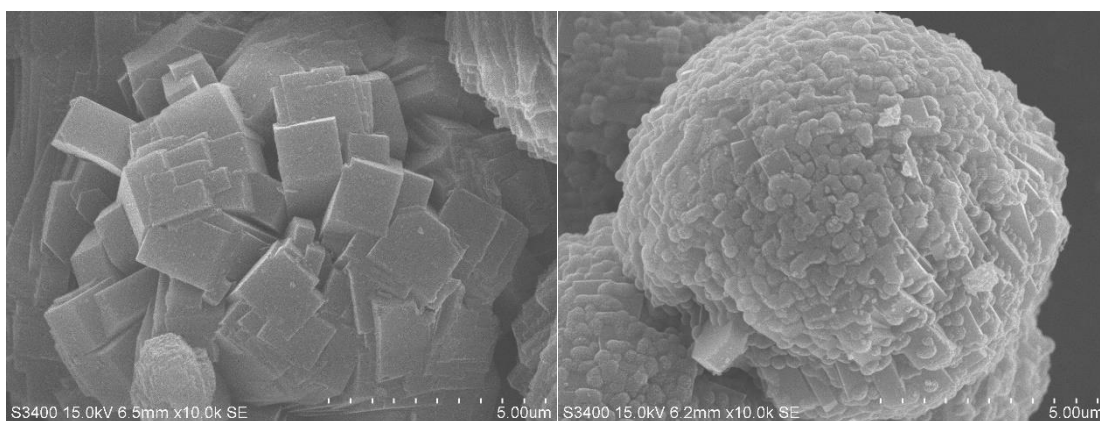
The morphologies of spent catalysts for both commercial HZSM-5 and synthesized HZSM-5 catalysts were observed by SEM after being used in ethanol dehydration for comparing with fresh catalysts. Since temperature programmed of ethanol dehydration reaction finished at 400 °C, catalysts deactivated by coke composition and it made the catalytic activity dropped. Figures 45 and 46 show the different between fresh and spent catalysts. It was observed that spent catalysts had small spherical particle covered on surface of both commercial HZSM-5 and synthesized HZSM-5 catalysts.



(a).

(b).

Figure 45 SEM image of fresh commercial HZSM-5 (a) and spent commercial HZSM-5 catalysts (b).



(a).

(b).

Figure 46 SEM image of fresh synthesized HZSM-5 (a) and spent synthesized HZSM-5 catalysts (b).

Figures 47 and 48 illustrate element distribution of commercial HZSM-5 and synthesized HZSM-5 catalysts. Each metal is represented by a different color such as blue color is silicon metal, green is aluminium and red is carbon. The amount of element distribution is reported in Tables 26 and 27 as weight and atomic percent. It was found that had carbon (coke) on surface of both catalysts and synthesized HZSM-5 catalyst had slight coke less than commercial HZSM-5 catalyst due to it had well catalytic activity than commercial HZSM-5 catalyst.

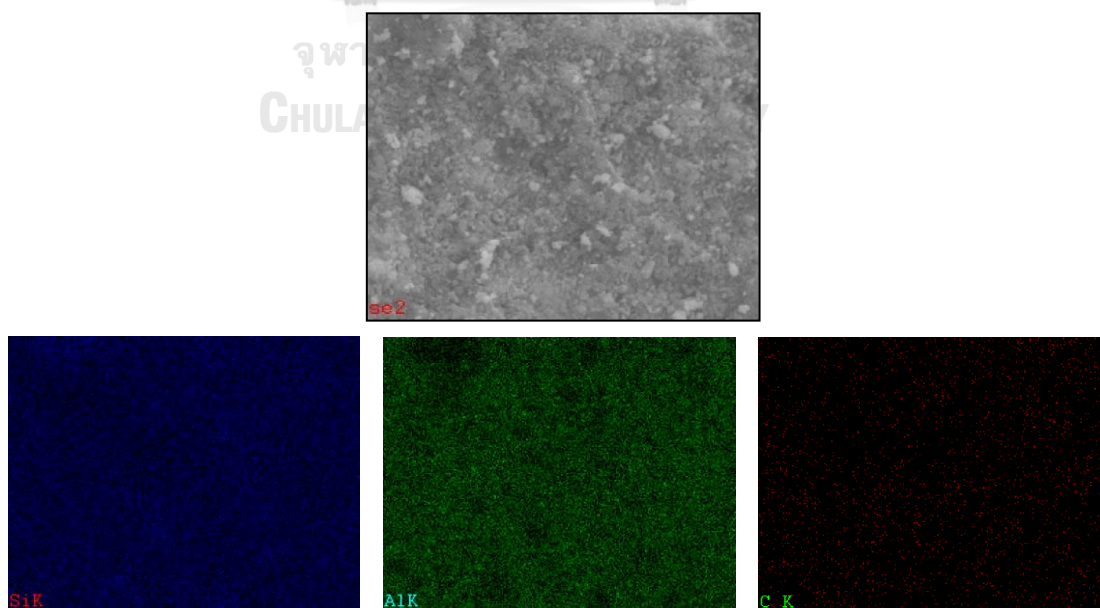


Figure 47 SEM-EDX of spent commercial HZSM-5 catalyst

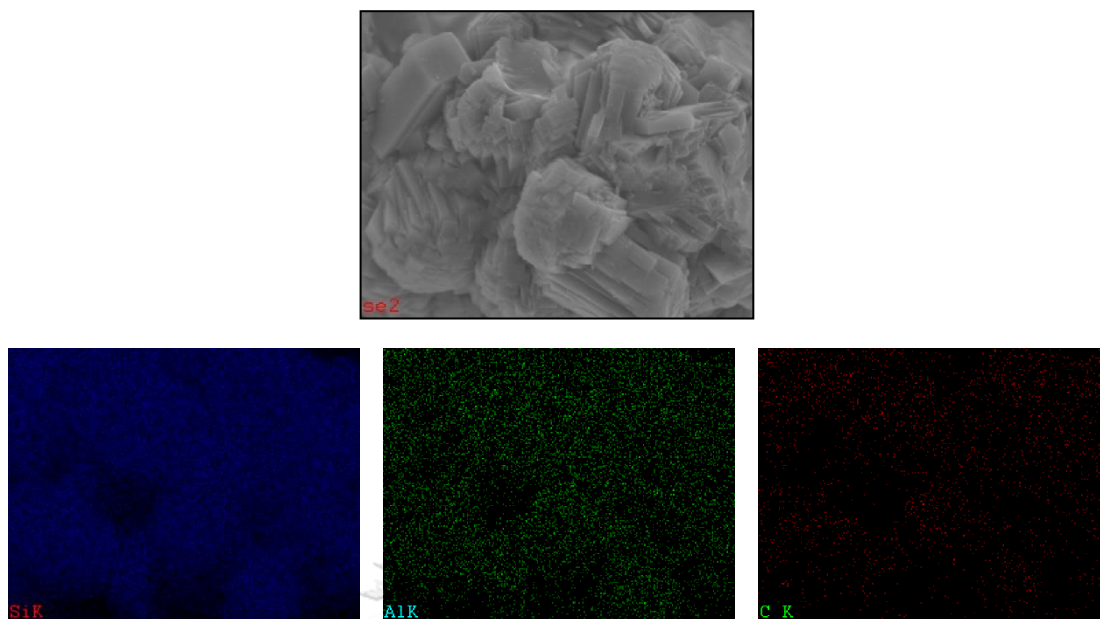


Figure 48 SEM-EDX of spent synthesized HZSM-5 catalyst

Table 26 Element distribution of commercial HZSM-5 and synthesized HZSM-5 catalysts (weight percent)

Catalysts	Element distribution (wt%)		
	Si	Al	C
Commercial HZSM-5	57.36	31.35	11.29
Synthesized HZSM-5	84.35	2.25	13.40

Table 27 Element distribution of commercial HZSM-5 and synthesized HZSM-5 catalysts (atomic percent)

Catalysts	Element distribution (at%)		
	Si	Al	C
Commercial HZSM-5	49.34	28.08	22.57
Synthesized HZSM-5	71.58	1.98	26.43

4.3.4 N₂ physisorption (BET&BJH)

N₂ physisorption is a technique that investigates surface area (BET method) , pore size , pore volume, pore size distribution (BJH method) and isotherm graph of studied catalyts. From Table 28, BET surface area, pore size and pore volume of commercial HZSM-5 and synthesized HZSM-5 catalyts were recorded and shown. Although synthesized HZSM-5 catalyst had larger BET surface area (296 m²/g) than the commercial HZSM-5 catalyts (258 m²/g), the pore size and pore volume were less than commercial HZSM-5 catalyts. Both of catalyts were mesoporous pore structure (pore size 2-50 nm). Furthermore, pore size of both catalyts can be predicted and they had hysteresis loop in isotherm graph.

Table 28 BET surface area, pore size and pore volume of commercial HZSM-5 and synthesized HZSM-5 catalyts

Sample	Surface area ^a (m ² /g)	Pore size ^b (nm)	Pore volume ^c (cm ³ /g)
Commercial HZSM-5	257.972	5.3	0.268361
Synthesized HZSM-5	296.265	2.6	0.030498

^a Determined from BET method

^{b,c} Determined from BJH desorption method

From Figure 49, N₂ adsorption-desorption isotherm graph of commercial HZSM-5 and synthesized HZSM-5 catalyts was investigated and plotted as type IV. Both of catalyts had hysteresis loops in range P/P₀ (0.5-0.9). It can be confirmed that both catalyts were mesoporous pore structure. Furthermore, amount of N₂ adsorption of commercial HZSM-5 catalyst was higher than synthesized HZSM-5 catalyst. Therefore, this data involved with pore volume in synthesized HZSM-5 catalyst, which had pore volume less than commercial HZSM-5 catalyst about 10 times.

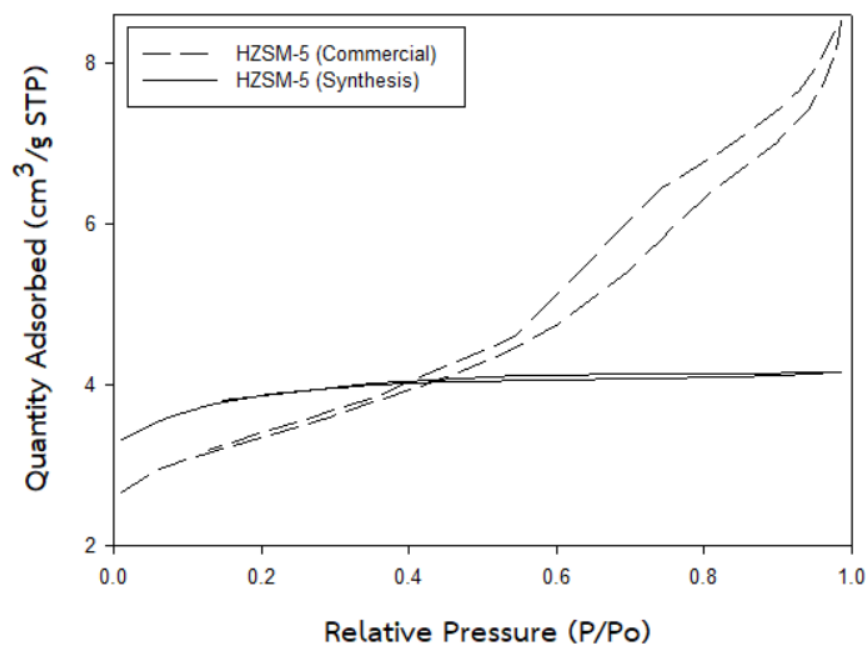


Figure 49 Isotherm graph of commercial HZSM-5 and synthesized HZSM-5 catalysts

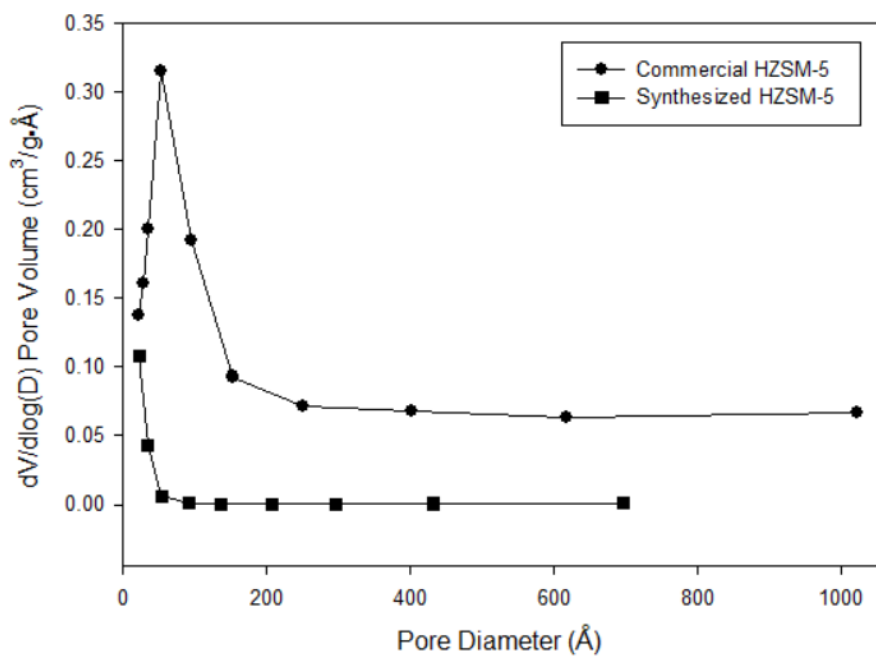


Figure 50 Pore size distribution of commercial HZSM-5 and synthesized HZSM-5 catalysts

Pore size distribution is plotted by pore volume versus pore diameter and displayed in Figure 50. Commercial HZSM-5 catalyst had distribution at low pore diameter about (50 Å or 5 nm). In case of synthesized HZSM-5 catalyst, it had similar distribution at low pore diameter but less than commercial HZSM-5 catalyst about (20 Å or 2 nm).

4.3.5 Ammonia temperature-programmed desorption (NH₃-TPD)

In part 4.3, acidity of each catalysts was detected by ammonia temperature-programmed desorption. From Figure 51, the desorption profile for both catalysts was divided into two desorption peaks; weak acid site and moderate to strong acid site, especially synthesized HZSM-5 catalyst had desorption peaks clearly. In order to calculate acidity, areas under peak were used to calculate. It seemed that the synthesized HZSM-5 catalyst had higher acidity than the commercial HZSM-5 catalyst. After calculation, Table 29 can be confirmed that the synthesized HZSM-5 catalyst had greater total acidity than the commercial HZSM-5 catalyst.

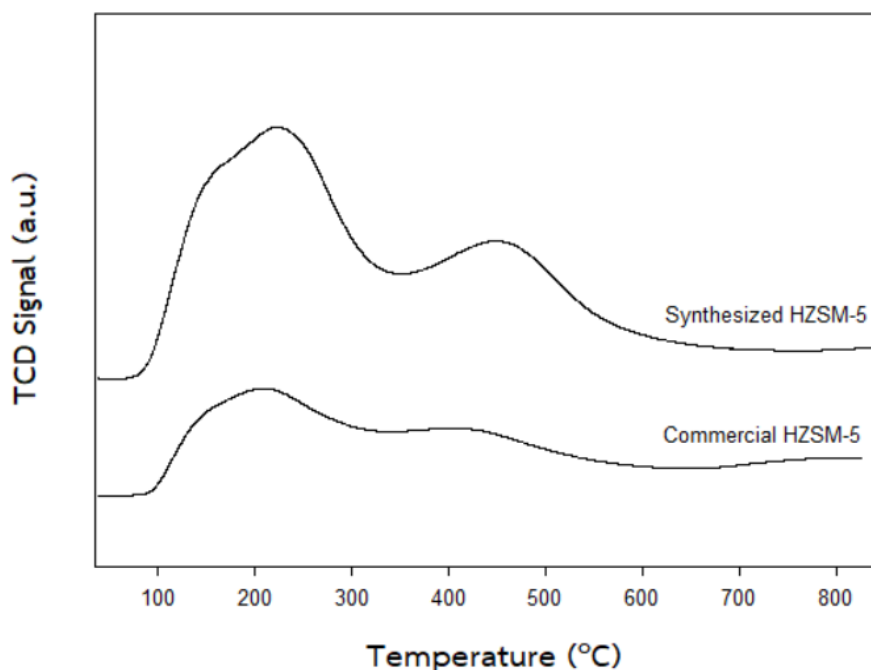


Figure 51 NH₃-TPD profiles of commercial HZSM-5 and synthesized HZSM-5 catalysts

Table 29 Total acidity of commercial HZSM-5 and synthesized HZSM-5 catalysts from NH₃-TPD.

Catalyst	Temperature (°C)		NH ₃ desorption ($\mu\text{mol NH}_3/\text{g}_{\text{cat}}$)		Total acidity ($\mu\text{mol NH}_3/\text{g}_{\text{cat}}$)
	1 st peak	2 nd peak	Weak	Medium to strong	
Commercial HZSM-5	200	410	439.39	517.65	957.04
Synthesized HZSM-5	210	439	1380.12	830.57	2210.69

4.3.6 Thermal gravimetric and differential analysis (TG/DTA)

Decomposition from temperature of fresh commercial HZSM-5 and synthesized HZSM-5 catalysts are characterized by TG/DTA technique and displayed in Figures 52 and 53. The thermal decomposition of both catalysts is started and recorded at 30 °C until 600 °C. From these results, it was separated into two zones. First zone refers to the temperature below 200 °C or it can be said this zone was vaporizing of water composition in both catalysts and the other zone may be volatilization of inorganic molecular in temperature above 200 °C. The amount of weight loss of both catalysts is shown in Table 30. From these data, it can be concluded that the synthesized HZSM-5 catalyst had higher moisture than the commercial HZSM-5 catalyst because synthesized HZSM-5 catalyst had high loss of weight in initial temperature (4.34 %), while commercial HZSM-5 catalyst had weight loss only 2.02 %. Although the synthesized HZSM-5 catalyst had high weight loss in initial temperature, the weight loss of this catalysts was minimal (0.67 %) when temperature increased more than 200 °C until 600 °C. In addition, the weight loss of commercial HZSM-5 catalyst was 1.1 %. In studied temperature range of 200 °C – 400 °C, both catalysts had only slight weight loss.

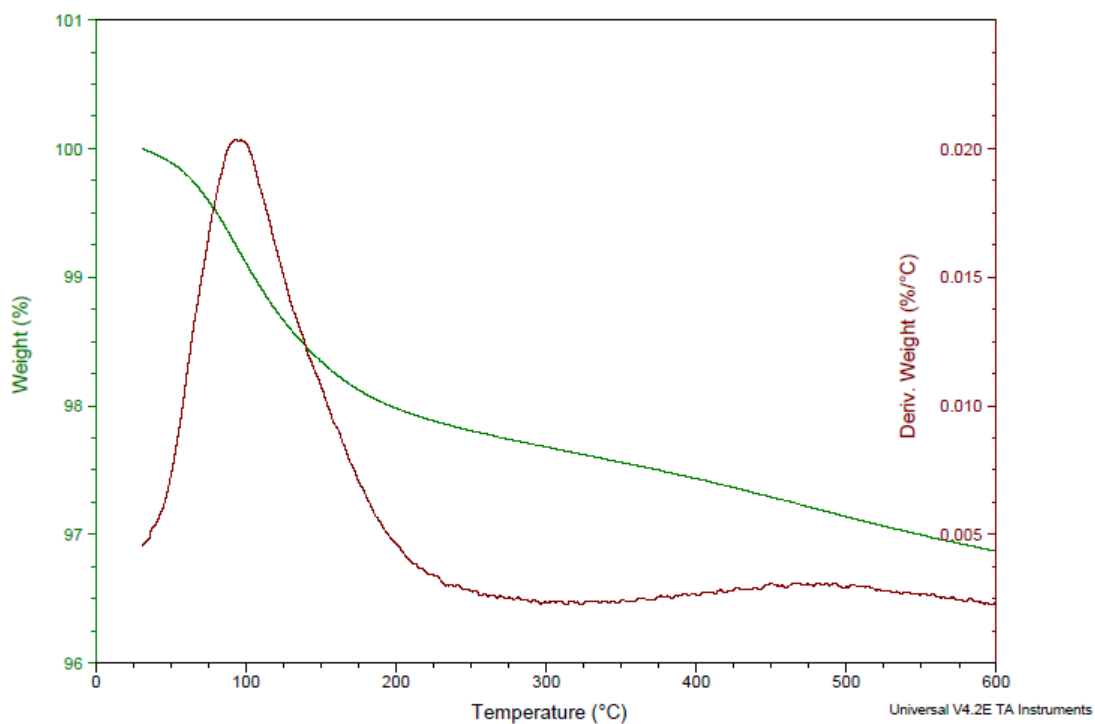


Figure 52 TG/DTA profile of commercial HZSM-5 catalyst

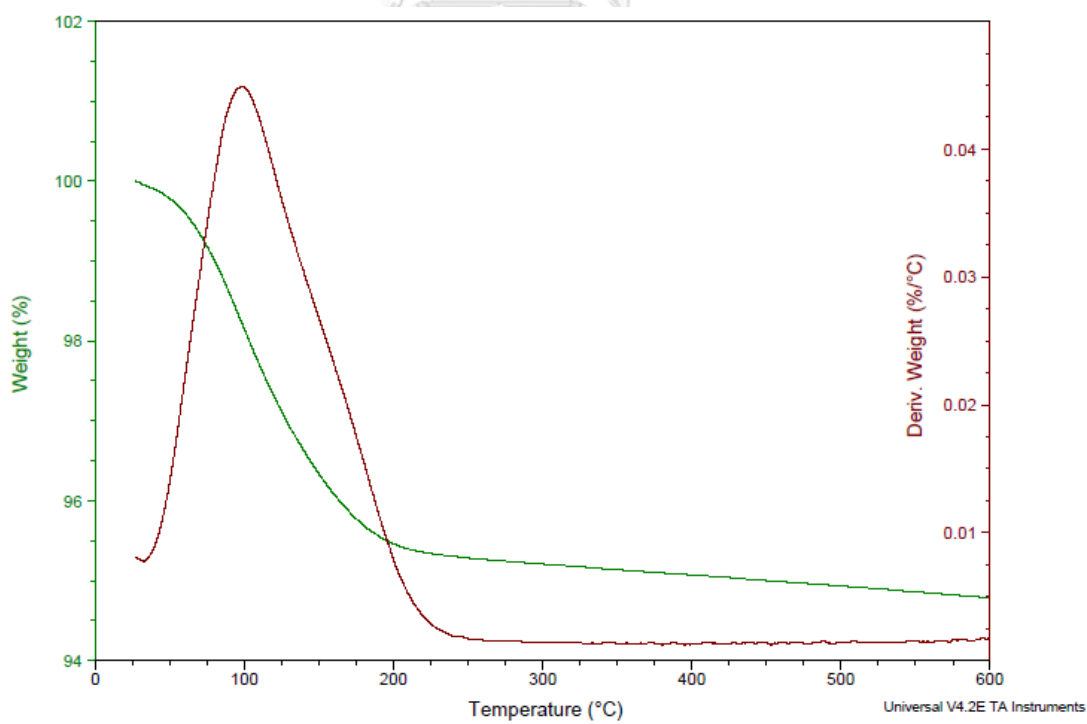


Figure 53 TG/DTA profile of synthesized HZSM-5 catalyst

Table 30 Weight loss of commercial HZSM-5 and synthesized HZSM-5 catalysts from TG/DTA

Catalysts	Weight at temperature (%)			
	30 °C	200 °C	400 °C	600 °C
Commercial HZSM-5	100.00	97.98	97.43	96.88
Synthesized HZSM-5	99.8	95.46	95.07	94.79

4.3.7 Ethanol dehydration reaction

Since ethanol dehydration reaction over commercial HZSM-5 catalyst was completed, the catalytic activity of this catalysts was compared with synthesized HZSM-5 catalyst in same condition and reaction. The mixture of products was analyzed by GC-FID and rearranged for plotting comparative graphs of conversion, diethyl ether yield, ethylene yield and acetaldehyde yield versus temperature in Figures 54 to 57.

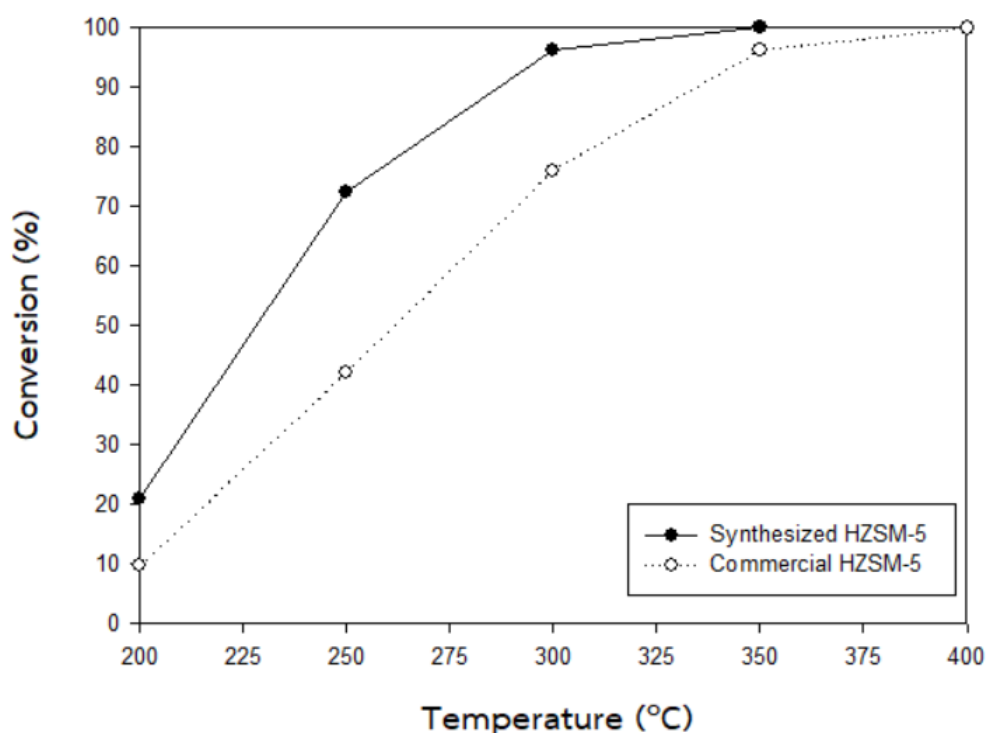


Figure 54 Catalytic activity of commercial HZSM-5 and synthesized HZSM-5 catalysts in ethanol dehydration reaction

Figure 54 shows the catalytic activity of both catalysts at temperature range 200 °C – 400 °C. It was found both catalysts had similar trend that conversion increased with raising temperature and synthesized HZSM-5 catalyst had higher activity than commercial HZSM-5 catalyst at all temperature range. The conversion at temperature of 200 °C of synthesized catalyst had high conversion over 20 %. Moreover, this catalyst had conversion more than 90 % starting from temperature 300 °C, whereas the commercial HZSM-5 catalyst had to use temperature 350 °C in order to obtain the conversion over 90 %. The reason that was attributed high catalytic activity in part 4.3 involved properties of catalyst such as BET surface area, total acidity, etc. same part 4.1 and part 4.2.

In Figure 55, ethylene yields of both of catalysts were calculated from the product of conversion and ethylene selectivity and plotted ethylene yield versus temperature.

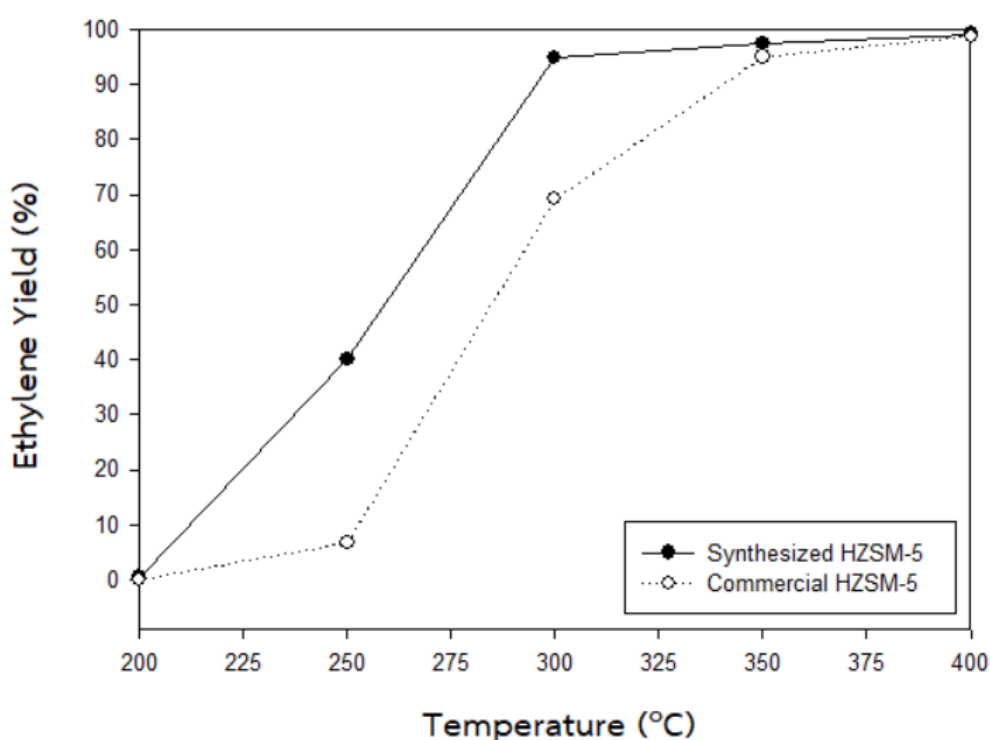


Figure 55 Ethylene yield of commercial HZSM-5 and synthesized HZSM-5 catalysts in ethanol dehydration reaction

Normally, ethanol dehydration reaction to ethylene is endothermic reaction. It prefers high temperature to obtain ethylene that has consistent with result from Figure 55. Both catalysts had poor ethylene yield at low temperature or it can be said that ethylene was not produced at low temperature (0% ethylene yield at 200 °C) and had well ethylene yield at high temperature. After temperature increased more than 200 °C, the synthesized HZSM-5 catalyst had greater ethylene yield than commercial HZSM-5 catalyst. In addition, ethylene yield of synthesized HZSM-5 catalyst was over 90 % at 300 °C. It was due to of ethylene was the main product at high temperature, so it had high selectivity. When calculated ethylene yield, it made high ethylene yield, too.

For diethyl ether yield, it is exothermic reaction. Therefore, it is main product at low temperature, but ethylene prefers to occur at high temperature. For this reason, it makes diethyl ether yield profile as shown in Figure 56.

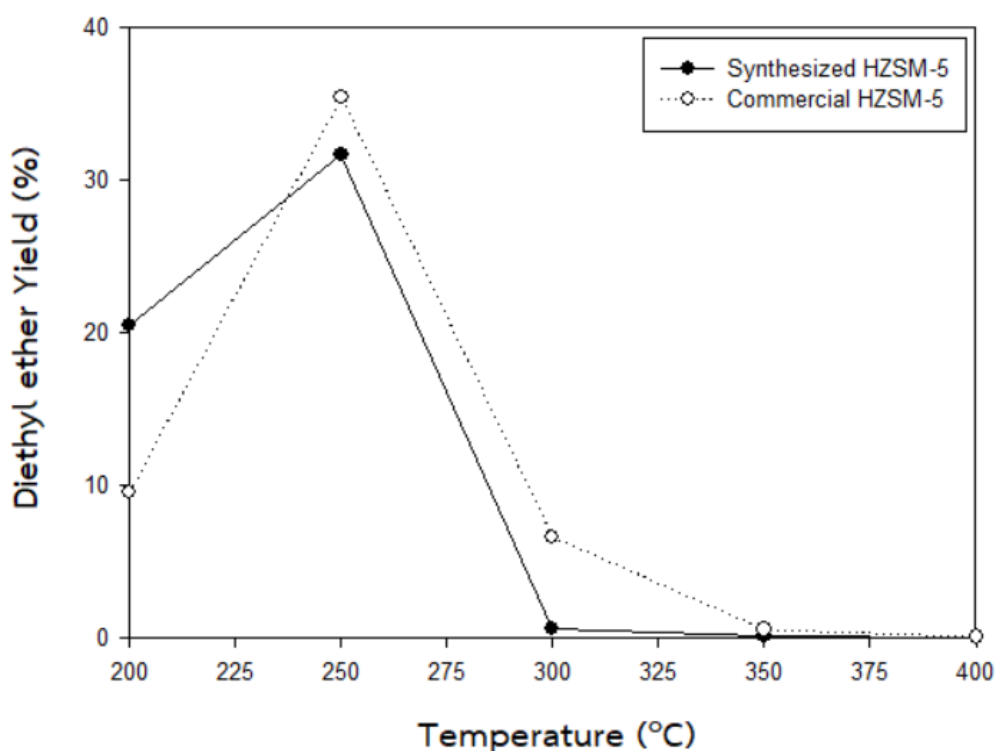


Figure 56 Diethyl ether yield of commercial HZSM-5 and synthesized HZSM-5 catalysts in ethanol dehydration reaction

Diethyl ether yield profile of both catalysts had similar trend. It increased until temperature up to 250 °C, and then diethyl ether yield decreased when temperature rased due to diethyl ether cracking and hydrolysis occurred ³³. Beside, the synthesized HZSM-5 catalyst had better activity than the commercial HZSM-5 catalyst in all temperature range and had higher diethyl ether yield at initial temperature about 20.4 %. However, commercial HZSM-5 catalyst had higer diethyl ether yield than the synthesized HZSM-5 catalyst after temperature over 250 °C. From Figure 56, it can be concluded that the optimal temperature that produced the highest diethyl ether yield of both catalysts was about 250 °C. Furthermore, the commercial HZSM-5 catalyst had diethyl ether yield over 35 % while synthesized HZSM-5 catalyst had only 32 % at temperature 250 °C.

Actually, acetaldehyde is a byproduct from ethanol dehydration reaction over zeolite catalysts such as HZSM-5. It slightly occurs after this reaction completed. Therefore, acetaldehyde yield is low at studied temperature as displayed in Figure 57.

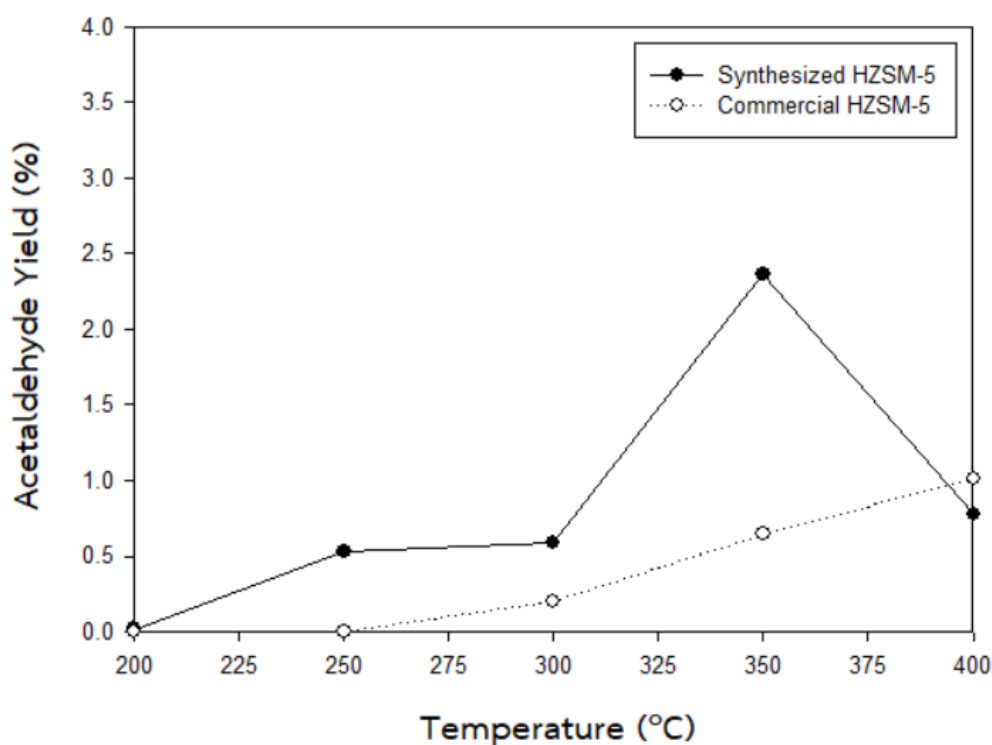


Figure 57 Acetaldehyde yield of commercial HZSM-5 and synthesized HZSM-5 catalysts in ethanol dehydration reaction

Figure 57 shows acetaldehyde yield profile for temperature of 200 °C to 400 °C. Acetaldehyde yield depended on temperature, so it increased when temperature increased due to dehydrogenation of ethanol reaction was endothermic reaction which preferred to occur at high temperature. From Figure 57, it can be concluded that acetaldehyde was the product that had the lowest yield among ethylene and diethyl ether. The synthesized HZSM-5 catalyst had higher acetaldehyde than the commercial HZSM-5 catalyst when temperature over 350 °C. It should be noted that the acetaldehyde yield dropped at temperature 400 °C over synthesized HZSM-5 catalyst. This is due to ethylene preferred to occur more than acetaldehyde so it made acetadehyde yield decreased.

Table 31 shows ethanol conversion from ethanol dehydration reaction at temperature from 200 °C - 400 °C , atmospheric pressure and WHSV 22.9 h⁻¹.

Table 31 Ethanol conversion of all catalysts

Catalysts	Ethanol conversion (%)				
	200 °C	250 °C	300 °C	350 °C	400 °C
ZSM-5 Si/Al 20	7.1	12.8	16.4	43.1	70.3
ZSM-5 Si/Al 40	2.8	9.4	12.0	20.5	38.2
ZSM-5 Si/Al 60	0.0	0.0	1.2	2.1	3.5
Commercial HZSM-5	9.6	42.1	75.9	96.1	99.8
P-HZSM-5	12.7	30.8	70.5	89.8	97.5
Pd-HZSM-5	22.3	60.73	94.8	99.3	100.0
Pd-P-HZSM-5	11.3	39.3	77.2	97.5	100.0
Pd-P-HZSM-5 (Co-impregnation)	12.7	48.1	84.1	97.4	100.0
Synthesized HZSM-5	20.9	72.3	96.1	100	100.0

From this data, ethanol conversion of all catalysts had increased when temperature increased. Modified HZSM-5 catalysts had the highest conversion at 200 °C. When temperature was over 200 °C , synthesized HZSM-5 catalysts had better activity than Pd-HZSM-5 catalysts.

CHAPTER 5

CONCLUSIONS AND RECOMMENDATIONS

In chapter 5, it concludes the experimental results in parts 4.1, 4.2 and 4.3 of the synthesized ZSM-5, HZSM-5, modified HZSM-5 and synthesized HZSM-5 catalysts that were tested via ethanol dehydration reaction and characterized with various techniques. In addition, the recommendations of ethanol dehydration reaction also include in this chapter. The results were compared in each parts and summed up as follows.

5.1 Conclusion

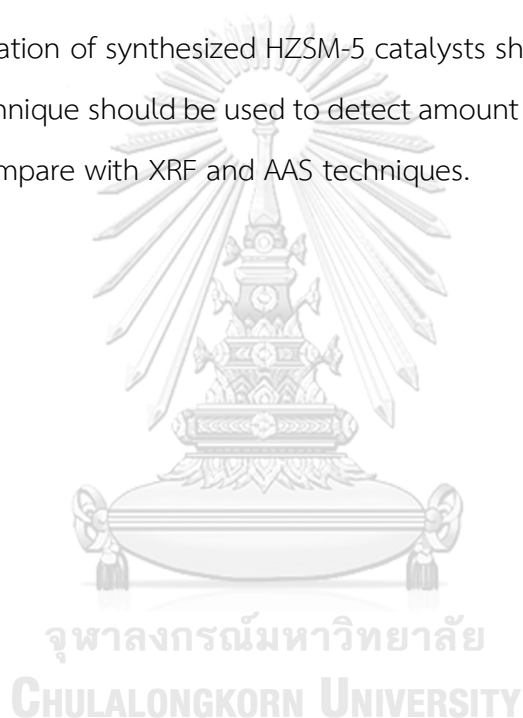
1. ZSM-5 catalysts with molar ratio of Si/Al = 20 exhibits the highest activity among other ratios (70.3 % ethanol conversion at 400 °C).
2. Increasing ratio of synthesized ZSM-5 catalysts by adding sodium silicate solution results in excess of silicon that joins together and forms into SiO₂ after calcination.
3. SiO₂ in ZSM-5 catalysts with molar ratio of Si/Al = 40 and 60 has effect on decreasing total acidity of catalysts.
4. The factors, which lead to the highest activity in ethanol dehydration reaction, are total acidity and physical properties such as surface area.
5. Palladium metal enhances activity of ethanol dehydration reaction.
 - a. Pd-HZSM-5 gives the highest activity among modified HZSM-5 catalysts. Moreover, it gives conversion over 90 % at temperature of 300 °C having almost 100 % of ethanol conversion at temperature 350 °C .
 - b. Increasing surface area and total acidity
 - c. Effect of palladium can facilitate ethylene formation at low temperature.

6. Effect of phosphoric acid on activity of ethanol dehydration reaction.
 - a. It decreases surface area and pore volume by pore blockage of phosphorus species.
 - b. It makes ethylene slightly occurs at low temperature, while for the commercial HZSM-5, ethylene does not occur at temperature of 200 °C.
 - c. Decreasing in surface area after impregnation with phosphoric acid effect on activity in ethanol dehydration. It decreases in activity when compared with commercial HZSM-5 catalysts.
 - d. Increasing of total acidity
7. Both of phosphoric acid and palladium metal do not affect morphology of HZSM-5 catalysts.
8. Bimetallic (phosphorus and palladium) impregnation affects ethylene formation at low temperature. It makes ethylene yield is slightly higher than monometallic impregnation.
9. Step by step impregnation and co-impregnation do not affect the morphology, physical properties and catalytic activity.
10. Synthesized HZSM-5 catalysts in ethanol dehydration reaction
 - a. It has actual molar ratio of Si/Al less than calculation (actual Si/Al 15.03) while commercial HZSM-5 catalysts has only (1.75).
 - b. Synthesized HZSM-5 catalyst has coke formation more than commercial HZSM-5 catalyst after ethanol dehydration complete.
 - c. For synthesis of ZSM-5 and HZSM-5 catalysts, they give total acidity more than commercial catalysts.
 - d. Synthesized HZSM-5 catalyst has weight loss in initial temperature (below 200 °C) more than commercial, but when temperature is over 200 °C, it has lower weight loss.

- e. Synthesized HZSM-5 catalysts has higher activity than commercial HZSM-5 catalyst and other catalysts in parts 4.1 and 4.2 when temperature is more than 200 °C

5.2 Recommendations

1. The stability of all catalysts should be studied in future.
2. Pyridine-IR technique should be used to investigate type of acid (Brønsted acid site and Lewis acid site).
3. Modification of synthesized HZSM-5 catalysts should be further studied.
4. ICP technique should be used to detect amount of element in bulk catalyst and compare with XRF and AAS techniques.



REFERENCES

1. Nejat, P.; Jomehzadeh, F.; Taheri, M. M.; Gohari, M.; Abd. Majid, M. Z., A global review of energy consumption, CO₂ emissions and policy in the residential sector (with an overview of the top ten CO₂ emitting countries). *Renewable and Sustainable Energy Reviews* **2015**, *43*, 843-862.
2. Bhattacharya, M.; Paramati, S. R.; Ozturk, I.; Bhattacharya, S., The effect of renewable energy consumption on economic growth: Evidence from top 38 countries. *Applied Energy* **2016**, *162*, 733-741.
3. Thatoi, H.; Dash, P. K.; Mohapatra, S.; Swain, M. R., Bioethanol production from tuber crops using fermentation technology: a review. *International Journal of Sustainable Energy* **2014**, *35* (5), 443-468.
4. Soh, J. C.; Chong, S. L.; Hossain, S. S.; Cheng, C. K., Catalytic ethylene production from ethanol dehydration over non-modified and phosphoric acid modified Zeolite H-Y (80) catalysts. *Fuel Processing Technology* **2017**, *158*, 85-95.
5. Kamsuwan, T.; Praserttham, P.; Jongsomjit, B., Diethyl Ether Production during Catalytic Dehydration of Ethanol over Ru- and Pt- modified H-beta Zeolite Catalysts. *J Oleo Sci* **2017**, *66* (2), 199-207.
6. Phung, T. K.; Proietti Hernández, L.; Lagazzo, A.; Busca, G., Dehydration of ethanol over zeolites, silica alumina and alumina: Lewis acidity, Brønsted acidity and confinement effects. *Applied Catalysis A: General* **2015**, *493*, 77-89.
7. Wu, C.-Y.; Wu, H.-S., Ethylene Formation from Ethanol Dehydration Using ZSM-5 Catalyst. *ACS Omega* **2017**, *2* (8), 4287-4296.
8. Chareonpanich, M.; Namto, T.; Kongkachuichay, P.; Limtrakul, J., Synthesis of ZSM-5 zeolite from lignite fly ash and rice husk ash. *Fuel Processing Technology* **2004**, *85* (15), 1623-1634.

9. Shirazi, L.; Jamshidi, E.; Ghasemi, M. R., The effect of Si/Al ratio of ZSM-5 zeolite on its morphology, acidity and crystal size. *Crystal Research and Technology* **2008**, *43* (12), 1300-1306.
10. Madeira, F. F.; Gnep, N. S.; Magnoux, P.; Vezin, H.; Maury, S.; Cadran, N., Mechanistic insights on the ethanol transformation into hydrocarbons over HZSM-5 zeolite. *Chemical Engineering Journal* **2010**, *161* (3), 403-408.
11. Phung, T. K.; Radikapratama, R.; Garbarino, G.; Lagazzo, A.; Riani, P.; Busca, G., Tuning of product selectivity in the conversion of ethanol to hydrocarbons over H-ZSM-5 based zeolite catalysts. *Fuel Processing Technology* **2015**, *137*, 290-297.
12. Van der Borght, K.; Galvita, V. V.; Marin, G. B., Ethanol to higher hydrocarbons over Ni, Ga, Fe-modified ZSM-5: Effect of metal content. *Applied Catalysis A: General* **2015**, *492*, 117-126.
13. Ramesh, K.; Jie, C.; Han, Y.-F.; Borgna, A., Synthesis, Characterization, and Catalytic Activity of Phosphorus Modified H-ZSM-5 selective ethanol dehydration. *Journal of industrial and engineering chemistry* **2010**, *49*, 4080-4090.
14. Kumar, N.; Nieminen, V.; Demirkan, K.; Salmi, T.; Murzin, D. Y.; Laine, E., Effect of synthesis time and mode of stirring on physico-chemical and catalytic properties of ZSM-5 zeolite catalysts. *Applied Catalysis A: General* **2002**, *235* (1-2), 113-123.
15. Jacobsen, C. J. H.; Madsen, C.; Houzvicka, J.; Schmidt, I.; Carlsson, A., Mesoporous Zeolite Single Crystals. *J. Am. Chem. Soc* **2000**, *122*, 7116-7117.
16. Zhou, J.; Hua, Z.; Liu, Z.; Wu, W.; Zhu, Y.; Shi, J., Direct Synthetic Strategy of Mesoporous ZSM-5 Zeolites by Using Conventional Block Copolymer Templates and the Improved Catalytic Properties. *ACS Catalysis* **2011**, *1* (4), 287-291.
17. Weitkamp, J., Zeolites and catalysis. *Solid State Ionics* **2000**, *131* (1-2).
18. Firoozi, M.; Baghalha, M.; Asadi, M., The effect of micro and nano particle sizes of H-ZSM-5 on the selectivity of MTP reaction. *Catalysis Communications* **2009**, *10* (12), 1582-1585.
19. Liu, N.; Zhu, X.; Hua, S.; Guo, D.; Yue, H.; Xue, B.; Li, Y., A facile strategy for preparation of phosphorus modified HZSM-5 shape-selective catalysts and its performances in disproportionation of toluene. *Catalysis Communications* **2016**, *77*, 60-64.

20. Chareonpanicha, M.; Boonfuenga, T.; Limtrakul, J., Production of aromatic hydrocarbons from Mae-Moh lignite *Fuel Processing Technology* **2002**, 79 (2), 171-179.
21. Huangfu, J.; Mao, D.; Zhai, X.; Guo, Q., Remarkably enhanced stability of HZSM-5 zeolite co-modified with alkaline and phosphorous for the selective conversion of bio-ethanol to propylene. *Applied Catalysis A: General* **2016**, 520, 99-104.
22. Zhang, M.; Yu, Y., Dehydration of Ethanol to Ethylene. *Industrial & Engineering Chemistry Research* **2013**, 52 (28), 9505-9514.
23. Pan, L. R., Development review of catalysts for ethanol dehydration to produce ethylene. *Speciality Petrochem* **1986**, 4, 41-64.
24. Pearson, D. E.; Tanner, R. D.; Picciotto, I. D.; Sawyer, J. S.; Jr, J. H. C., phosphoric acid systems. 2. catalytic conversion of fermentation ethano to ethylene. *Ind. Eng. Chem. Prod. Res. Dev.* **1981**, 20 (4), 734-740.
25. Pines, H.; Haag, W., Alumina: Catalyst and Support. I. Alumina, its Intrinsic Acidity and Catalytic Activity. *Journal of the American Chemical Society* **1960**, 2471-2483.
26. Zhu, X. R., Dehydration of bioethanol into ethylene over modified nano-scale HZSM-5 catalysts. . *Dalian University of Technology: Dalian* **2007**.
27. Mizuno, N.; Misnno, M., Heteropolyacid catalysts. *Current Opinion in Solid State and Materials Science* **1997**, 2 (1), 84-89.
28. Machado, N.; Calsavara, V.; Astrath, N.; Matsuda, C.; Paesanojunior, A.; Baesso, M., Obtaining hydrocarbons from ethanol over iron-modified ZSM-5 zeolites. *Fuel* **2005**, 84 (16), 2064-2070.
29. Zaki, T., Catalytic dehydration of ethanol using transition metal oxide catalysts. *J Colloid Interface Sci* **2005**, 284 (2), 606-13.
30. Varisli, D.; Dogu, T.; Dogu, G., Ethylene and diethyl-ether production by dehydration reaction of ethanol over different heteropolyacid catalysts. *Chemical Engineering Science* **2007**, 62 (18-20), 5349-5352.
31. Zhang, D.; Wang, R.; Yang, X., Effect of P Content on the Catalytic Performance of P-modified HZSM-5 Catalysts in Dehydration of Ethanol to Ethylene. *Catalysis Letters* **2008**, 124 (3-4), 384-391.

32. Zhan, N.; Hu, Y.; Li, H.; Yu, D.; Han, Y.; Huang, H., Lanthanum–phosphorous modified HZSM-5 catalysts in dehydration of ethanol to ethylene: A comparative analysis. *Catalysis Communications* **2010**, *11* (7), 633-637.
33. Phung, T. K.; Busca, G., Diethyl ether cracking and ethanol dehydration: Acid catalysis and reaction paths. *Chemical Engineering Journal* **2015**, *272*, 92-101.
34. Bagal, L. K.; Patil, J. Y.; Vaishampayan, M. V.; Mulla, I. S.; Suryavanshi, S. S., Effect of Pd and Ce on the enhancement of ethanol vapor response of SnO₂ thick films. *Sensors and Actuators B: Chemical* **2015**, *207*, 383-390.
35. Chen, B.; Lu, J.; Wu, L.; Chao, Z., Dehydration of bio-ethanol to ethylene over iron exchanged HZSM-5. *Chinese Journal of Catalysis* **2016**, *37* (11), 1941-1948.
36. de Oliveira, T. K. R.; Rosset, M.; Perez-Lopez, O. W., Ethanol dehydration to diethyl ether over Cu-Fe/ZSM-5 catalysts. *Catalysis Communications* **2018**, *104*, 32-36.
37. Zhang, X.; Lin, L.; Zhang, T.; Liu, H.; Zhang, X., Catalytic dehydration of lactic acid to acrylic acid over modified ZSM-5 catalysts. *Chemical Engineering Journal* **2016**, *284*, 934-941.
38. Abd Rashid, R.; Shamsudin, R.; Abdul Hamid, M. A.; Jalar, A., Low temperature production of wollastonite from limestone and silica sand through solid-state reaction. *Journal of Asian Ceramic Societies* **2018**, *2* (1), 77-81.
39. Li, J.; Ma, H.; Sun, Q.; Ying, W.; Fang, D., Effect of iron and phosphorus on HZSM-5 in catalytic cracking of 1-butene. *Fuel Processing Technology* **2015**, *134*, 32-38.
40. Figueiredo, A. L.; Araujo, A. S.; Linares, M.; Peral, Á.; García, R. A.; Serrano, D. P.; Fernandes, V. J., Catalytic cracking of LDPE over nanocrystalline HZSM-5 zeolite prepared by seed-assisted synthesis from an organic-template-free system. *Journal of Analytical and Applied Pyrolysis* **2016**, *117*, 132-140.



Appendix A

Calculation catalysts preparation

For ZSM-5 catalysts with molar ratio of Si/Al 20 was prepared by hydrothermal method. In experiment part 4.1, Sodium silicate solution, aluminium nitrate nonahydrate and tetrapropylammonium bromide were mixed in distilled water.

Precursor

- | | | |
|---|--|--------------------|
| - Sodium silicate solution
(≈ 27 wt% SiO_2) | SiO_2 | M.W. = 60 g / mol |
| - Aluminium nitrate nonahydrate | $\text{Al}(\text{NO}_3)_3 \cdot 9\text{H}_2\text{O}$ | M.W. = 375 g / mol |
| - Tetrapropylammonium bromide
(TPABr) | $\text{C}_{16}\text{H}_{36}\text{BrN}$ | M.W. = 266 g / mol |

Calculation Substance

SiO_2

Based on 1 mol of SiO_2	60	g
27% SiO_2 from Sodium silicate solution	222.22	g
Density of Sodium silicate solution	1.39	g/cm^3
There is 60 g of SiO_2 in Sodium silicate solution 222.22 g or 159.85 cm^3		

$\text{Al}(\text{NO}_3)_3 \cdot 9\text{H}_2\text{O}$

Based on 0.05 mol of $\text{Al}(\text{NO}_3)_3 \cdot 9\text{H}_2\text{O}$	375×0.05	g
$\text{Al}(\text{NO}_3)_3 \cdot 9\text{H}_2\text{O}$	18.75	g

$\text{C}_{16}\text{H}_{36}\text{BrN}$

Based on 0.03 mol of $\text{C}_{16}\text{H}_{36}\text{BrN}$	266×0.03	g
$\text{C}_{16}\text{H}_{36}\text{BrN}$	7.98	g

Molar ratio of Si : Al : TPABr (Si/Al 1/0.05 or 20)

Si : Al : TPABr (Molar ratio)	1 : 0.05 : 0.03
Si : Al : TPABr (Gram ratio)	159.85 : 18.75 : 7.98
Si : Al : TPABr (Gram ratio)	15.985 : 1.875 : 0.798

Appendix B

Calculation catalysts preparation by incipient wetness impregnation

Metal Loading 0.5 % of Pd on HZSM-5 catalyst by incipient wetness impregnation

Precursor

- 10% Tetraamminepalladium(II)nitrate in H₂O M.W. = 298.53 g / mol
(Pd(NO₃)₂•4(NH₃))
- Palladium M.W. = 106.42 g / mol

Based on solution 100 ml , it has 10 ml of Pd(NO₃)₂•4(NH₃)

Density of Tetraamminepalladium(II)nitrate 1.03 g / cm³

Concentration of Pd(NO₃)₂•4(NH₃)

$$\frac{10}{100} \% \times 1000 \frac{\text{cm}^3}{\text{L}} \times 1.03 \frac{\text{g}}{\text{cm}^3} \times \frac{1}{298.53} \frac{\text{mol}}{\text{g}} = 0.345 \frac{\text{mol}}{\text{L}}$$

Based on Pd-HZSM-5 catalyst 1 g

There is 0.005 g of palladium in HZSM-5 catalysts 1 - 0.005 g

Therefore 0.995 g of HZSM-5 catalysts

For Palladium 0.005 g 0.005/106.42 mol

Palladium 0.00004698 mol

For mole balance equation

$$\begin{aligned} N_1 &= N_2 \quad \text{or} \quad C_1 V_1 = C_2 V_2 \\ 0.345 \times V_1 \text{ (mol/L)} &= 0.00004698 \text{ mol} \\ V_1 &= 0.0001361 \text{ L} \\ V_1 &= 136.1 \text{ } \mu\text{L} \end{aligned}$$

136.1 μL of 10% Tetraamminepalladium(II)nitrate in H₂O is used to prepare 0.5% wt Pd-HZSM-5 catalysts

Pore volume of 1 g HZSM-5 catalyst = 550 μL

Thus, It must add distilled water equal 550 - 136.1 = 413.9 μL

Metal Loading 5 % of P on HZSM-5 catalyst by incipient wetness impregnation

Precursor

- 85% Phosphoric acid (H_3PO_4) M.W. = 98 g / mol
- Phosphorus M.W. = 31 g / mol

Based on solution 100 ml , it has 85 ml of H_3PO_4

Density of Phosphoric acid 1.71 g / cm^3

Concentration of Phosphoric acid

$$\frac{85}{100} \% \times 1000 \frac{\text{cm}^3}{\text{L}} \times 1.71 \frac{\text{g}}{\text{cm}^3} \times \frac{1 \text{ mol}}{98 \text{ g}} = 14.832 \frac{\text{mol}}{\text{L}}$$

Based on P-HZSM-5 catalyst 1 g

There is 0.05 g of phosphorus in HZSM-5 catalysts 1 - 0.05 g

Therefore 0.95 g of HZSM-5 catalysts

For Phosphorus 0.05 g 0.05/31 mol

Phosphorus 0.001613 mol

For mole balance equation

$$N_1 = N_2 \quad \text{or} \quad C_1 V_1 = C_2 V_2$$

$$14.832 \times V_1 \text{ (mol/L)} = 0.001613 \text{ mol}$$

$$V_1 = 0.00010875 \text{ L}$$

$$V_1 = 108.75 \text{ } \mu\text{L}$$

108.75 μL of 85% Phosphoric acid is used to prepare 5% wt P-HZSM-5 catalysts

Pore volume of 1 g HZSM-5 catalyst = 550 μL

Thus, It must add distilled water equal 550 - 108.75 = 441.25 μL

Metal Loading 0.5% of Pd and 5 % of P on HZSM-5 catalyst by incipient wetness Co-impregnation

Precursor

- 10% Tetraamminepalladium(II)nitrate in H₂O M.W. = 298.53 g / mol
(Pd(NO₃)₂•4(NH₃))
- Palladium M.W. = 106.42 g / mol
- 85% Phosphoric acid (H₃PO₄) M.W. = 98 g / mol
- Phosphorus M.W. = 31 g / mol

Based on solution 100 ml , it has 10 ml of Pd(NO₃)₂•4(NH₃) and 85 ml of H₃PO₄

Density of Tetraamminepalladium(II)nitrate 1.03 g / cm³

Density of Phosphoric acid 1.71 g / cm³

Concentration of Pd(NO₃)₂•4(NH₃)

$$\frac{10}{100} \% \times 1000 \frac{\text{cm}^3}{\text{L}} \times 1.03 \frac{\text{g}}{\text{cm}^3} \times \frac{1}{298.53} \frac{\text{mol}}{\text{g}} = 0.345 \frac{\text{mol}}{\text{L}}$$

Concentration of Phosphoric acid

$$\frac{85}{100} \% \times 1000 \frac{\text{cm}^3}{\text{L}} \times 1.71 \frac{\text{g}}{\text{cm}^3} \times \frac{1}{98} \frac{\text{mol}}{\text{g}} = 14.832 \frac{\text{mol}}{\text{L}}$$

Based on P-HZSM-5 catalyst 1 g

There is 0.05 g of phosphorus in HZSM-5 catalysts 1 - 0.05 g

And There is 0.005 g of palladium in HZSM-5 catalysts 0.95-0.005

Therefore 0.945 g of HZSM-5 catalysts

For Palladium 0.005 g 0.005/106.42 mol

Palladium 0.00004698 mol

For Phosphorus 0.05 g 0.05/31 mol

Phosphorus 0.001613 mol

For mole balance equation

$$\begin{aligned}
 N_1 &= N_2 \quad \text{or} \quad C_1V_1 = C_2V_2 \\
 0.345 \times V_1 \text{ (mol/L)} &= 0.00004698 \text{ mol} \\
 V_1 &= 0.0001361 \text{ L} \\
 V_1 &= 136.1 \text{ } \mu\text{L}
 \end{aligned}$$

136.1 μL of 10% Tetraamminepalladium(II)nitrate in H_2O is used to prepare 0.5% wt Pd-HZSM-5 catalysts

For mole balance equation

$$\begin{aligned}
 N_1 &= N_2 \quad \text{or} \quad C_1V_1 = C_2V_2 \\
 14.832 \times V_1 \text{ (mol/L)} &= 0.001613 \text{ mol} \\
 V_1 &= 0.00010875 \text{ L} \\
 V_1 &= 108.75 \text{ } \mu\text{L}
 \end{aligned}$$

108.75 μL of 85% Phosphoric acid is used to prepare 5% wt P-HZSM-5 catalysts

Total of 10% Tetraamminepalladium(II)nitrate in H_2O and Phosphoric acid

$$= 136.1 + 108.75 = 244.85 \text{ } \mu\text{L}$$

Pore volume of 1 g HZSM-5 catalyst = 550 μL

Thus, It must add distilled water equal $550 - 244.85 = 305.15 \text{ } \mu\text{L}$

Appendix C

Modification ZSM-5 catalyst by ion-exchange

ZSM-5 catalysts was modified with 1 M NH_4NO_3 by ion-exchange method

Precursor

- Ammonium nitrate (NH_4NO_3) M.W. 80 g / mol

Based on 1 M of NH_4NO_3

For solution	1,000 ml	consists of NH_4NO_3	1 mol
		consists of NH_4NO_3	80 g

Adding NH_4NO_3 80 g into distilled water for preparing 1 M of NH_4NO_3

ZSM-5 catalyst was mixed with 1 M NH_4NO_3 for 2 h. over 3 round and washed with distilled water until pH equal or near 7 after that it was dried at 110 °C for 24 h. Finally, it was calcined with air at 550 °C for 4.5 h.

Appendix D

Calibration curve of Reactant and Product

The calibration curve was calculated by injection substance into GC-FID and detected by chromatogram in area of substance versus amount of injection substance. The calibration curve of reactant and product were shown in Figure AC 1-4

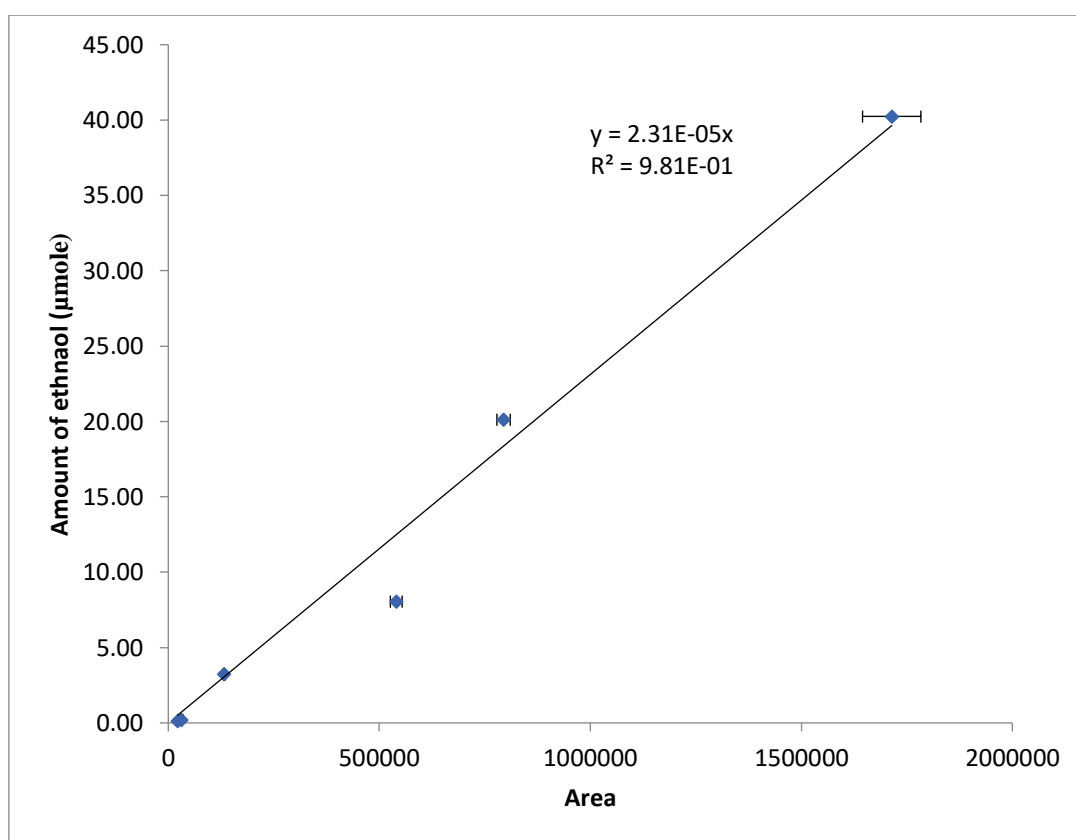


Figure AC 1. The calibration curve of ethanol

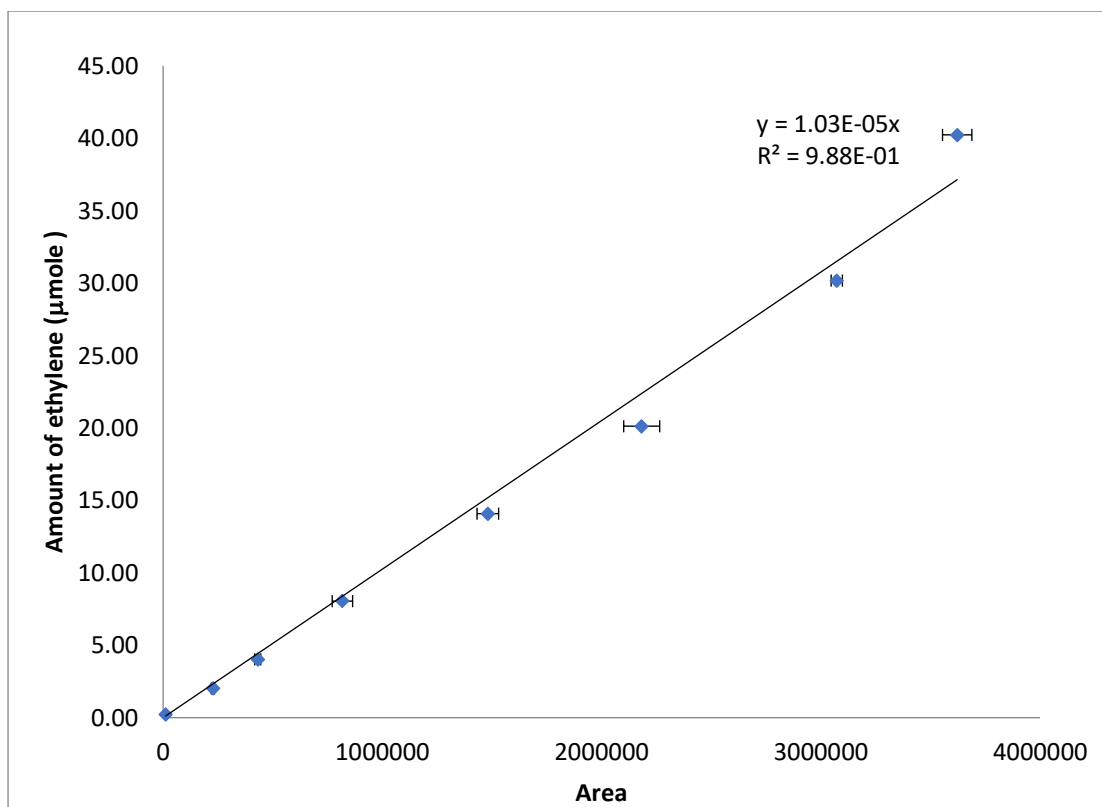


Figure AC 2. The calibration curve of ethylene

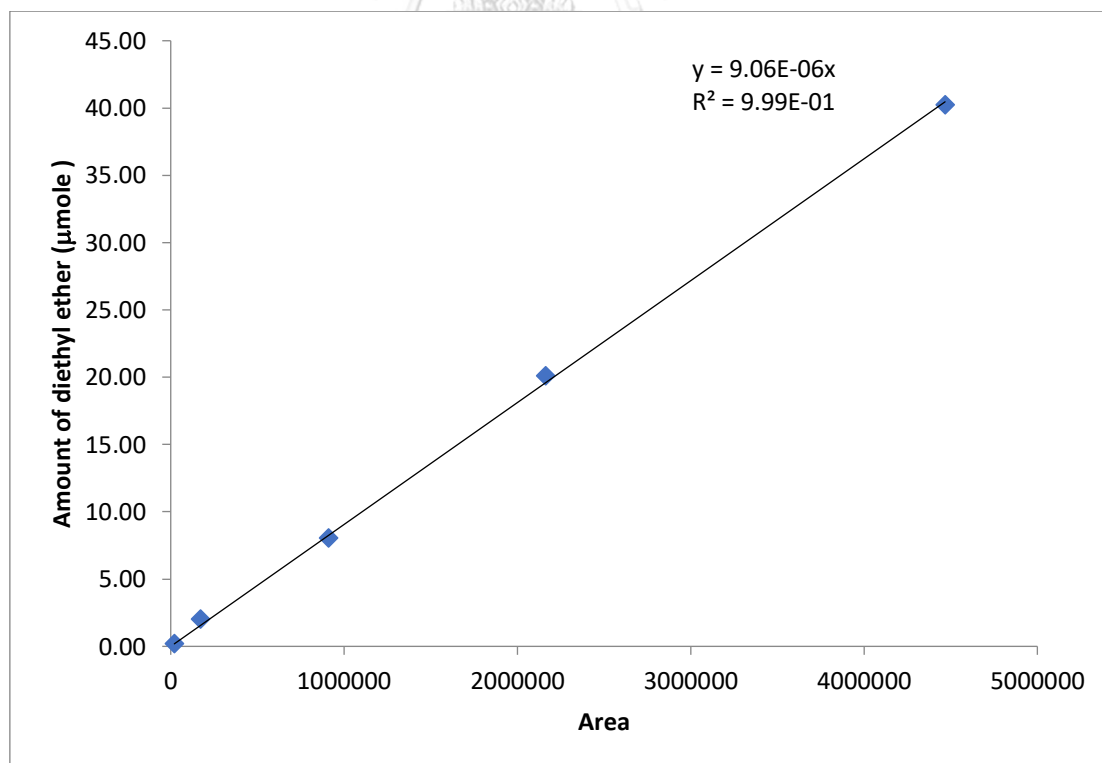


Figure AC 3. The calibration curve of diethyl ether

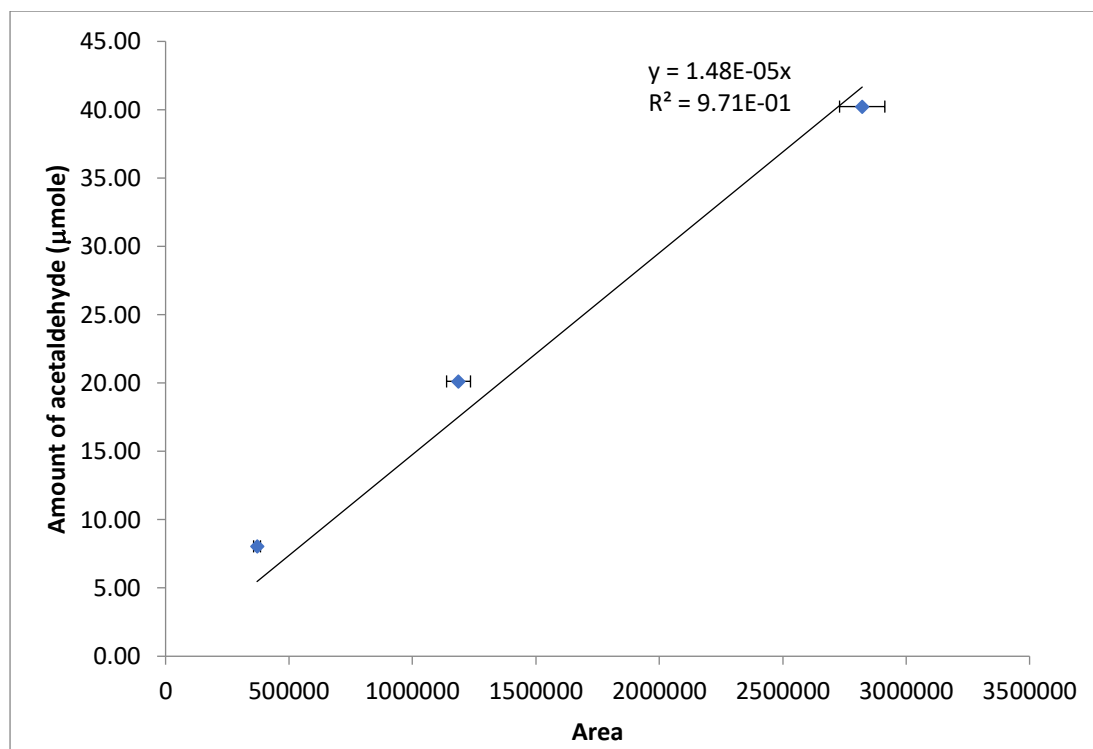


Figure AC 4. The calibration curve of acetaldehyde



Appendix E

Calculation of acidity catalysts from NH₃-TPD

Acidity of catalysts were detected by ammonia temperature programmed desorption. The calibration curve of ammonia gas is shown in Figure AE 1.

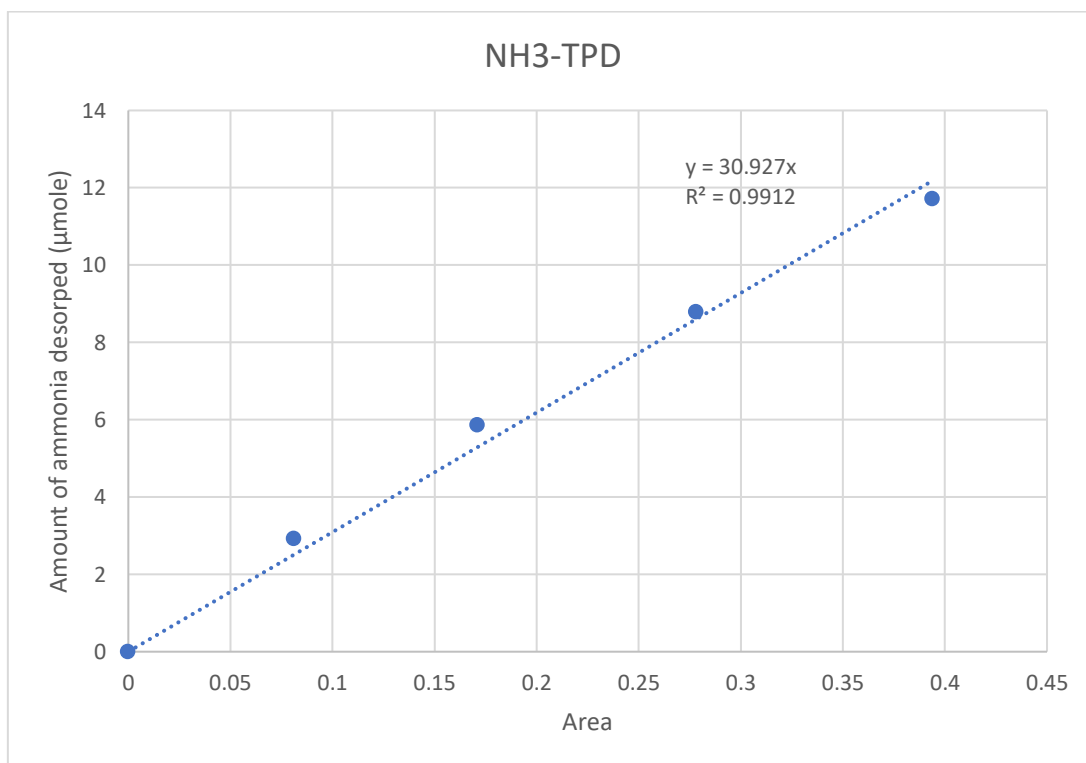


Figure AE 1. Calibration curve of ammonia

$$\text{Total Acidity} = \frac{\text{Mole of desorbed NH}_3 (\mu\text{mole NH}_3)}{\text{Weight of used catalyst (g)}}$$

Where, mole of desorbed NH₃ were calculation from calibration curve

$$\begin{aligned} \text{Mole of desorbed NH}_3 (\mu\text{mole NH}_3) &= \text{Area under curve of TCD signal} \times 30.93 \\ &(\text{slope of calibration curve from desorption of} \\ &\text{ammonia gas}) \end{aligned}$$

Appendix F

Calculation of conversion , selectivity, yield rate of reaction and WHSV

Conversion

$$\text{Reactant conversion (\%)} = \frac{\text{Mole of reactant after reaction completed}}{\text{Mole of reactant before reaction completed}} \times 100 \%$$

Selectivity

$$\text{Product selectivity (\%)} = \frac{\text{Mole of desired product}}{\text{Total moles of all product}} \times 100 \%$$

Yield

$$\text{Product yield (\%)} = \text{Product selectivity} \times \text{Reactant conversion}$$

Rate of reaction

$$\begin{aligned} \text{Rate of reaction} &= \frac{\text{Ethanol feed rate} \times \text{Ethanol conversion (\%)}}{\text{(mole ethanol/h)}} \\ \text{(mole ethanol/kg}_{\text{cat}} \cdot \text{h)} &= \frac{0.0821 \times \text{Temperature} \times \text{Amount of used}}{\text{(L} \cdot \text{atm/mol} \cdot \text{K)} \quad \text{(K)} \quad \text{catalysts (kg)}} \end{aligned}$$

Weight hourly space velocity

$$\text{WHSV (h}^{-1}\text{)} = \frac{\text{Mass flow rate of reactant (g/h)}}{\text{Weight of catalyst in reactor (g)}}$$

Calculate %wt of Si from %at

$$\begin{aligned} \text{\%wt of Si} &= \frac{\text{\%at of Si} \times \text{atomic weight of Si}}{(\text{\%at of Si} \times \text{atomic weight of Si}) + (\text{\%at of Al} \times \text{atomic weight of Al})} \\ &\quad + (\text{\%at of O} \times \text{atomic weight of O}) \end{aligned}$$

Appendix G

Catalytic activity, selectivity, yield and rate of reaction of product over all catalysts

Table AF 1 Conversion, selectivity, yield and rate of reaction from ethanol reaction at 200 °C

Catalysts	Conversion (%)	Product selectivity (%)		
		Ethylene	Diethyl ether	Acetaldehyde
ZSM-5 Si/Al 20	7.1	0.0	100.0	0.0
ZSM-5 Si/Al 40	2.8	0.0	100.0	0.0
ZSM-5 Si/Al 60	0.0	0.0	0.0	0.0
Commercial HZSM-5	9.6	0.0	100.0	0.0
P-HZSM-5	12.7	0.5	99.3	0.2
Pd-HZSM-5	22.3	3.8	92.6	3.6
Pd-P-HZSM-5	11.3	12.6	83.8	3.6
Pd-P-HZSM-5 (Co-impregnation)	12.7	11.4	84.2	4.4
Synthesized HZSM-5	20.9	2.1	98.8	0.1

Catalysts	Rate of reaction (mole ethanol/kg _{cat} ·h)	Product yield (%)		
		Ethylene	Diethyl ether	Acetaldehyde
ZSM-5 Si/Al 20	90.9	0.0	7.1	0.0
ZSM-5 Si/Al 40	60.6	0.0	2.8	0.0
ZSM-5 Si/Al 60	0.0	0.0	0.0	0.0
Commercial HZSM-5	213.1	0.0	9.6	0.0
P-HZSM-5	272.3	0.1	12.6	0.0
Pd-HZSM-5	472.9	0.9	20.7	0.8
Pd-P-HZSM-5	231.8	1.4	9.5	0.4
Pd-P-HZSM-5 (Co-impregnation)	270.6	1.4	10.7	0.6
Synthesized HZSM-5	463.8	0.4	20.5	0.0

Table AF 2 Conversion, selectivity, yield and rate of reaction from ethanol reaction at 250 °C

Catalysts	Conversion (%)	Product selectivity (%)		
		Ethylene	Diethyl ether	Acetaldehyde
ZSM-5 Si/Al 20	12.8	4.9	94.3	0.8
ZSM-5 Si/Al 40	9.4	3.1	85.7	11.17
ZSM-5 Si/Al 60	0.0	0.0	100.0	0.0
Commercial HZSM-5	42.1	15.9	84.1	0.0
P-HZSM-5	30.8	14.9	84.9	0.2
Pd-HZSM-5	60.7	79.8	19.1	1.1
Pd-P-HZSM-5	39.3	73.6	25.6	0.8
Pd-P-HZSM-5 (Co-impregnation)	48.1	69.6	26.8	3.7
Synthesized HZSM-5	72.3	55.6	43.7	0.7

Catalysts	Rate of reaction (mole ethanol/kg _{cat} •h)	Product yield (%)		
		Ethylene	Diethyl ether	Acetaldehyde
ZSM-5 Si/Al 20	148.3	0.6	12.1	0.1
ZSM-5 Si/Al 40	108.9	0.3	8.1	1.1
ZSM-5 Si/Al 60	0.0	0.0	0.0	0.0
Commercial HZSM-5	487.7	6.7	35.4	0.0
P-HZSM-5	356.8	4.6	26.2	0.1
Pd-HZSM-5	703.5	48.5	11.6	0.6
Pd-P-HZSM-5	455.3	29.0	10.1	0.3
Pd-P-HZSM-5 (Co-impregnation)	557.2	33.4	12.9	1.8
Synthesized HZSM-5	837.5	40.2	31.6	0.5

Table AF 3 Conversion, selectivity, yield and rate of reaction from ethanol reaction at 300 °C

Catalysts	Conversion (%)	Product selectivity (%)		
		Ethylene	Diethyl ether	Acetaldehyde
ZSM-5 Si/Al 20	16.4	32.4	66.5	1.1
ZSM-5 Si/Al 40	12.0	11.0	84.5	4.5
ZSM-5 Si/Al 60	1.2	0.0	0.0	100.0
Commercial HZSM-5	75.9	91.0	8.7	0.3
P-HZSM-5	70.5	92.6	7.2	0.2
Pd-HZSM-5	94.8	98.5	0.5	1.0
Pd-P-HZSM-5	77.2	95.0	3.5	1.5
Pd-P-HZSM-5 (Co-impregnation)	84.1	94.7	3.9	1.4
Synthesized HZSM-5	96.1	98.7	0.7	0.6

Catalysts	Rate of reaction (mole ethanol/kg _{cat} •h)	Product yield (%)		
		Ethylene	Diethyl ether	Acetaldehyde
ZSM-5 Si/Al 20	173.4	5.3	10.9	0.2
ZSM-5 Si/Al 40	126.9	1.3	10.1	0.5
ZSM-5 Si/Al 60	12.7	0.0	0.0	1.24
Commercial HZSM-5	802.5	69.1	6.6	0.2
P-HZSM-5	745.4	65.3	5.1	0.2
Pd-HZSM-5	1002.4	93.5	0.4	0.9
Pd-P-HZSM-5	816.3	73.3	2.7	1.2
Pd-P-HZSM-5 (Co-impregnation)	889.2	79.6	3.2	1.2
Synthesized HZSM-5	1016.1	94.8	0.6	0.6

Table AF 4 Conversion, selectivity, yield and rate of reaction from ethanol reaction at 350 °C

Catalysts	Conversion (%)	Product selectivity (%)		
		Ethylene	Diethyl ether	Acetaldehyde
ZSM-5 Si/Al 20	43.1	80.2	18.4	1.4
ZSM-5 Si/Al 40	20.5	43.3	51.5	5.2
ZSM-5 Si/Al 60	2.1	4.2	0.6	95.2
Commercial HZSM-5	96.1	98.8	0.5	0.7
P-HZSM-5	89.8	98.1	1.5	0.4
Pd-HZSM-5	99.3	97.5	0.2	2.3
Pd-P-HZSM-5	97.5	98.3	0.2	1.5
Pd-P-HZSM-5 (Co-impregnation)	97.4	98.2	0.3	1.5
Synthesized HZSM-5	100	97.5	0.1	2.4

Catalysts	Rate of reaction (mole ethanol/kg _{cat} •h)	Product yield (%)		
		Ethylene	Diethyl ether	Acetaldehyde
ZSM-5 Si/Al 20	419.1	34.6	7.9	0.6
ZSM-5 Si/Al 40	199.4	8.9	10.6	1.1
ZSM-5 Si/Al 60	20.4	0.1	0.0	2.0
Commercial HZSM-5	934.6	95.0	0.5	0.6
P-HZSM-5	873.3	88.0	1.3	0.4
Pd-HZSM-5	965.7	96.8	0.2	2.3
Pd-P-HZSM-5	948.2	95.9	0.2	1.4
Pd-P-HZSM-5 (Co-impregnation)	947.2	95.6	0.3	1.5
Synthesized HZSM-5	972.5	97.5	0.1	2.4

Table AF 5 Conversion, selectivity, yield and rate of reaction from ethanol reaction at 400 °C

Catalysts	Conversion (%)	Product selectivity (%)		
		Ethylene	Diethyl ether	Acetaldehyde
ZSM-5 Si/Al 20	70.3	95.6	2.5	1.9
ZSM-5 Si/Al 40	38.2	83.6	12.7	3.7
ZSM-5 Si/Al 60	3.5	10.3	3.8	85.9
Commercial HZSM-5	99.8	98.9	0.1	1.0
P-HZSM-5	97.5	99.3	0.1	0.5
Pd-HZSM-5	100.0	97.2	0.3	2.6
Pd-P-HZSM-5	100.0	98.7	0.1	1.2
Pd-P-HZSM-5 (Co-impregnation)	100.0	99.2	0.1	0.7
Synthesized HZSM-5	100.0	99.2	0.0	0.8

Catalysts	Rate of reaction (mole ethanol/kg _{cat} •h)	Product yield (%)		
		Ethylene	Diethyl ether	Acetaldehyde
ZSM-5 Si/Al 20	632.9	67.2	1.7	1.4
ZSM-5 Si/Al 40	343.9	31.9	4.8	1.4
ZSM-5 Si/Al 60	31.5	0.4	0.1	3.0
Commercial HZSM-5	898.4	98.8	0.1	1.0
P-HZSM-5	877.7	96.9	0.1	0.5
Pd-HZSM-5	900.2	97.1	0.3	2.6
Pd-P-HZSM-5	900.2	98.7	0.1	1.2
Pd-P-HZSM-5 (Co-impregnation)	900.2	99.2	0.1	0.7
Synthesized HZSM-5	900.2	99.2	0.0	0.8

VITA

Mr. Nattawat Nampipat was born on February 21th, 1994 in Bangkok, Thailand. He graduated Bachelor degree of Chemical Engineering from Kasetsart University, Bangkok ,Thailand in Mar 2016. He decided to study in Master degree of Chemical Engineering at Chulalongkorn University, Bangkok, Thailand since 2016





จุฬาลงกรณ์มหาวิทยาลัย
CHULALONGKORN UNIVERSITY